KH-98-1 Leg 3 Cruise Report

RV Hakuho Maru
Ocean Research Institute
University of Tokyo

KH98-1 Cruise LEG.3

1998.3.2~3.16 Pohnpei-Tokyo

Name	Title	Institute	E-mail address
Teruaki Ishii	Associate Professor	ORI, Univ. of Tokyo	ishii@ori.u-tokyo.ac.jp
(Chief Scientist of the Mission)			
Toshitaka Gamo	Associate Professor	ORI, Univ. of Tokyo	gamo@ori.u-tokyo.ac.jp
Hiroaki Toh	Research Associate	ORI, Univ. of Tokyo	toh@ori.u-tokyo.ac.jp
Hiroshi Hasumoto	Research Associate	ORI, Univ. of Tokyo	hasumoto@ori.u-tokyo.ac.jp
Shoji Kitagawa	Technical Staff	ORI, Univ. of Tokyo	kitagawa@ori.u-tokyo.ac.jp
Eiichiro Araki	Graduate Student	ORI, Univ. of Tokyo	araki@ori.u-tokyo.ac.jp
Satoru Haraguchi	Graduate Student	ORI, Univ. of Tokyo	haraguti@ori.u-tokyo.ac.jp
Kei Okamura	Graduate Student	ORI, Univ. of Tokyo	okamura@ori.u-tokyo.ac.jp
Yukiko Hirata -Kotake	Research Fellow	ORI, Univ. of Tokyo	yhirata@ori.u-tokyo.ac.jp
Junichiro Ishibashi	Research Associate	Univ. of Tokyo	ishi@eqchem.s.u-tokyo.ac.jp
Yoshiro Nishio	Graduate Student	Univ. of Tokyo	nishio@geol.s.u-tokyo.ac.jp
Tadanori Goto	Research Fellow	ERI, Univ. of Tokyo	goto@utada-sun.eri.u-tokyo.ac.jp
Hiroshi Sato	Graduate Student	Univ. of Tsukuba	satohiro@arsia.geo.tsukuba.ac.jp
Yasutaka Hayasaka	Research Associate	Hiroshima Univ.	hayasaka@geol.sci.hiroshima-u.ac.jp
Takeaki Maejima	Graduate Student	Hiroshima Univ.	take@geol.sci.hiroshima-u.ac.jp
Toshiro Yamanaka	Graduate Student	Kyushu Univ.	ezmikasa@planet.geo.kyushu-u.ac.jp
Toru Yamashiro	Research Associate	Kagoshima Univ.	toru@oce.eng.kagoshima-u.ac.jp
Eiichiro Nakayama	Associate Professor	Univ. of Shiga Prefec.	nakayama@ses.usp.ac.jp
Hajime Obata	Research Fellow	Univ. of Shiga Prefec.	obata@ses.usp.ac.jp
Harue Masuda-Nakaya	Associate Professor	Osaka City Univ.	harue@sci.osaka-cu.ac.jp
Hidetsugu Taniguchi	Lecturer	Komazawa Univ. High Sch.	hidetani@pb3.so-net.ne.jp
Thomas J. Mueller	Senior Scientist	Inst. fuer Meereskunde, Kiel	tmueller@ifm.uni-kiel.de
Dieter Carlsen	Mooring Engineer	Inst. fuer Meereskunde, Kiel	dcarlsen@ifm.uni-kiel.de

TRACK CHART

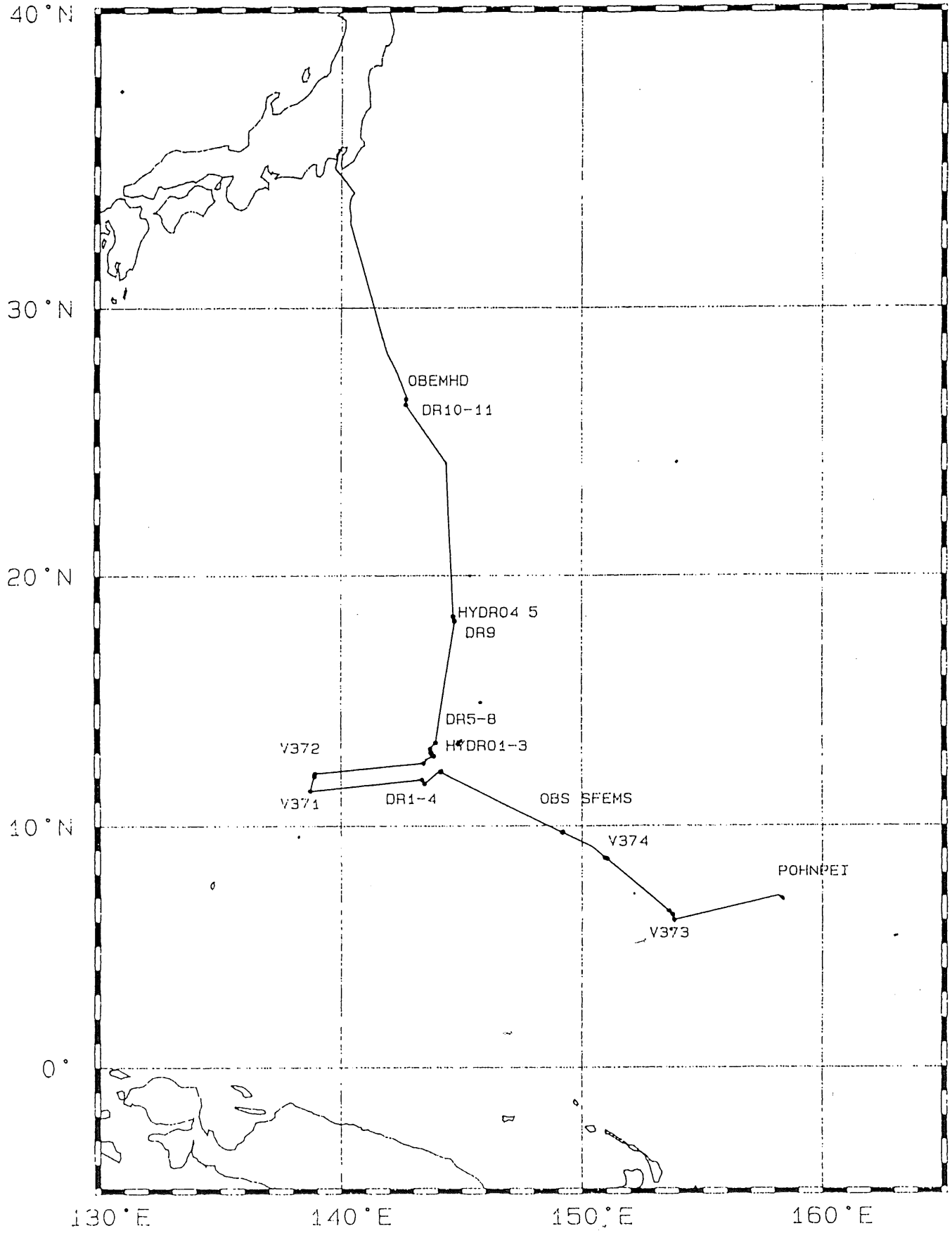
40°N
30°N
20°N
10°N
0°
130°E
140°E
150°E
160°E
OBEMHD
DR10-11
HYDRO4 5
DR9
DR5-8
HYDRO1-3
V372
V371
DR1-4
OBS SFEMS
V374
POHNPEI
V373

LEG. 3
Working Schedule

Leg.1	1	2	3	4	5	6	7	8	9	10	11	12	13	14	15	16	17	18	19	20	21	22	23	24
Mar. 02. 98'	a difference time									Ponpei Departure														
	JST+2																							
Mar. 03. 98'								St.373-1 CTD-CMS						St.373 CTD-CMS				St.373-2 CTD-CMS						
								06 00.29N, 153 47.15E						06 14.54N,153 43.47E				06 23.80N,153 33.99N						
												Start to retreive of CM(12:15-14:08)												
Mar. 04. 98'								St.374-1 CTD-CMS							St.374 CTD-CMS					St.374-2 CTD-CMS				
								08 37.34N,150 58.99E							08 39.53N,150 56.61E					08 39.62N,150 55.11E				
	1:00:(JST+1)											Start to retreive of CM(12:15-15:11)												
Mar. 05. 98'						OBS & SFEMS Retreive																		
						(06::11-13:30)															1:00:(JST+0)			
Mar. 06. 98'									St.kh98-1 DR-1						St.kh98-1 DR-2								St.kh98-1	
									12 13.12N,144 06.23E						12 15.53N,144 04.58E								11 43.67N	
Mar. 07. 98'	DR-3				St.kh98-1 DR-4																			
	143 26.47E				11 53.89N,143 20.15E																			
Mar. 08. 98'		St.371 CTD-CMS													St.372 CTD-CMS				St.372-1 CTD-CMS			St.372-2 CTD-CMS		
		11 26.63N,138 41.40E													12 06.93N,138 52.3E				12 02.30N,138 52.11E				12 09.32N	
							Start to retreive of CM(06:55-09:32)						Start to retreive of CM(12:35-14:43)											
Mar. 09. 98'																			St.kh98-1 DR-5				St.Hydro-1	
	138 53.31E																		12 33.91N,143 24.83E					
Mar. 10. 98'	CTD-CMS			St.kh98-1 DR-6				St.Hydro-2 CTD-CMS				St.kh98-1 DR-7				St.kh98-1 DR-8				St.Hydro-3 CTD-CMS			
	12 43.04N,143 31.95E			12 51.99N,143 50.02E				12 58.26N,143 44.53E				12 58.44N,143 43.65E					13 09.19N,143 40.61E				13 23.75N,143 55.21E		
Mar. 11. 98'																St.Hydro-4 CTD-CMS				St.kh98-1 DR-9				
																18 12.82N,144 42.30E				18 12.7N,144 42.97E				
Mar. 12. 98'																							St.Hydro-5	
																							18 23.54N	
Mar. 13. 98'	CTD-CMS														St.kh98-1 DR-10				St.kh98-1 DR-11					
	144 38.97E														26 30.24N,142 39.45E				26 30.13N,142 39.45E					
Mar. 14. 98'																								
Mar. 15. 98'																								
Mar. 16. 98'										Arrived at Tokyo														

	----- 02 MAR.98 (GMT) -----			
373-1	21:09	06°00.850N	153°47.039E	4065m CTD-CMS START
373-1	22:31	06°00.290N	153°47.149E	4101m CTD-CMS DEEPEST
373-1	23:34	05°59.970N	153°47.289E	4060m CTD-CMS FINISH
	----- 03 MAR.98 (GMT) -----			
V-373	03:32	06°14.540N	153°43.499E	4075m CTD-CMS START
V-373	04:54	06°14.540N	153°43.469E	4077m CTD-CMS DEEPEST
V-373	05:54	06°14.520N	153°43.279E	4078m CTD FINISHED
373-2	07:14	06°23.930N	153°34.039E	3781m CTD-CMS START
373-2	07:58	06°23.880N	153°34.019E	3778m SUNSET & PUT ON REGULATION LIGHTS
373-2	08:33	06°23.800N	153°33.999E	3787m CTD-CMS DEEPEST
373-2	09:33	06°23.590N	153°33.929E	3787m CTD-CMS FINISH
374-1	22:43	08°36.990N	150°59.840E	4940m CTD-CMS START
	----- 04 MAR.98 (GMT) -----			
374-1	00:28	08°37.340N	150°58.990E	4973m CTD-CMS DEEPEST
374-1	01:45	08°37.760N	150°58.370E	4996m CTD-CMS FINISH
V-374	02:15	08°38.620N	150°56.670E	4994m RELEASE FOR CM
V-374	02:27	08°38.500N	150°56.380E	4990m POPPING UP OF CM
V-374	02:31	08°38.460N	150°56.280E	4986m START TO RETREIVE OF CM
V-374	05:11	08°38.810N	150°54.110E	4499m FINISHED TO RETREIVE OF CM
V-374	05:49	08°38.660N	150°56.870E	4982m CTD-CMS START
V-374	07:21	08°39.530N	150°56.610E	4935m CTD-CMS DEEPEST
V-374	08:08	08°39.640N	150°56.590E	4936m SUNSET & PUT ON REGULATION LIGHTS
V-374	08:38	08°39.770N	150°56.530E	4943m CTD-CMS FINISH
V-374	09:01	08°39.340N	150°55.650E	4924m CTD-CMS START
374-2	10:36	08°39.620N	150°55.110E	4840m CTD-CMS DEEPEST
374-2	11:52	08°39.800N	150°54.830E	4552m CTD-CMS FINISH
EMB	20:11	09°43.880N	149°09.700E	5356m RELEASE FOR OBS-EMB
OBM	20:38	09°44.930N	149°09.980E	5372m COMMENCED TEST OF OBM
	----- 05 MAR.98 (GMT) -----			
OBM	00:19	09°44.900N	149°10.140E	5374m RELEASE FOR OBM
OBM	02:53	09°44.710N	149°09.650E	5373m POPPING UP OF OBM
OBM	03:02	09°44.870N	149°09.690E	5369m START TO RETREIVE OF
OBM	03:05	09°44.860N	149°09.630E	5370m FINISHED TO RETREIVE OF OBM
	----- 06 MAR.98 (GMT) -----			
D-1	00:38	12°13.120N	144°06.400E	6284m DREDGE START DOWN
D-1	02:37	12°13.120N	144°06.230E	5702m DREDGE ON BOTTOM (02H29M)
D-1	04:16	12°13.200N	144°05.680E	5497m DREDGE OFF BOTTOM
D-1	04:26	12°13.200N	144°05.600E	5476m DREDGE OFF BOTTOM
D-1	05:40	12°13.190N	144°04.170E	4578m DREDGE ON DECK
D-2	06:35	12°15.200N	144°07.180E	5973m DREDGE START DOWN
D-2	08:38	12°15.840N	144°05.190E	4828m DREDGE ON BOTTOM
D-2	10:24	12°15.530N	144°04.580E	4298m DREDGE OFF BOTTOM
D-2	11:26	12°15.050N	144°03.660E	4005m DREDGE ON DECK
D-3	14:41	11°43.650N	143°26.300E	6014m DREDGE START DOWN
D-3	16:27	11°43.670N	143°26.470E	6039m DREDGE ON BOTTOM
D-3	18:11	11°45.340N	143°26.250E	5233m DREDGE OFF BOTTOM
D-3	19:33	11°45.230N	143°26.980E	5514m DREDGE ON DECK
D-4	20:47	11°54.040N	143°19.980E	3338m DREDGE START DOWN
D-4	21:50	11°53.890N	143°20.150E	3195m DREDGE ON BOTTOM
	----- 07 MAR.98 (GMT) -----			
D-4	00:03	11°53.960N	143°21.970E	2296m DREDGE OFF BOTTOM
D-4	00:38	11°53.980N	143°22.090E	2287m DREDGE ON DECK
V-371	17:18	11°25.780N	138°41.860E	4788m CTD-CMS START
V-371	18:49	11°26.630N	138°41.400E	4754m CTD-CMS DEEPEST
V-371	20:39	11°27.570N	138°41.430E	4795m CTD-CMS FINISH
V-371	20:59	11°26.580N	138°42.670E	4853m SUNRISE & PUT OFF REGULAION LIGHTS
V-371	21:24	11°25.690N	138°43.350E	4671m RELEASE FOR CM (V-371)
V-371	21:55	11°25.544N	138°43.712E	4676m POPPING UP OF CM
V-371	22:12	11°26.150N	138°43.930E	4666m START TO RETREIVE OF CM
V-371	22:25	11°26.100N	138°43.750E	4676m START TO RETREIVE OF
	----- 08 MAR.98 (GMT) -----			
V-371	00:32	11°26.340N	138°42.350E	4849m FINISHED TO RETREIVE OF V-371
V-372	03:35	12°05.880N	138°52.790E	4659m RELEASE FOR CM
V-372	04:30	12°05.910N	138°52.710E	4623m POPPING UP OF CM
V-372	04:33	12°05.920N	138°52.650E	4607m START TO RETREIVE OF CM
V-372	05:43	12°06.230N	138°51.120E	4578m FINISHED TO RETREIVE OF CM
V-372	06:16	12°05.990N	138°53.050E	4711m CTD-CMS START
V-372	07:48	12°06.930N	138°52.310E	4932m CTD-CMS DEEPEST
V-372	08:54	12°07.560N	138°52.070E	4886m SUNSET & PUT ON REGULATION LIGHTS
V-372	09:09	12°07.700N	138°52.550E	4953m CTD-CMS FINISH
372-1	10:08	12°01.500N	138°52.420E	4598m CTD-CMS START
372-1	11:29	12°02.300N	138°52.110E	4678m CTD-CMS DEEPEST

372-1	12:41	12°02.990N	138°51.690E	4659m	CTD-CMS FINISH
372-2	13:29	12°08.800N	138°53.820E	4627m	CTD-CMS START
372-2	14:56	12°09.320N	138°53.310E	4616m	CTD-CMS DEEPEST
372-2	16:32	12°10.080N	138°52.850E	4646m	CTD-CMS FINISH
----- 09 MAR.98 (GMT) -----					
D-05	10:48	12°33.860N	143°24.770E	2752m	DREDGE START DOWN
D-05	11:43	12°33.910N	143°24.830E	2691m	DREDGE ON BOTTOM
D-05	13:49	12°33.860N	143°25.710E	2082m	DREDGE OFF BOTTOM
D-05	14:23	12°33.750N	143°25.920E	2228m	DREDGE ON DECK
D-06	19:35	12°52.150N	143°49.790E	2350m	DREDGE START DOWN
D-06	20:24	12°51.990N	143°50.020E	2486m	DREDGE ON BOTTOM
D-06	21:59	12°51.270N	143°50.650E	2222m	DREDGE ON DECK
HYD-2	23:17	12°58.460N	143°44.680E	2606m	CTD-CMS START
----- 10 MAR.98 (GMT) -----					
HYD-2	00:09	12°58.540N	143°44.470E	2738m	CTD-CMS DEEPEST
HYD-2	00:45	12°58.260N	143°44.570E	2489m	CTD-CMS DEEPEST
HYD-2	00:51	12°58.260N	143°44.520E	2480m	CTD-CMS DEEPEST
HYD-2	02:00	12°57.930N	143°44.400E	2707m	CTD-CMS FINISH
D-07	02:21	12°58.580N	143°43.550E	3344m	DREDGE START DOWN
D-07	03:26	12°58.440N	143°43.650E	3222m	DREDGE ON BOTTOM
D-07	05:10	12°58.040N	143°44.900E	2722m	DREDGE OFF BOTTOM
D-07	05:44	12°58.100N	143°45.000E	2825m	DREDGE ON DECK
D-07	05:56	12°58.090N	143°44.850E	2674m	CHANGED PROPULSION TO DIESEL ENGINE
D-07	05:56	12°58.090N	143°44.840E	2664m	SLOW AHEAD ENGINES
D-07	05:59	12°58.220N	143°44.760E	2552m	s/co on 342°
D-08	08:15	13°08.720N	143°41.420E	2927m	DREDGE ON BOTTOM
D-08	08:35	13°09.040N	143°40.990E	2975m	DREDGE OFF BOTTOM
D-08	08:35	13°09.040N	143°40.980E	2964m	SUNSET & PUT ON REGULATION LIGHTS
D-08	09:05	13°09.190N	143°40.610E	2975m	DREDGE OFF BOTTOM
D-08	09:47	13°09.720N	143°40.610E	3161m	DREDGE ON DECK
HYD-3	11:27	13°23.680N	143°55.270E	1501m	CTD-CMS START
HYD-3	12:10	13°23.750N	143°55.210E	1494m	CTD-CMS DEEPEST
HYD-3	13:12	13°23.200N	143°55.160E	1797m	CTD-CMS FINISH
----- 11 MAR.98 (GMT) -----					
HC-1	07:44	18°12.560N	144°41.680E	3818m	CTD-CMS START
HC-1	09:15	18°12.820N	144°42.300E	3702m	CTD-CMS DEEPEST
HC-1	10:35	18°12.600N	144°42.180E	3734m	CTD-CMS FINISH
D-09	10:50	18°12.940N	144°41.990E	3721m	DREDGE START DOWN
D-09	11:53	18°12.940N	144°42.060E	3718m	DREDGE ON BOTTOM
D-09	12:41	18°12.700N	144°42.970E	3819m	DREDGE OFF BOTTOM
D-09	13:33	18°13.290N	144°43.570E	3726m	DREDGE ON DECK
HYD-5	14:41	18°23.940N	144°38.640E	3610m	CTD-CMS START
HYD-5	15:53	18°23.540N	144°38.970E	3598m	CTD-CMS DEEPEST
HYD-5	17:18	18°22.920N	144°38.980E	3695m	CTD-CMS FINISH
----- 13 MAR.98 (GMT) -----					
D-10	05:55	26°30.290N	142°39.560E	2586m	DREDGE START DOWN
D-10	06:35	26°30.240N	142°39.450E	2566m	DREDGE ON BOTTOM
D-10	08:18	26°30.130N	142°37.650E	2018m	DREDGE OFF BOTTOM
D-10	08:56	26°30.120N	142°37.510E	1965m	DREDGE ON DECK
D-11	10:25	26°42.880N	142°40.590E	2007m	DREDGE START DOWN
D-11	11:06	26°43.110N	142°40.640E	1996m	DREDGE ON BOTTOM
D-11	12:37	26°43.060N	142°42.870E	1814m	DREDGE OFF BOTTOM
D-11	13:10	26°43.100N	142°43.870E	1836m	DREDGE ON DECK

U: The circulation of the intermediate and deep water masses in the western tropical Pacific.

Leg 3: Mueller, Carlsen, Yamashiro, Kitagawa, Hasumoto et al.

Introduction

In the world oceans, four major layers of water masses play an important role in the interoceanic and interhemispheric water mass exchange and associated heat transport. Looking from top to bottom in a subtropical gyre, they are (i) warm near-surface and thermocline waters, (ii) intermediate waters of low salinity of subpolar origin, (iii) deep water which major part stems from the deep convection areas in the northern North Atlantic, and (iv) bottom water which major part origins from the Wedell Sea.

While most of the warm near-surface and thermocline waters of the subtropics are caught in their wind-driven gyre circulation, some of it is needed to compensate for losses of surface water due to vertical convection in remote areas which drives the large scale ocean thermohaline circulation. Thus, the convection-poor North Pacific provides some warm near-surface water that flows to the Indian Ocean through the Indonesian Passage, is transported around the tip of South Africa into the South Atlantic and from there along the northeast coast of Brazil into the northern North Atlantic where the North Atlantic Deep Water (NADW) is convectively formed in the Labrador and Greenland Seas. This in turn makes its way southward in a deep western boundary current along the American continental shelf break, mixes with Circumpolar Deep Water in the Antarctic Circumpolar Current (ACC), and finally through western boundary currents feeds the Indian and Pacific Oceans with deep water which compensates for their losses of warm surface waters to the North Atlantic.

The most important intermediate water is the Antarctic Intermediate Water (AAIW). It is formed in the ACC and is injected to the southern subtropical oceans. In the Atlantic, it can be traced far north of the equator. In the Pacific it can be identified at least up to the North Equatorial Counter Current where it meets the North Pacific Intermediate Water (NPIW). Thus, it also plays an important role in the world ocean thermohaline circulation.

As this general picture of the thermohaline circulation is known since long, details of flow paths and transports as well as mixing processes and mixing rates beteween the layers are not. One area is the western tropical Pacific with its complicated topographic structure.

The TROPAC experiment

In co-operation with Prof. K. Taira from the Ocean Research Institute (ORI) at the University of Tokyo, the programme TROPAC has been set up at the Institut fuer Meereskunde in Kiel, Germany, by Prof. G. Siedler and Dr. W. Zenk. The two major goals of TROPAC are:

- to search for the pathways that the AAIW takes as it crosses the equator northward, probably along the coast of New Guinea, and as it meets the NPIW.

- to identify passages that are deep enough to let the deep water pass from the Eastern Caroline Basin into the Western Mariane Basin and to measure its transport.

Methods

The water masses are traced with hydrographic stations, including measurements of dissolved oxygen, nutrients and the anthropogenic CFCs F11, F12 and CCl4. A net of stations covering the East Caroline Basin has been performed during the first TROPAC cruise on the German R/V SONNE, cruise 113, in October/November 1996.

To measure the flow in the AAIW level directly, subsurface floats of RAFOS type have been deployed during SONNE 113. They are tracked acoustically by moored sound sources. The mission time of the floats ends by June 1998 when they will surface and transmit their data via the ARGOS satellite system for further analysis. Moorings V375 and V376, that have been deployed during SONNE 113 north of New Guinea and that carry one sound source each, will be in site until July 1998. Float data are expected from June 1998 on.

Four other moorings were deployed in passages that are thought to be able to let deep water pass from the East Caroline Basin across the Caroline Ridge (V373 near the Losap Atoll, Fig. U1; V374 near East Fayou, Fig. U2) and the South Honshu Ridge (V372, V371; Fig. U3) into the Western Mariane Basin. These moorings carry current meters to measure the deep flow. Two of them (V371 and V374) in addition have one sound source and one current meter in the AAIW level.

Purpose of TROPAC during R/V Hakuho Maru cruise KH98-1/3

- to recover moorings V371 to V374

- to obtain additional CTD-O2 stations close to the mooring positions to identify the water mass properties and level thicknesses for transport calculations.

Preliminary results

All four moorings were recovered as scheduled without delay (Fig. U4 - U7). One current meter was flooded (Tab. U1) and one lost its rotor during the deployement so that no speed could be measured. All data were read from the storing unit to PC, despiked, calibrated and corrected for clock drifts. The overall data quality is good after the first inspection (Tab. U1).

Across each of the passages at V373 near the Loasap Atoll, at V374 near East Fayou and at V372 in the South Honshu Ridge, three CTD-O2 stations with a SeaBird 911 were obtained. Bottle samples for salinity and oxygen sensor calibration were taken near the surface, above the bottom and at full 1000 m depths. The vertical profiles of temperature, salinity and oxygen of the central casts of these and a single cast taken at V371 are shown in Figures U8 - U11, respectively.

Further analysis will be performed in the Institut fuer Meereskunde, Kiel.

Table U1: Inventory of TROPAC moorings V371 to V374

ID	Lat N Lon E DDD MM.MM	Water depth m	Layed Recovery	Instrument depth m	ID	Sensors	Remarks
V371	11 25.65 138 43.60	4720	13 Oct 1996 08 Mar 1998	712 772	RCM00094 SoSo12	VTCP	
				3220	RCM10662	VTC	
				3720	RCM11662	VT	
				4220	RCM09728	VT	
				4670	RCM11617	VT	
V372	12 06.0 138 53.1	4620	14 Oct 1996 08 Mar 1998	3120	RCM12004	VT P	
				3620	RCM09832	VVT	no speed from day 125 on
				4120	RCM09344	VT	
				4570	RCM09730	VT	no speed from day 438 on
V373	06 14.5 153 43.5	4096	29 Oct 1996 03 Mar 1998	1900	RCM12005	VT P	
				2400	RCM09831	VT	
				2900	RCM09820	VTC	
				3400	RCM09313	VTC	
				3900	RCM09323	flooded, no data	
				4040	RCM11621	VT	no speed due to rotor loss during deployement
V374	08 38.6 150 56.9	4984	27 Oct 1996 04 Mar 1998	757 817	RCM10077 SoSo13	VTCP	
				2830	RCM09727	VTC	
				3330	RCM09731	VT	
				3830	RCM09732	VTC	
				4270	RCM11618	VT	

Legend: RCM is Aanderaa (vector averaging) current meter RCM8; sampling rate 120 minutes; V denotes current vector, T temperature, C conductivity, P pressure sensors; where no pressure is measured, high resolution temperature (-2 to 6 C) is measured in addition. SoSo is Webb Research RAFOS sound source for RAFOS float tracking.

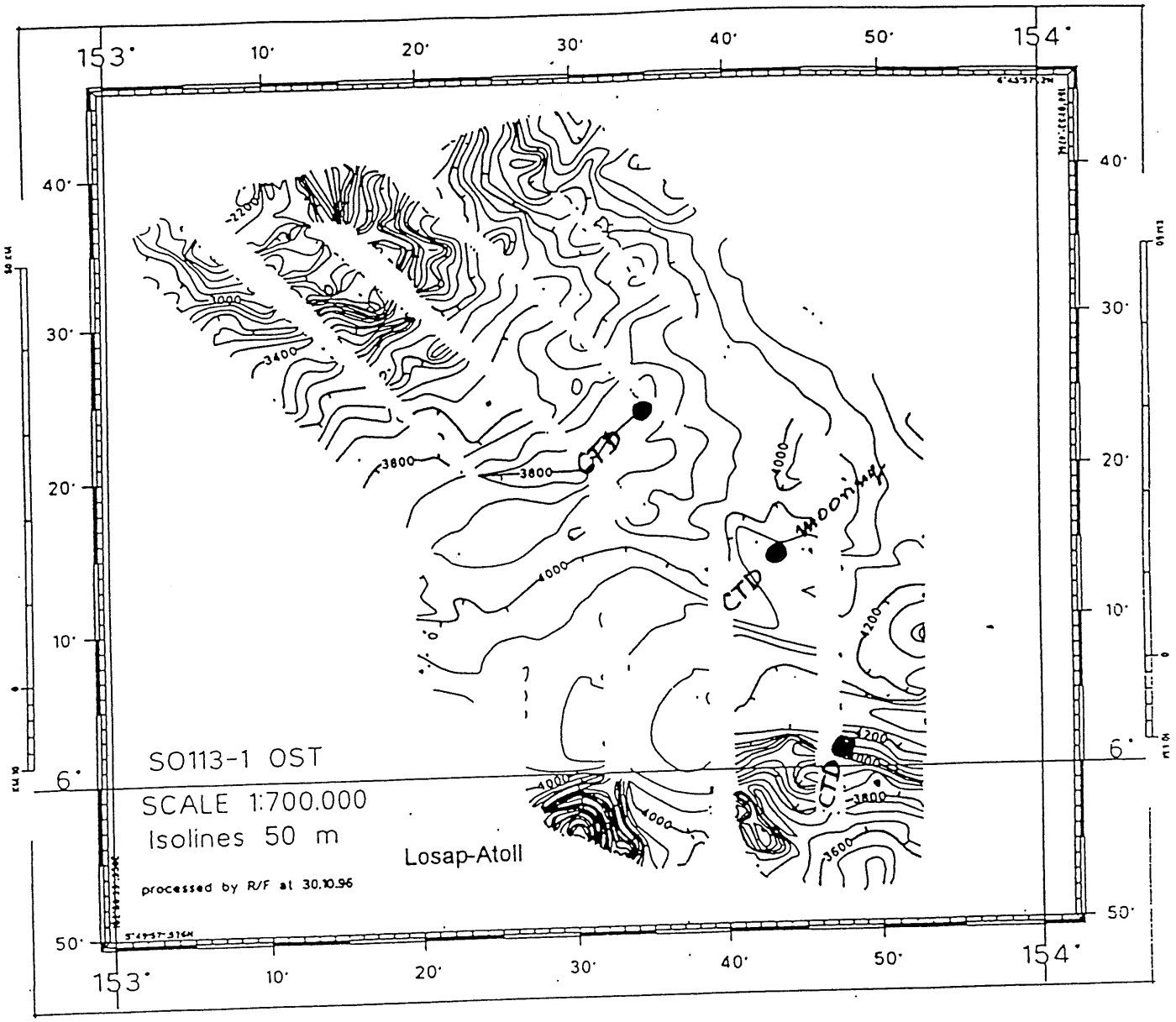

mooring V373

Fig. 11

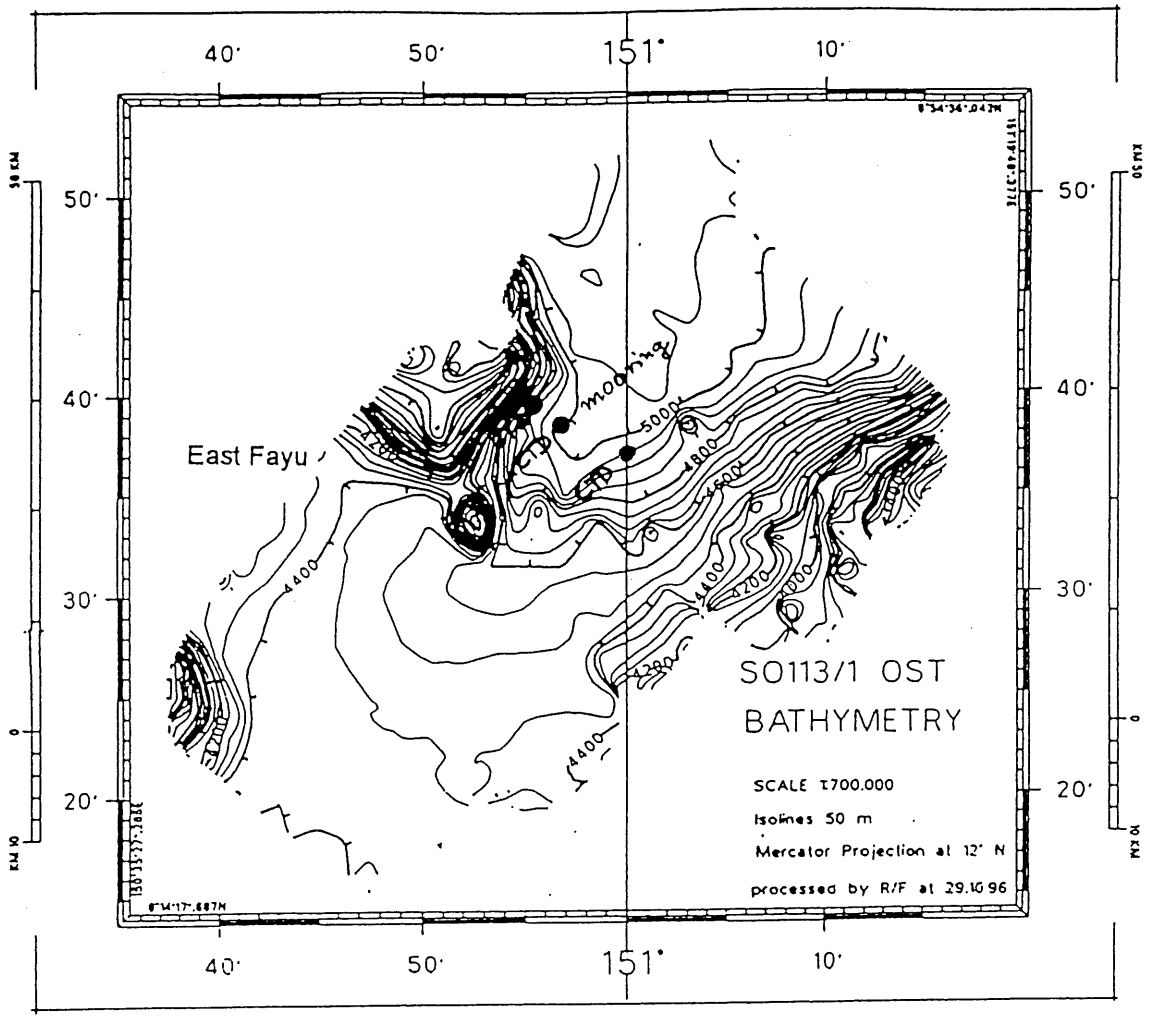

mooring V 374

Fig 12

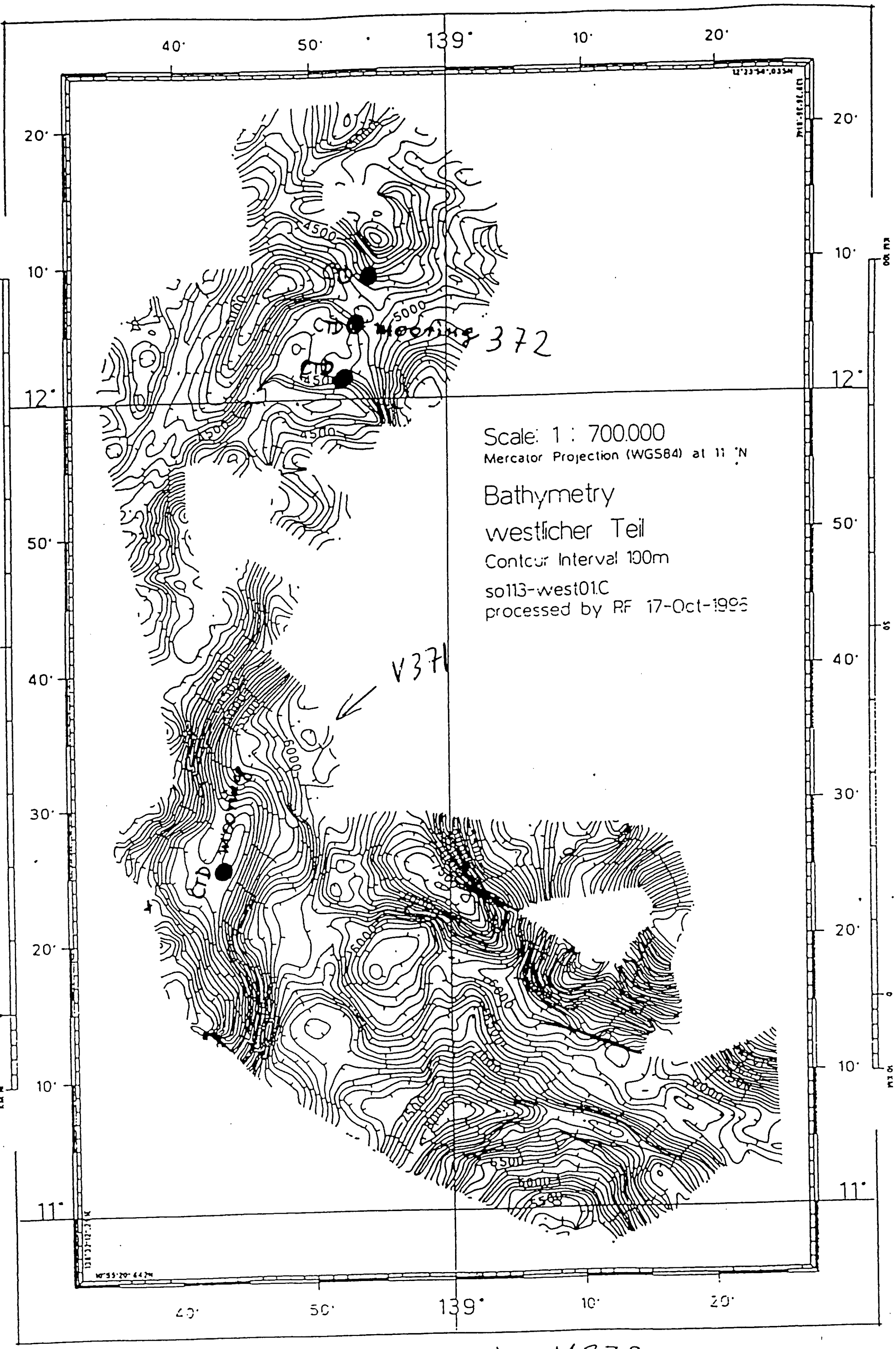

mooring V372
V371

Fig U3

UTC+10 | UTC +9

Einsatz-tiefe in m	Bodenab-stand in m	Reck in %	Ist-Länge in m	Gerätetyp und Nr.:	Rotor los	Gerät ins Wasser	Gerät aus dem Wasser	Rotor fest
622	4098		V	Senderschwim. S.Freq.: — Argos #: 5507		8:13	07:14	
652	4068		30	14xBenthos		8:16		
			60	10xBenthos				
712	4008		Aanderaa RCM 8	A-VTP 94	8:20	8:23	07:26	08.20
			60	Schallgeber Nr. 12		8:30		
772	3948			Blubb		8:33		
			100	6xBenthos		8:38		
912	3808		40	Blubb		8:40		
			100	Blubb		8:45		
			100	Blubb		8:49		
			100	Blubb		8:52		
			100					
			200					
		1200m+9%R = ca 1308m	200	Blubb		9:12	8.24	
			200					
		460m+9%R = ca500m	200					
			460	4xBenthos		10:15		
3220	1500		Aanderaa RCM 8	A-VTLA 10662	10:03	10:15	09:05	09:19
		460m+9%R = ca500m	460			10:33		
3720	1000	460m+9%R = ca 500m	Aanderaa RCM 8	A-VTA ~~11663~~ 11622	10:16	10:33	09:05	09:09
			460	4xBenthos		10:50		
4220	500		Aanderaa RCM 8	A-VTA 9728	10:34	10:50	09:20	09:20
		450m+10%R = ca 500m	200					
			200	4xBenthos		11:06		
4670	50		Aanderaa RCM 8	A-VTA 11617	10:50	11:06	09:32	09 40
			Oceano AT 661 RT 161	Ak.Auslöser Nr. 31 Nr. 729		11:07		
			0.75K	Std. dampfen		13:15		
			50					
			2.00K					
4720	00		1000KG					

Nirosta 8mm/Teylon

Perlon 11mm

Tiefe

● Schäkel-Ring-Schäkel ∞ Wirbel

Entwurf: D.Carlsen | Gezeichnet: D.Carlsen

Schiff/Expedition F.S. Sonne 113	Schiff/Expedition Hakuho Maru	Verankerungs Nr.: V 371 / MA
Auslegedatum 13.10.96	Aufnahmedatum 08.03.98	Institut für Meereskunde Kiel Physik
Protokollführer-in B.Klein	Protokollführer-in T M	Seegebiet: Pazifischer Ozean
Lottiefe 4726/4799 m (HS)	von Tiefe 06:22 UTC+9	Position: (Decca,GPS,) 11°25,65 N 138°43,60E
auf Tiefe 13.55	Zeitmeridian UTC = Bordzeit - 10 Std.	

Fig. 14

UTC +10 / UTC +9

Einsatz-tiefe in m	Bodenab-stand in m	Reck in %	Ist-Länge in m	Gerätetyp und Nr.:	Rotor los	Gerät ins Wasser	Gerät aus dem Wasser	Rotor fest
				Senderschwim. S.Freq.:27.035 Mhz		14:43		
3020 ~~1900~~	1600		0.75 K					
3070 ~~1950~~	1950		50	10xBenthos		14:46		
			50	8xBenthos		14:50		
3120 ~~2000~~	2000		Aanderaa RCM 8	A-VTP 12004	14:47	14:50	14:11	14:13
			460	3xBenthos		15:18		
3620 ~~2500~~	1000		Aanderaa RCM 8	A-VTA 9832	14:51	15:18	14:22	14:24
		460m+9% R = ca 500m	460	3xBenthos		15:41		
4120 ~~3000~~	500		Aanderaa RCM 8	A-VTA 9344	15:20	15:41	14:34	14:35
			200	4xBenthos		16:00		
		450m+10% R = ca 500m	200	A-VT 9730 AK.Auslöser Nr. 868	15:42	16:00	14:42	14:44
4570 ~~3450~~	50		Aanderaa RCM 8			16:00		
			Oceano RT161			16:21		
			0.75 K					
			50					
4620 ~~3500~~	00		2.00 K					
			950 KG					

Perlon 11mm

● Schäkel-Ring-Schäkel ∞ Wirbel

Entwurf: D.Carlsen | Gezeichnet: D.Carlsen

Schiff/Expedition F.S. Sonne 113	Schiff/Expedition Hakuho Maru	Verankerungs Nr.: V 372 / MB
Auslegedatum 14.10.96	Aufnahmedatum 08.03.98	Institut für Meereskunde Kiel Physik
Protokollführer-in S.Becker	Protokollführer-in T.J.M	Seegebiet: Pazifischer Ozean
Lottiefe 4618 m	von Tiefe 12:34 UTC+9	Position: (Decca,GPS,etc) 12°06,0N 138°53,1E
auf Tiefe 16.33	Zeitmeridian UTC = Bordzeit -10Std.	

Fig. 115

UTC +10 | UTC +11 UTC +11

Einsatz-tiefe in m	Bodenab-stand in m	Reck in %	Ist-Länge in m	Gerätetyp und Nr.:	Rotor los	Gerät ins Wasser	Gerät aus dem Wasser	Rotor fest
		1900	2300	Senderschwim. S. Freq.:27.035 Mhz		12:37		
1840 1950	2250		0,75 K 50	10xBenthos		12:40		
			50	8xBenthos		12:43		
1900 2000	2200		Aanderaa	A-VTP 12005	12:41	12:43	13:19	13:25
			460	3xBenthos		12:59		
2400 2500	1700		Aanderaa	A-VTA 9831	12:45	12:59	13:34	13:36
			RCM 8 460	3xBenthos		13:12		
2900 3000	1200		Aanderaa	A-VTLA 9820	12:59	13:12	13:45	13:52
			RCM 8 460	3xBenthos		13:39		
3400 3500	700		Aanderaa	A-VTLA 9313	13:13	13:39	13:57	14:02
		460m+9% R = ca 500m	RCM 8 460	3xBenthos		13:55		
3900 4000	200		Aanderaa	A-VTLA 9323	13:42	13:55	abgeschossen	
			RCM 8 100 30	4xBenthos		14:00	14:08	
		180m+10% R = ca 200m						
4040 4150	50		Aanderaa	A-VTA 11621	13:56	14:00		Signal Reflektor
			RCM 8 Oceano RT161	Ak.Auslöser 888		14:00	Tauch	
			0.75 K 50 2.00 K	1:42 Std. dampfen		15:42		
4096 4200	00		950 KG					

Perlon 11mm

● Schäkel-Ring-Schäkel ∞ Wirbel

Entwurf: D.Carlsen | Gezeichnet: D.Carlsen

Schiff/Expedition F.S. Sonne 113	Schiff/Expedition Hakuho Maru	Verankerungs Nr.: V 373 / MC
Auslegedatum 29.10.96	Aufnahmedatum 03.03.98	Institut für Meereskunde Kiel Physik
Protokollführer-in S. Becker	Protokollführer-in T/M	Seegebiet: Pazifischer Ozean
Lottiefe 4096-4091 m (IIS)	von Tiefe 12:12 UTC+11	Position: (Decca,GPS,etc) 06°14,5N 153°43,5E
auf Tiefe 16.03	Zeitmeridian UTC = Bordzeit - 10 Std.	

F.j. 116

UTC +10 | UTC + 10

Einsatz-tiefe in m	Bodenab-stand in m	Reck in %	Ist-Länge in m	Gerätetyp und Nr.:	Rotor los	Gerät ins Wasser	Gerät aus dem Wasser	Rotor fest
667 ~~692~~	4318			Senderschwim. S.Freq.: —— Argos #:		10:30		
697 ~~722~~	4288		30	14x~~Benthos~~		10:32		
			60	10xBenthos		10:37		
757 ~~782~~	4228		Aanderaa RCM 8	A-VTP 10077	10:34	10:37	13:08	13:11
			60					
817 ~~842~~	4168		Niro 8mm / Tevlon	Schallgeber 13		10:44		
957 ~~982~~	4028		100	Blubb		10:47		
			40	6xBenthos		10:50		
			100	Blubb		10:54		
			100	Blubb		10:57		
			100	Blubb		11:00		
			100	Blubb		11:04		
			100					
		1260m+9%R = ca1373m	100	Tow	Ausziehen			
			100					
			100	Blubb		11:19		
			200	Blubb		11:23		
			200					
			460	4xBenthos		11:50		
2830 ~~2855~~	2185		Aanderaa RCM 8	A-VTL 9727	11:27	11:50	14:15	14:20
		460m+9%R = ca 500m	460	4xBenthos		12:10		
3330 ~~3355~~	1655		Aanderaa RCM 8	A-VTA 9731	11:55	12:10	14:12	14:14
		460m+9% R = ca 500m	460					
				4xBenthos		12:30		
3830 ~~3855~~	1155		Aanderaa RCM 8	A-VTA 9732	12:25	12:30	14:37	14:40
		400m+10%R = ca 440m	200					
			200	3xBenthos		12:45		
4270 ~~4295~~	715		Aanderaa RCM 8	A-VTA 11618	12:43	12:45	14:50	14:51
			200					
		650m+10%R = ca 715m	200					
			100					
			100	3xBenthos		13:08		
4935 ~~4960~~	50		Oceano AT 661 RT 161	Ak.Auslöser Nr. 30 Nr. 889		13:08	15:15	/
			0.75 K	~		13:19	Ceil	
			50					
			2.00 K					
4985 ~~5010~~	00		1000 KG					

● Schäkel-Ring-Schäkel ∞ Wirbel

Entwurf: D.Carlsen | Gezeichnet: D.Carlsen

Schiff/Expedition F.S. Sonne 113	Schiff/Expedition Hakuho Maru	Verankerungs Nr.: V 374 / MD
Auslegedatum 27.10.96	Aufnahmedatum 04.03.1998	Institut für Meereskunde Kiel Physik
Protokollführer-in S.Becker	Protokollführer-in T J M	Seegebiet: Pazifischer Ozean
Lottiefe 4984 (HS)	von Tiefe 12:12	Position: (Decca,GPS,etc) 08°38,6N 150°56.9E
auf Tiefe 14.00	Zeitmeridian UTC = Bordzeit - 10Std.	

Fig. 47

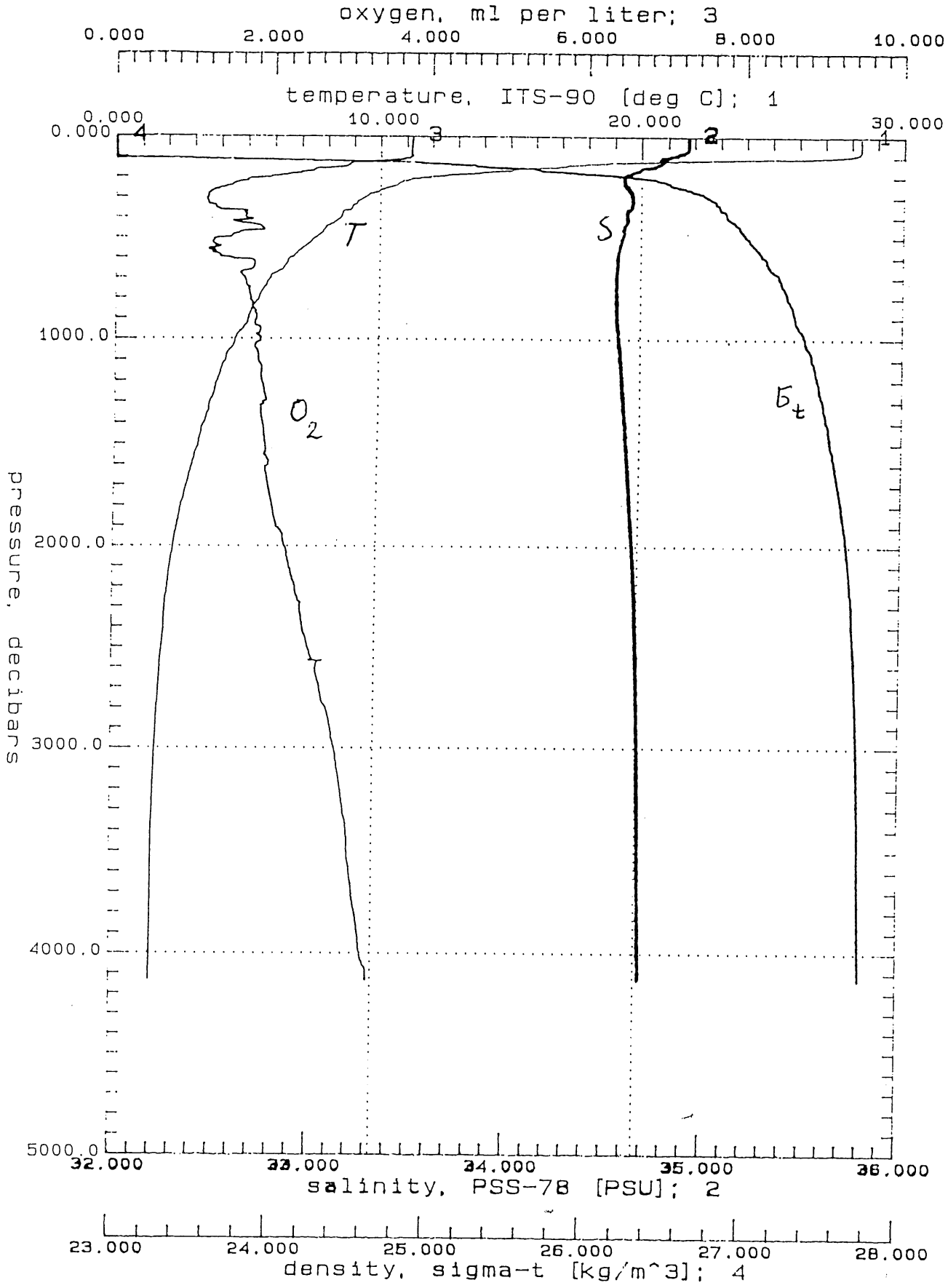

V37301.CNV: HAKUHO-MARU KH-98-1

Fig. 18

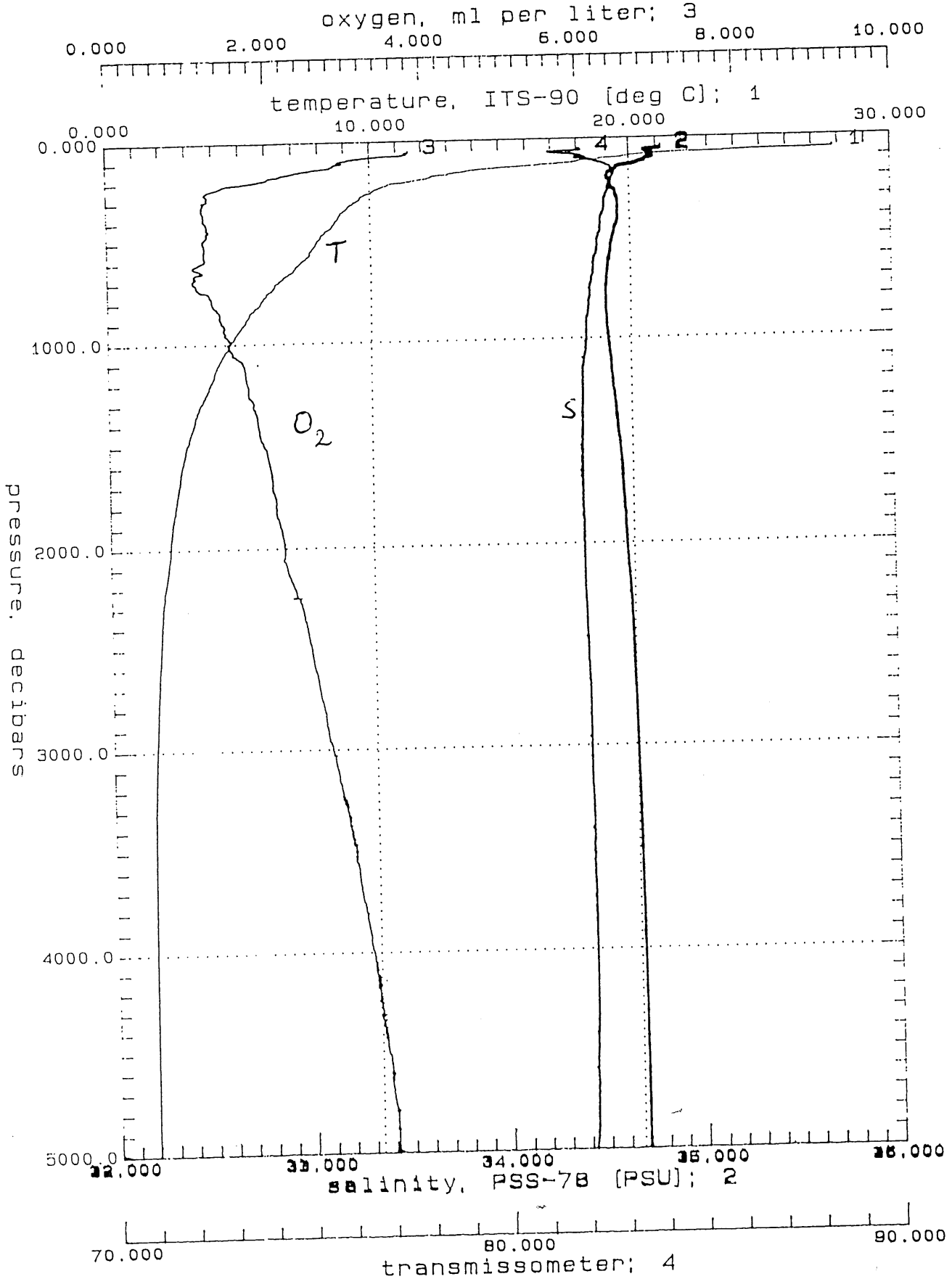

V374D.CNV: HAKUHO-MARU KH-98-1

Fig 49

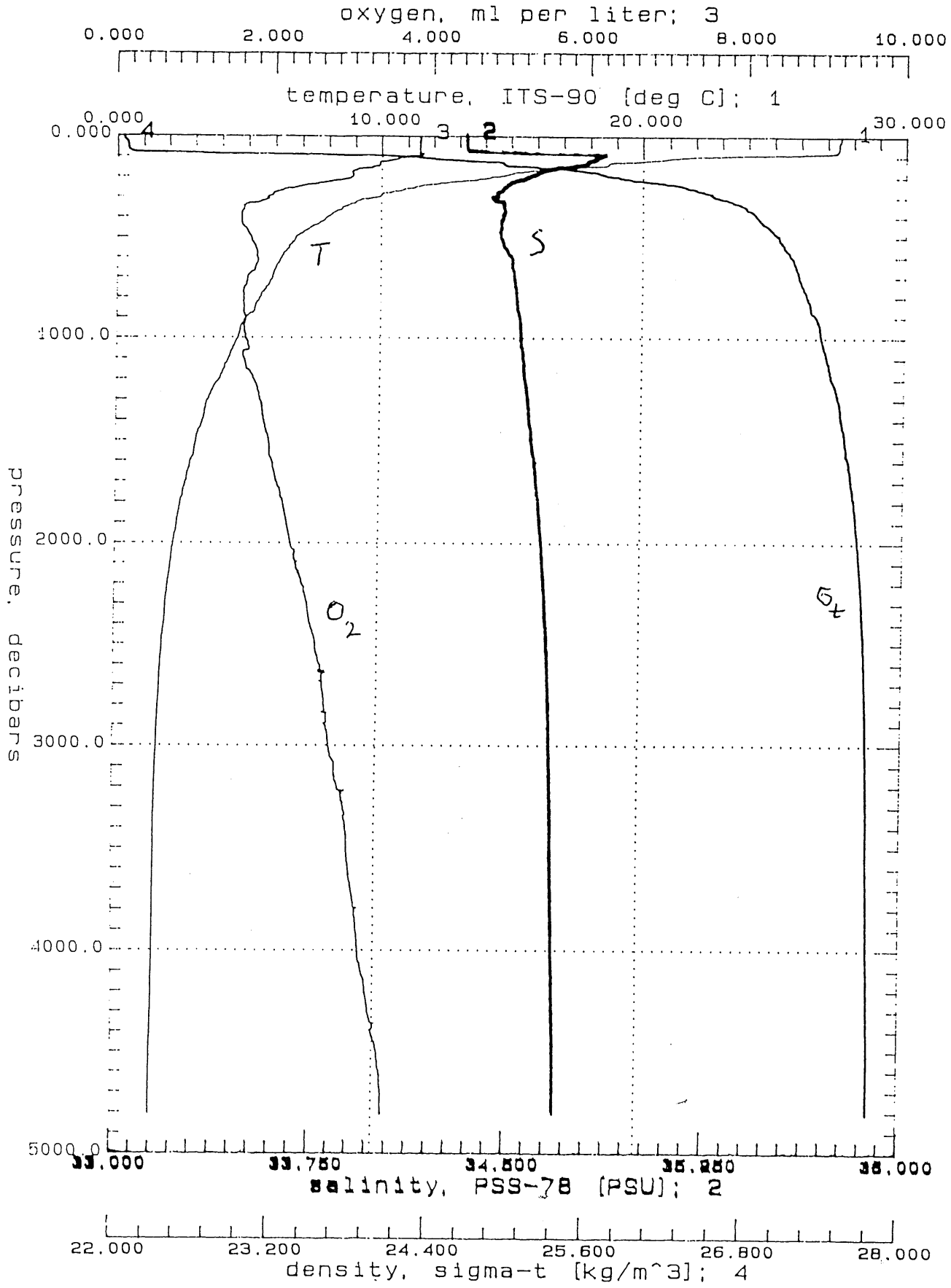

V372D.CNV: HAKUHO MARU KH-98-1

Fig. 10

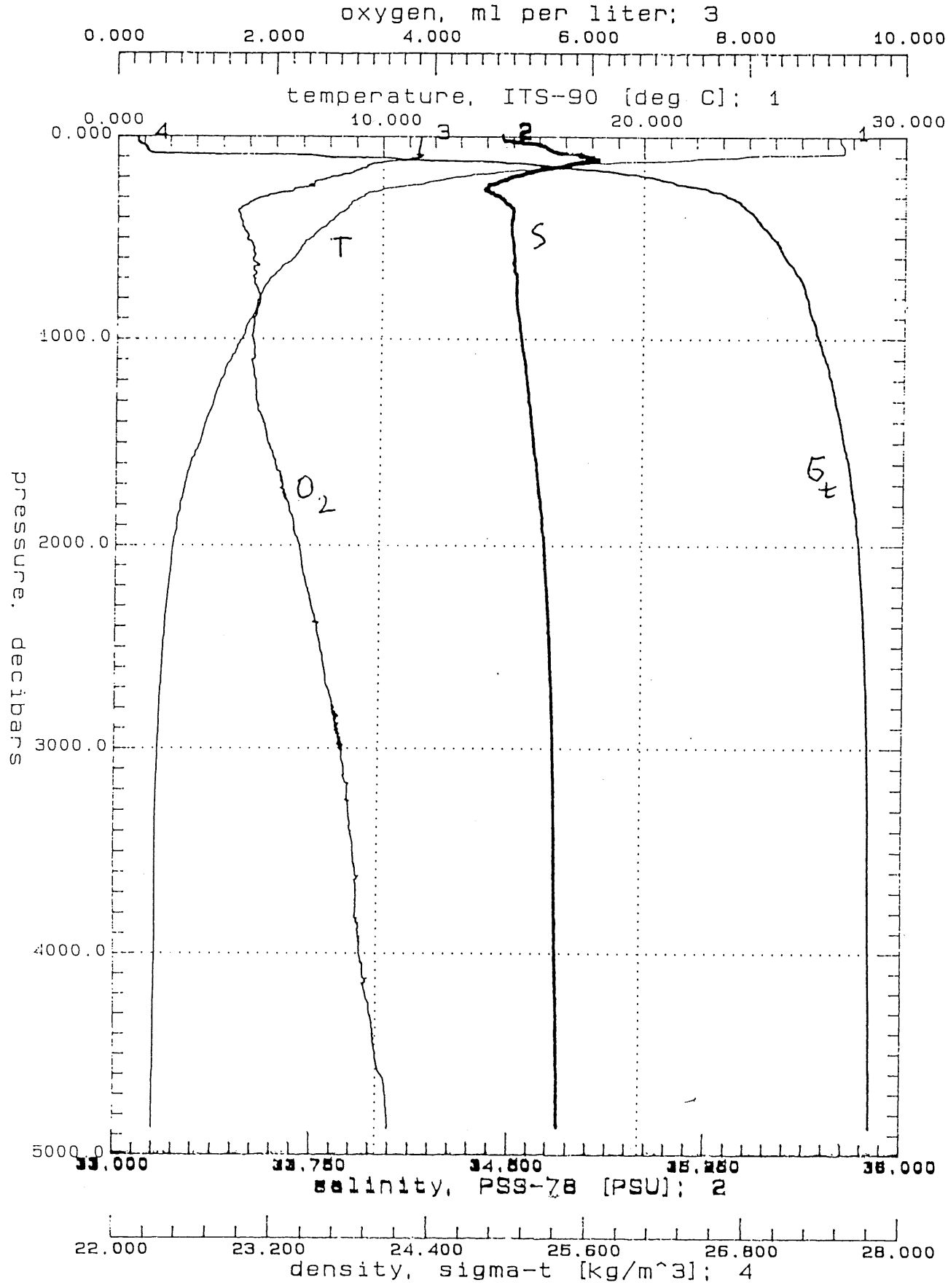

V371D.CNV: HAKUHO MARU KH-98-1

Fig 11

Seafloor Magnetotellurics of Western Pacific Upper Mantle - OBEM Study [Leg 3] -

Hiroaki TOH* and Tadanori GOTO**

*Ocean Research Institute, University of Tokyo, JAPAN
**Earthquake Research Instiute, University of Tokyo, JAPAN

1. Introduction

Three OBEM's were successfully retrieved during Leg 2 and Leg 3. Since nobody from Team OBEM joined Leg 2, the membres of Team OBS kindly completed the recovery of one instrument installed at the Ontong-Java Plateau (OJP). This report briefly summarizes what has been done in Leg 3 because other information such as the objectives, instruments and so on has already been included in the on-board report of Leg 1 (Toh and Nagaya, 1998).

2. Sea Experiment in Leg 3

Table 1 shows a summary of the recoveries conducted in Leg 2 and Leg 3. One of the three OBEM's deployed during Leg 1 was retrieved by Team OBS in Leg 2 without any difficulty except for a slight acoustic noise generated by ship's 3.5 kHz subbottom profiler. The remaining two OBEM's were recovered during Leg 3. Before recovering SFEMS, several acoustic rangings were measured to complement those conducted in Leg 1. They were:

Latitude (N)	Longitude (E)	Depth (m)	Slant Range (m)
9 44.87'	149 09.96'	5372	5658
9 44.82'	149 09.60'	5381	5424
9 44.93'	149 10.16'	5374	5838 (5476?)

Acoustic communication through ATM attached to SFEMS was also tried, which turned out impossible at distances farther than about two nautical miles. It was not until SFEMS came up around 3600 m depth that we're able to talk to the instrument. Furthermore, transmission of considerable amount of data could not be achieved due to frequent mistranslation of the transmitted characters. We succeeded in receiving time stamps and sending monitor-on/off commands. However, parameter readings often failed due to acoustic noises, not to mention to the data retrieval itself. This clearly outlined the limitations of the ATM presently adopted for SFEMS even with its maximum rate of 1200 baud as well as the inability of the on-board software controling the ATM. The ATM should be replaced by other ATM of higher performance in the future.

Recovery of OBEM-HD was done at the cost of one broken electrode arm due

to a little bit rough sea at the time of the night recovery. Clock drift of OBEM-HD was successfully measured as well as TT4 while that of SFEMS could not be conducted since SFEMS sent back time stamps in units of the sampling interval whenever tried.

3. Data

Figure 1 shows a sample plot of the EM data collected at OJP. Binary data stored in either SRAM's or flash memories of each instrument were dumped to a PC via serial connection at a rate of 9600 baud with an exception of the SRAM's equipped with a variograph of SFEMS. This may be due to a failure in an external current loop-RS232C converter. Anyway, the variograph data were also successfully dumped from a backup memory of other interface board. The dumped data were found to cover almost all the installation term as listed in Table 1 without any serious failure. Raw data expanded in ASCII format were corrected for spikes and jumps by pairs of UNIX shellscripts and FORTRAN source codes: (CORRECT, correct.f), (CORRECTG, correctg.f) and (CORRECTT, correctt.f & ave.f) after visual inspection. Quality of all the magnetic data is satisfactory especially for SFEMS which yielded not only temporal vector magnetic field by its variograph but also absolute measurements of the geomagnetic total force by its Overhauser proton precession magnetometer. (Its Hx-component, however, was often suffered from wrong bias correction as large as 409600 nT, which was easily corrected by subtraction.) Figure 2 compares the differences between synthetic geomagnetic total forces and respective absolute values. It is evident from the figure that the fluxgate-type variograph drifted as much as approximately 7 nT over 120000 samples, i.e., 0.167 nT/day. Deviations from the major trend may be attributed to incorrect scale factors of each axis of the variograph, which we assumed here as unity.

The most time consuming part of the data editing was electric field correction. Except for OBEM-HD, the electric fields were filled with many spikes and jumps. As for TT4, some of them may be due to bad electrodes attached to the specific instrument. First 1485 records of TT4 have been removed off due to overscale (> 10 mV) of Ex-component. Figure 3 shows their large self potentials and relatively high drift rates after recovery compared with those of SFEMS and OBEM-HD. However, it is unlikely that the noises can be attributed to the electrodes used in the case of SFEMS since they seem stable and have much less self potentials inbetween. Another possible reason for the noises is mischoice of the recording format. OBEM-HD performed 2-byte, viz., full recording of the electric field while SFEMS and TT4 did 1-byte, namely, differential recording for the sake of memory saving. This may lead to misrecording of the electric field if the temporal change of the field is too rapid to be within 40 μV/sample. Anyway, we think main objectives of this expedition can be attained by the data collected to this date since there're significant amount of good electric data even for SFEMS and TT4.

Acknowledgments

We're grateful to the crew membres of R/V Hakuho-Maru for their skillful help at the time of recovery. Our sincere thanks are also forwarded to the OBS group in Leg 2 and 3 that kindly offered a joint experiment with us.

REFERENCES

Toh, H. and Y. Nagaya, Seafloor Magnetotellurics of Western Pacific Upper mantle - OBEM study -, this issue, 1998.

Figure and Table Captions

Table 1 Summary table of the recoveries.

Fig. 1 Sample plot of Hy (top) and Ex (bottom) components.

Fig. 2 Difference between the synthetic and absolute geomagnetic total force.

Fig. 3 Electrode drift after recovery.

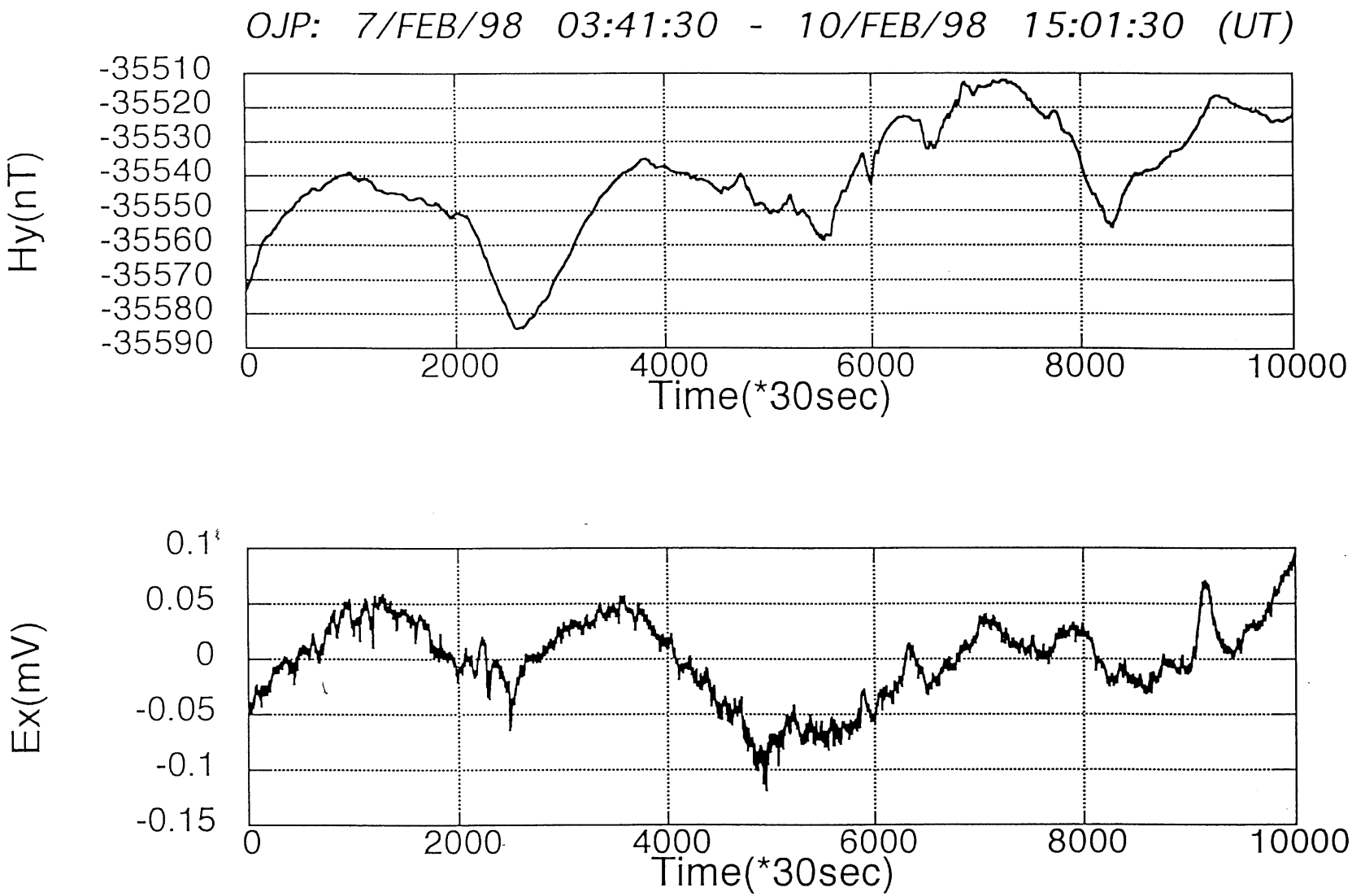
OJP: 7/FEB/98 03:41:30 - 10/FEB/98 15:01:30 (UT)
Hy(nT)
-35510
-35520
-35530
-35540
-35550
-35560
-35570
-35580
-35590
0
2000
4000
6000
8000
10000
Time(*30sec)
Ex(mV)
0.1
0.05
0
-0.05
-0.1
-0.15
0
2000
4000
6000
8000
10000
Time(*30sec)

Fig. 1

Table. 1

Apparatus	Recovery	Ascending Speed	Record Start	Record End	Sampling Rate	Sample Number	Unit	Timer Drift
TT4	24/Feb/'98 20:13 UT	---	26/JAN/'98 12:24:00 UT	24/Feb/'98 20:12:30 UT	30sec	84457	nT, mV/km, deg.	-3 sec / 37 days
SFEMS	05/Mar/'98 02:50 UT	29.9m/min (0.5m/sec)	22/JAN/'98 00:01:30 UT	04/Mar/'98 20:52:00 UT	30sec	120581	nT, mV/km, deg.	---
OBEM-HD	12/Mar/'98 18:50 UT	35.5m/min (0.6m/sec)	19/JAN/'98 00:01:30 UT	12/Mar/'98 13:05:00 UT	30sec	151327	nT, mV/km, deg.	+5 sec / 54 days

Fig. 2

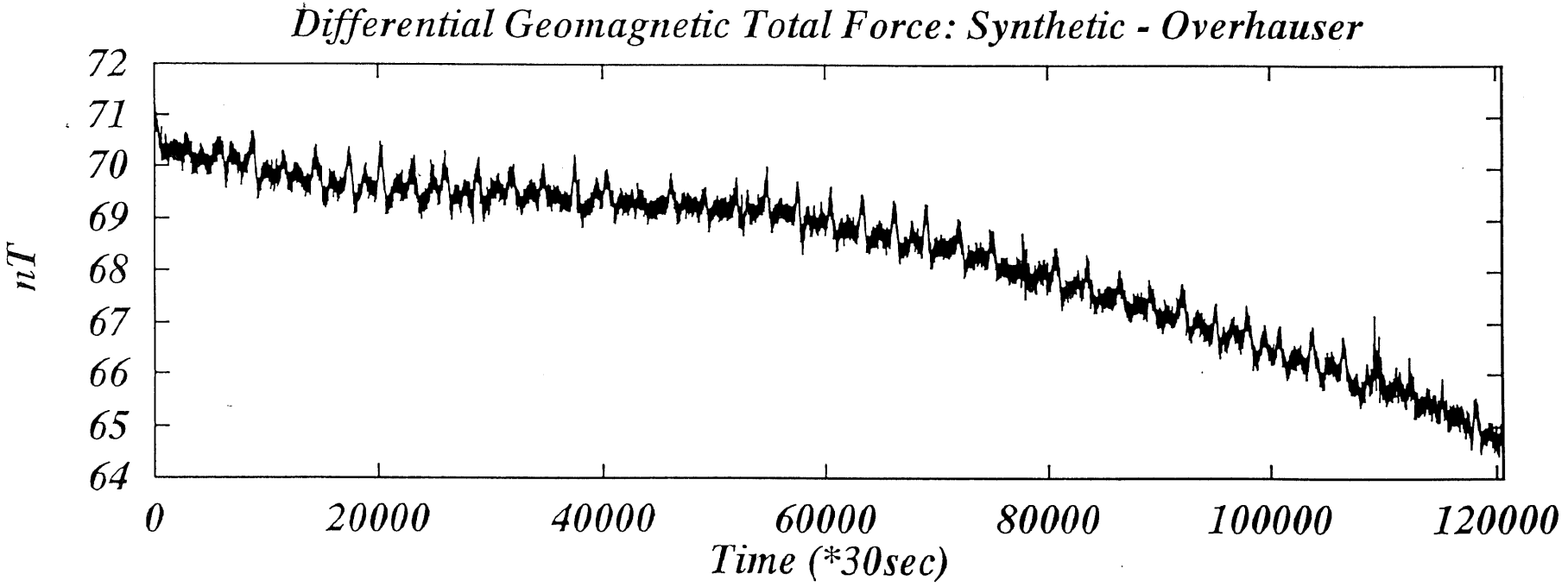

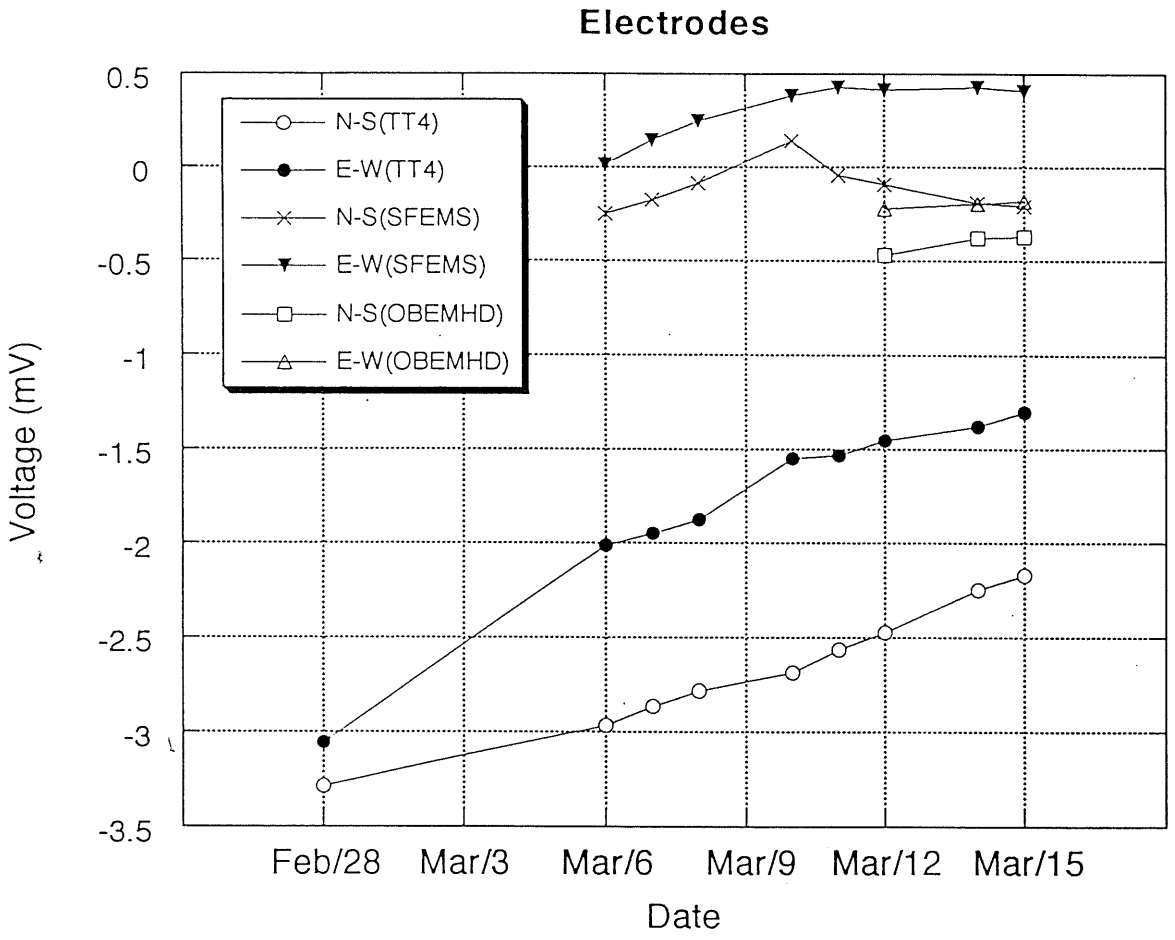
Electrodes
0.5
0
-0.5
-1
-1.5
-2
-2.5
-3
-3.5
Voltage (mV)
N-S(TT4)
E-W(TT4)
N-S(SFEMS)
E-W(SFEMS)
N-S(OBEMHD)
E-W(OBEMHD)
Feb/28
Mar/3
Mar/6
Mar/9
Mar/12
Mar/15
Date

Fig. 3

Petrological studies on the geological cross section exposed along the Southern Mariana trench inner wall during KH98-1 (Leg3) cruise.

Ishii, Haraguchi, Hirata, Hayasaka, Maejima, Sato, Taniguchi, Masuda, Yamanaka and Nishio

Inner trench wall of the Southern Mariana shows very steep slope with about 600 km wide having an EWE strike and a southward dip of about 12°-15° (Fig. 1), which is much steeper locally than along the northern to middle part of the Mariana trench. The depth of the escarpment extends from 4000 m to more than 10000 m, up to about 11000 m deep at the Challenger Deep (10915 m ?), assumed as the deepest trench in the world. The steep escarpment and deep trench could be induced by the oblique subduction of the Pacific Plate underneath the Philippine Sea Plate, that is, the trench trend is nearly parallel to the plate motion vector and is dominated today by strike-slip motion.

It can be assumed that the escarpment is a huge fault plane, if so outcrops of a series of the geological cross section including upper mantle, lower crust and upper crust for the island-arc system with back-arc spreading may be observed along the escarpment with about 600 km wide. The system includes the West Mariana Ridge (remnant arc) - Mariana Trough (back arc basin) - Mariana Arc (active arc + remnant arc) - Mariana Forearc - Mariana Trench from the west to the east.

Many topographic highs are recognized along the Izu-Ogasawara-Mariana forearc region (Fryer et al., 1985, Tayler and Smoot, 1984). A number of igneous rocks including lavas (boninitic rocks and arc-type rocks), gabbroes and serpentinized peridotites; so called ophiolitic rocks were dredged and drilled from those sea mounts by several investigators (Bloomer 1983, Ishii 1985, Ishii et al., 1992). Ophiolitic rocks were also reported from some dredge sites along the Southern Mariana inner wall (Bloomer and Hawkins, 1983, Ishii et al., 1993). Those rocks were originated from the upper parts of the mantle wedge including the overlying crustal materials.

Box type chain-bag dredges (TIORI-type) were prepared for KH98-1 Cruise. The assembles of the dredges used during KH98-1 Cruise are illustrated in Figs. 1-1 and -2, showing main wire, heavy chain (with attached heavy weight and small pipe dredge), fuse wire (with attached parallel life wire) and the main chain-bag dredge.

Main wire : installed winch wire of the R/V Hakuho-maru for scientific observation. It is piano wire of 14 mm diameter, 15000 m long, 0.815 kg weight per one meter (i.e. about 7 ton for 10000 m in the sea water) and having a 16.9 ton breaking strength.

Heavy chain : heavy chain (18 mm diameter, 5 m long and 25 kg weight) is used to stabilize the dredge assemblage and was joined to the main wire with a 3 ton swivel and shackles. Three weights (200 kg weight and two 50 kg pipe dredge type weights) were moreover linked to the heavy chin to add additional stability and provide additional possible sampling.

200 kg weight : the weight is used to assure the dredge is on the bottom as can be observed by the tension meter in the operation room, and was linked by shackles to the heavy chain together with a 1 ton swivel, fuse wire (8 mm diameter, 25 cm long) and life wires (8 mm diameter, 100 cm long).

50 kg weight (=small pipe dredge type weight) : this pipe dredge (50 kg weight, 30 cm diameter and 50 cm long) serves both as a stabilizing weight and common small dredge. It was also linked to the heavy chain in the same manner as the 200 kg weight, as shown in Fig. 1-1.

Fuse wire : fuse wire (8 mm diameter, 25 cm long and a 2.5 ton breaking strength) was prepared to release the dredge from big bites that might damage the main wire. It was jointed to the heavy chain with a 3 ton swivel and shackles in the dredge assemblages. In the case of the TIORI-type dredge, however, two additional fuse wires (8 mm diameter, 50 cm and 100 cm long) were connected as shown in Fig. 1-2, so that the TIORI-type dredge can be hauled toward the different direction by the second fuse wire if the first fuse wire is broken due to anchoring. The third fuse wire is designed to work in the same manner as the second fuse wire should, if the second fuse wire was broken. The change in hauling direction can hopefully release the dredge from bites

that might damage the main wire and anchoring.

Life wire : one end of the life wire (10 mm diameter, 7 m long, 3.9 ton breaking strength) is connected parallel with fuse wires and another end is linked with one winding at the upper middle part of the chain-bag. The life wire is designed to close and recover the chain-bag dredge with rock samples secured in the lower part of the chain-bag in the case all fuse wires are broken by a big bite or anchoring.

The TIORI type dredge(=box chain-bag dredge) is an improved design of the Norwalk type box chain-bag dredge, by Teruaki ISHII, Ocean Research Institute, University of Tokyo. As shown in Fig.1-1, it consists of box type jaw (60 x 45 cm mouth, 60 x 27 cm throat, 16 cm deep) having a steel handle (26 mm diameter, 85 cm long) and a steel chain-bag (6 mm diameter, 100 cm long) with a stainless steel (5 mm thick) box type bucket (27 x 60 x 50 cm). The bucket can recover all kinds of geological samples including soft sediments, sands, pebbles and large rocks. It was jointed with shackles to the 25 cm fuse wire together with the second (50 cm long) and the third (100 cm long) fuse wires as mentioned above.

Four dredge sites KH98-1D01, D02, D03 and D04 were selected in the Southern Mariana trench inner wall as shown in Table 1 and Fig. 2. Five dredge hauls were carried out in the Mariana Trough (see Masuda et al. in this volume). Additional two dredge sites KH98-1D10 and D11 were selected in the Ogasawara forearc as shown in Table 1 and Fig. 3.

The outline of the dredge hauls are shown in the followings.

References :

Bloomer, S. H. 1983. JGR

Bloomer, S. H., and Hawkins, J. W., 1983. Gabbroic and ultramafic rocks from the Mariana Trench: an island arc ophiolite. *In* Hayes, D.E. (Ed.), *The Tectonic and Geologic Evolution of Southeast Asian Seas and Islands: Part II*: Am. Geophys. Union, Geophys. Monogr. Ser., 27:294-317.

Fryer, P., Ambos E. L., and Huson D. M., 1985. Origin and emplacement of

Mariana forearc sea mounts. *Geology,* 13:774-777.

Ishii, T., 1985. Dredged samples from the Ogasawara fore-arc seamount or "Ogasawara Paleoland" - "fore-arc ophiolite". *In* Nasu, N., Kushiro, I., et al. (Eds.), *Formation of Active Ocean Margins.*: Tokyo (Terra Scientific Publ. Co.), 307-342.

Ishii, T., Robinson, P. T., Maekawa, H., and Fiske, R., 1992. Petrological studies of peridotites from diapiric serpentinite seamounts in the Izu-Ogasawara-Mariana forearc, Leg 125. *In* Fryer, P., Pearce, J. A., and Stokking, L. B. (Eds.), *Proc. ODP, Init. Repts.,* 125 (Scientific Results): College Station, TX (Ocean Drilling Program),125, xxx-yyy.

Ishii, T., Segawa, J., 1993. Dredged rocks during KH92-1 cruise from . In Segawa, J., (Ed.), Preliminary Report of the Hakuho Maru Cruise KH92-1, aaa-bbb.

Taylor, B., and Smoot, N. C., 1984. Morphology of Bonin fore-arc submarine canyons. *Geology,* 12:724-727.

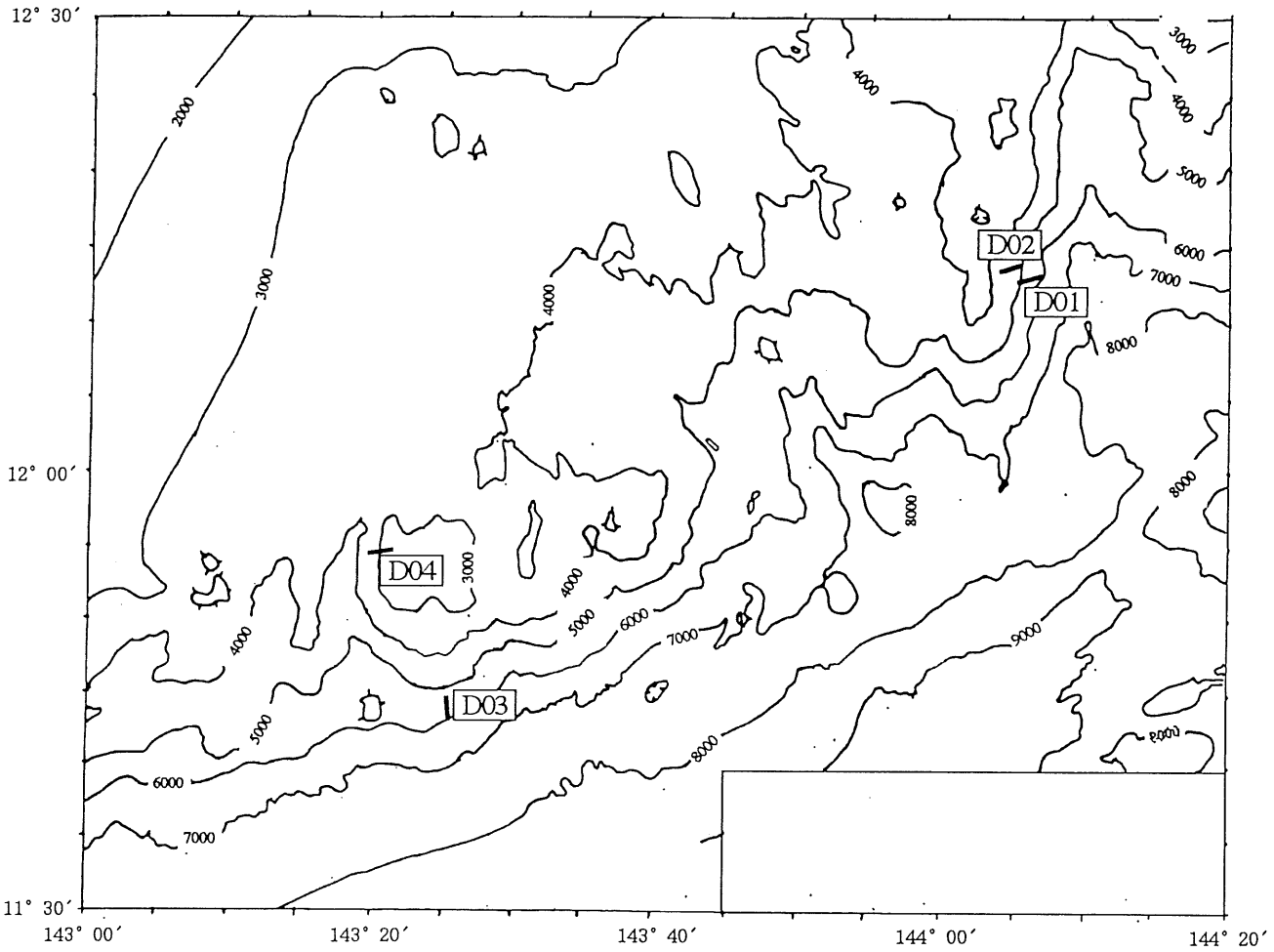
12° 30′
12° 00′
11° 30′
143° 00′
143° 20′
143° 40′
144° 00′
144° 20′
D01
D02
D03
D04
2000
3000
4000
5000
6000
7000
8000
9000

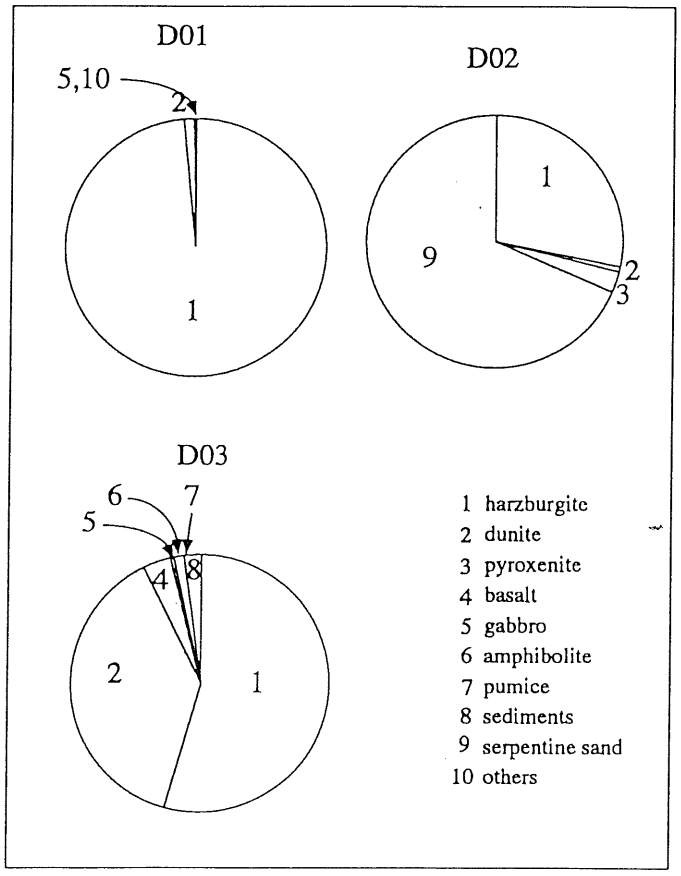
D01
5,10
2
1
D02
1
9
2
3
D03
6
7
5
4
8
2
1
1 harzburgite
2 dunite
3 pyroxenite
4 basalt
5 gabbro
6 amphibolite
7 pumice
8 sediments
9 serpentine sand
10 others

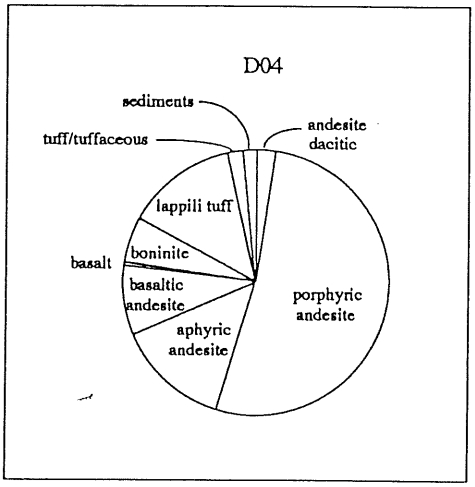
D04
sediments
tuff/tuffaceous
andesite
dacitic
lappili tuff
basalt
boninite
basaltic andesite
aphyric andesite
porphyric andesite

Fig 2

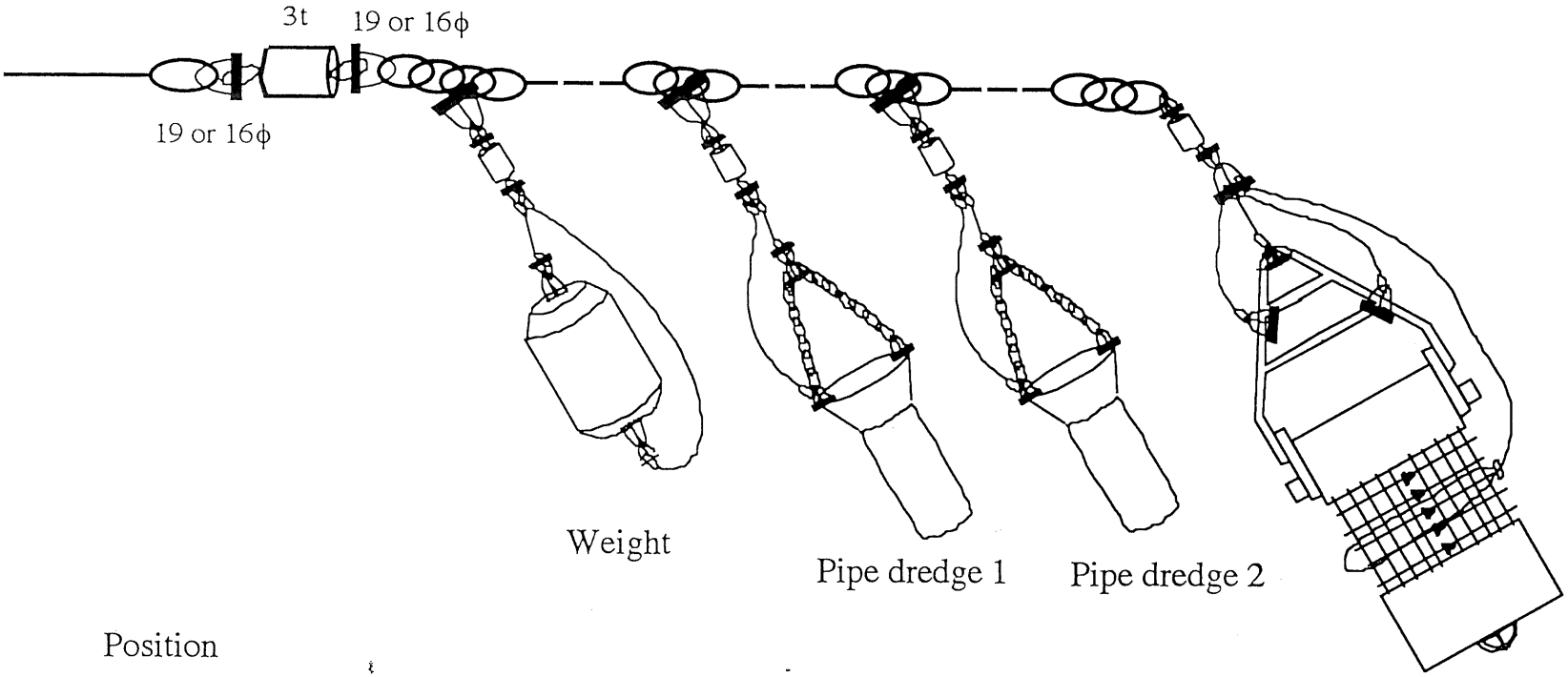
3t
19 or 16ϕ
19 or 16ϕ
Weight
Pipe dredge 1
Pipe dredge 2
Main dredge

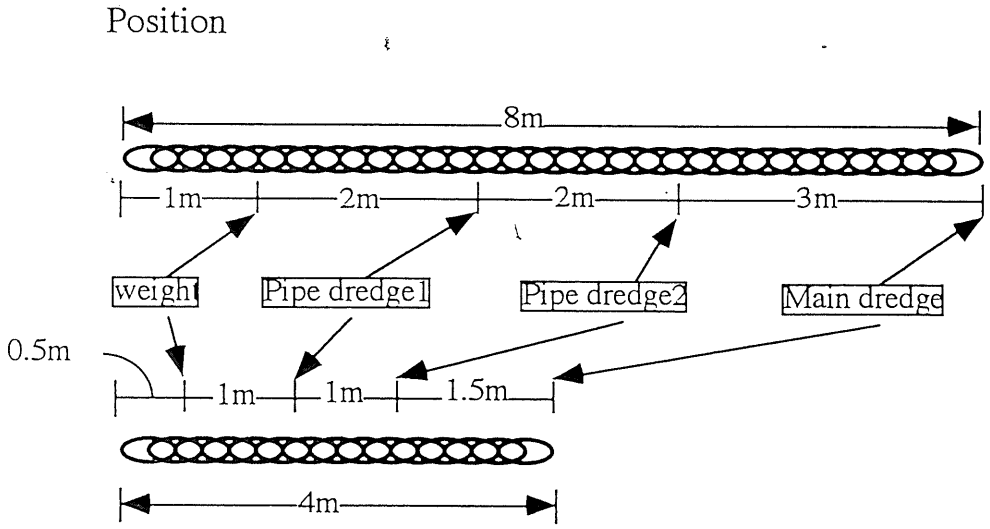
Position
8m
1m
2m
2m
3m
weight
Pipe dredge1
Pipe dredge2
Main dredge
0.5m
1m
1m
1.5m
4m

Fig 1-1

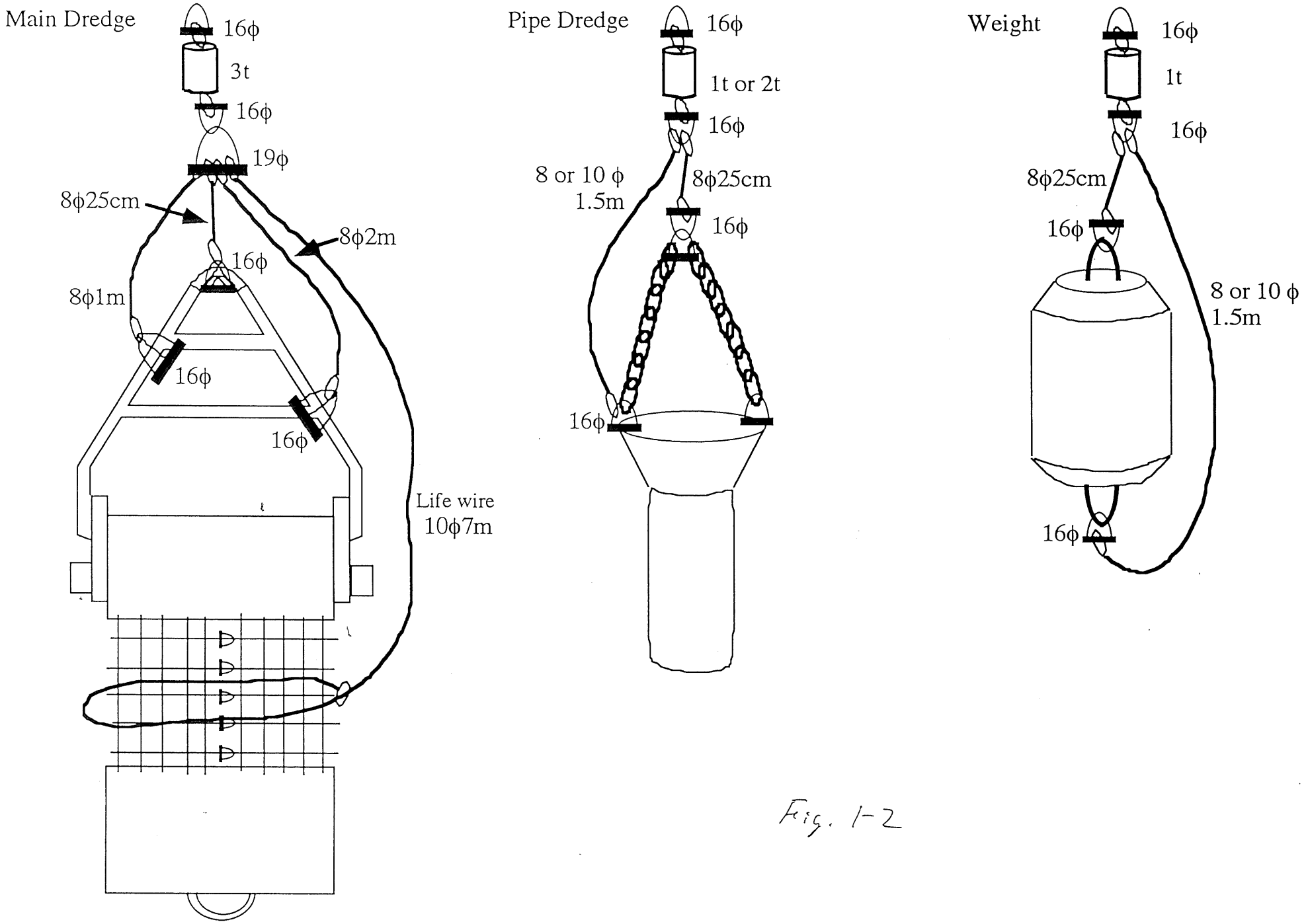
Main Dredge
16ϕ
3t
16ϕ
19ϕ
8ϕ25cm
8ϕ2m
16ϕ
8ϕ1m
16ϕ
16ϕ
Life wire
10ϕ7m
Pipe Dredge
16ϕ
1t or 2t
16ϕ
8 or 10 ϕ
1.5m
8ϕ25cm
16ϕ
16ϕ
Weight
16ϕ
1t
16ϕ
8ϕ25cm
16ϕ
8 or 10 ϕ
1.5m
16ϕ

Fig. 1-2

DREDGE LOG

Date 6 Mar. '98 Ship Hakuhō-maru Cruise KH98-1 Station D01

Location Southwest of the Guam Island

Weather fine Wind _____ Sea Calm

Bottom Topography _____

Type of Dredge Norwalk type dredge Add. Wt. 400 kg

Time lowered 9 h 40 m

Uncorr. Water Depth 6265 m

Initial Time on Bottom 11 h 29 m

Uncorr. Water Depth 5843 m Corr. Water Depth _____ m

Wier Length 5880 m Wire Angle _____ °

Ship Position Lat. 12°13.07N Long. 144°06.38E

Direction of haul _____ ° Ship Speed _____ kt (till h m)

Speed Wire in 12 m/min (from 12h45m) Winch No. 1

Final Time on Bottom 13 h 26 m

Uncorr. Water Depth 5388 m Corr. Water Depth _____ m

Wier Length 5525 m Wire Angle _____ °

Ship Position Lat. 12°13.20N Long. 144°05.60

Time surfaced 14 h 38 m

Condition of Haul _____

Dredged Materials _____

Directed by _____

DREDGE LOG

Date 6 Mar. '98 Ship Hakuhō-maru Cruise KH98-1 Station D2

Location Southwest of the Guam Island

Weather fine Wind _____ Sea Calm

Bottom Topography _____

Type of Dredge Norwalk type dredge Add. Wt. 400 kg

Time lowered 15 h 37 m

Uncorr. Water Depth 5979 m

Initial Time on Bottom 17 h 39 m

Uncorr. Water Depth 4880 m Corr. Water Depth _____ m

Wier Length 5160 m Wire Angle _____ °

Ship Position Lat. 12°15.83N Long. 144°05.19E

Direction of haul _____ ° Ship Speed _____ kt (till h m)

Speed Wire in 12 m/min (from 18h32m) Winch No. 1

Final Time on Bottom 19 h 24 m

Uncorr. Water Depth 4292 m Corr. Water Depth _____ m

Wier Length 4637 m Wire Angle _____ °

Ship Position Lat. 12°15.64N Long. 144°04.64E

Time surfaced 20 h 23 m

Condition of Haul _____

Dredged Materials _____

Directed by _____

DREDGE LOG

Date 6 Mar. '98 Ship Hakuhō-maru Cruise KH98-1 Station D3

Location Southwest of the Guam Island

Weather fine Wind _____ Sea Calm

Bottom Topography

Type of Dredge Norwalk type dredge Add. Wt. 400 kg

Time lowered 23 h 44 m

Uncorr. Water Depth 5986 m

Initial Time on Bottom 1 h 26 m

Uncorr. Water Depth 6016 m Corr. Water Depth _____ m

Wier Length 6053 m Wire Angle _____ °

Ship Position Lat. 11°43.'66N Long. 143°26.'46E

Direction of haul _____ ° Ship Speed _____ kt(till h m)

Speed Wire in 12 m/min (from 2 h 57 m) Winch No. 1

Final Time on Bottom 3 h 10 m

Uncorr. Water Depth 5123 m Corr. Water Depth _____ m

Wier Length 6040 m Wire Angle _____ °

Ship Position Lat. 11°45.'35N Long. 143°26.'25E

Time surfaced 4 h 31 m

Condition of Haul

Dredged Materials

Directed by

DREDGE LOG

Date 7 Mar. '98 Ship Hakuhō-maru Cruise KH98-1 Station D04

Location Southwest of the Guam Island

Weather fine Wind _____ Sea Calm

Bottom Topography

Type of Dredge Norwalk type dredge Add. Wt. 400 kg

Time lowered 5 h 47 m

Uncorr. Water Depth 3337 m

Initial Time on Bottom 6 h 50 m

Uncorr. Water Depth 3239 m Corr. Water Depth _____ m

Wier Length 3279 m Wire Angle _____ °

Ship Position Lat. 11°53.'89N Long. 143°20.'15E

Direction of haul _____ ° Ship Speed _____ kt(till h m)

Speed Wire in 12 m/min (from 7 h 59 m) Winch No. 1

Final Time on Bottom 9 h 04 m

Uncorr. Water Depth 2289 m Corr. Water Depth _____ m

Wier Length 2301 m Wire Angle _____ °

Ship Position Lat. 11°53.'96N Long. 143°21.'98E

Time surfaced 9 h 35 m

Condition of Haul

Dredged Materials

Directed by

DREDGE LOG

Date 13 Mar '98 Ship Hakuhō-maru Cruise KH98-1 Station D10

Location East of the Haha-jima Island

Weather Cloudy and Rainy Wind W 10 m/s Sea rough

Bottom Topography mud

Type of Dredge Norwalk type dredge Add. Wt. 400 kg

Time lowered 14 h 47 m

Uncorr. Water Depth 2578 m

Initial Time on Bottom 15 h 36 m

Uncorr. Water Depth 2569 m Corr. Water Depth ____ m

Wier Length 2781 m Wire Angle 0 °

Ship Position Lat. 26°30.24N Long. 142°39.43E.

Direction of haul ____ ° Ship Speed 1.0 kt (till 15 h 38 m)

Speed Wire in 12 m/min (from 16 h 38 m) Winch No. 1

Final Time on Bottom 17 h 18 m

Uncorr. Water Depth 2010 m Corr. Water Depth ____ m

Wier Length 2404 m Wire Angle ____ °

Ship Position Lat. 26°30.13N Long. 142°37.65E.

Time surfaced 17 h 54 m

Condition of Haul

Dredged Materials

Directed by

DREDGE LOG

Date 13 Mar '98 Ship Hakuhō-maru Cruise KH98-1 Station D11

Location East of the Haha-jima Island

Weather Rainy Wind W 10 m/s Sea rough.

Bottom Topography

Type of Dredge Norwalk type dredge Add. Wt. 400 kg

Time lowered 19 h 17 m

Uncorr. Water Depth 1988 m

Initial Time on Bottom 20 h 06 m

Uncorr. Water Depth 1988 m Corr. Water Depth ____ m

Wier Length 2015 m Wire Angle ____ °

Ship Position Lat. 26°43.11N Long. 142°40.65E.

Direction of haul 90 ° Ship Speed 1.0 kt (till 20 h 31 m)

Speed Wire in 12 m/min (from 21 h 12 m) Winch No. 1

Final Time on Bottom 20 h 37 m

Uncorr. Water Depth 1814 m Corr. Water Depth ____ m

Wier Length 1945 m Wire Angle 30 °

Ship Position Lat. 26°43.06N Long. 142°~~44~~. 42.88E.

Time surfaced 22 h 06 m

Condition of Haul

Dredged Materials

Directed by

Sample No.	Diameter L	M	S	Round-ness	Wt. (g)	Mn-coating	Lithology & Remarks
D01-001	270	200	140	0.30	7900	n.	tectonized harzburgite strongly serpentinized of its peripheral zone.
002	210	85	80	0.20	2650	n.	tectonized harzburgite serpentinized of its peripheral zone, serpentine vein, saussuritized plagioclase.
003	130	110	80	0.20	1970	n.	tectonized harzburgite serpentinized of its peripheral zone, serpentine vein.
004	140	120	70	0.20	1480	n.	serpentinized harzburgite. Opx; bastite, strongly serpentinized of its peripheral zone.
005	170	90	30	0.20	690	n.	tectonized harzburgite strongly serpentinized of its peripheral zone.
006	90	60	60	0.20	460	n.	serpentinized harzburgite, weakly serpentine veins developping.
007	130	80	30	0.20	420	n.	tectonized harzburgite, altered strongly of its peripheral zone. saussuritized plagioclase.
008	120	50	30	0.20	390	n.	serpentinized harzburgite. Opx; bastite.
009	100	80	30	0.20	270	n.	serpentinized tectonized harzburgite. serpentine vein developping.
010	90	70	50	0.20	365	n.	serpentinite orginally harzburgite.
011	70	50	40	0.20	170	n.	tectonized harzburgite. Opx; bastite, saussuritized plagioclase.
012	80	50	40	0.20	100	n.	strongly altered (talc?) harzburgite. Pseudomorphic texture
013	70	40	25	0.20	90	n.	strongly altered (talc?) harzburgite. Pseudomorphic texture
014	60	30	25	0.20	115	n.	tectonized harzburgite.
015	55	50	30	0.30	110	n.	tectonized harzburgite. serpentine veins.
016	60	40	30	0.30	95	n.	tectonized harzburgite. serpentine veins.
017	50	40	35	0.20	90	n.	serpentinized harzburgite.
018	50	35	30	0.30	95	n.	serpentinized harzburgite, saussuritized plagioclase.
019	40	40	30	0.30	85	n.	serpentinized harzburgite. serpentine veins, bastite texture.
020	60	40	40	0.30	95	n.	altered harzburgite. serpentine vein.
021	70	50	40	0.30	95	n.	serpentinized harzburgite.
022	100	50	30	0.20	100	n.	serpentinite originally dunite.
023	55	45	30	0.20	65	n.	serpentinite originally harzburgite.
024	50	35	30	0.20	50	n.	strongly serpentinized tectonized harzburgite.
025	50	35	30	0.20	75	n.	serpentinized harzburgite.
026	30	30	30	0.20	35	n.	strongly altered (talc?) serpentinite originally harzburgite.
027	50	40	25	0.20	55	n.	serpentinized harzburgite.
028	40	30	25	0.20	40	n.	strongly altered (talc?) serpentinite originally harzburgite.
029	40	35	25	0.20	40	n.	serpentinized harzburgite.
030	40	30	15	0.20	25	n.	serpentinized harzburgite.
031	35	30	20	0.20	25	n.	strongly altered (talc?) serpentinite originally harzburgite.
032	35	30	25	0.20	30	n.	serpentinized harzburgite.
033	55	40	25	0.20	35	n.	strongly altered (talc?) serpentinite originally harzburgite.
035	35	25	30	0.20	20	n.	serpentinized harzburgite. saussuritized plagioclase.
036	30	30	15	0.20	20	n.	serpentinized harzburgite.
037	40	25	20	0.20	15	n.	strongly altered (talc?) serpentinite originally harzburgite.
038	50	25	15	0.20	15	n.	serpentinized harzburgite. serpentinite of its peripheral zone.
039	35	25	15	0.20	15	n.	serpentinized harzburgite. serpentine veins.
101	35	25	10	0.20	15	n.	talc.
102	25	20	8	0.20	2	n.	talc.
201	50	30	15	0.20	20	n. to f.	dorelite.
202	30	25	15	0.40	10	n.	microgabbro.
301					1020		pebbls of ultramafic rocks.
302					340		mud.
D02-001	150	140	50	0.40	1650	n.	serpentinized harzburgite with serpentine veins.
002	170	80	40	0.20	820	n.	weakly serpentinized harzburgite.
003	130	80	55	0.40	1080	n.	weakly serpentinized harzburgite.
004	160	90	80	0.30	1100	n.	weakly serpentinized harzburgite.
005	130	75	45	0.30	520	n.	weakly serpentinized harzburgite, strongly serpentinized of its peripheral zone.
006	80	70	60	0.40	390	n.	serpentinized orthopyroxenite.
007	95	80	70	0.40	540	n.	serpentinized harzburgite.
008	85	50	30	0.30	150	n.	serpentinized harzburgite.

Sample No.	Diameter L	M	S	Round-ness	Wt. (g)	Mn-coating	Lithology & Remarks
D02-009	65	55	25	0.30	100	n.	serpentinite.
010	70	55	45	0.20	230	n.	serpentinized dunite and harzburgite.
011	70	55	35	0.30	220	n.	serpentinized harzburgite.
012	100	80	40	0.20	340	n.	serpentinized harzburgite, serpentine veins.
013	90	50	40	0.30	230	n.	orthopyroxenite, serpentine veins of its peripheral zone.
014	75	50	35	0.20	135	n.	serpentinized harzburgite.
015	60	40	30	0.20	100	n.	serpentinized harzburgite.
016	70	45	45	0.40	170	n.	serpentinized harzburgite.
017	45	40	40	0.40	150	n.	serpentinized harzburgite.
018	60	40	25	0.20	80	n.	serpentinized harzburgite.
019	85	40	16	0.20	45	n.	serpentinized dunite.
020	55	40	25	0.30	70	n.	serpentinized dunite, strongly peripheral zone.
021	40	35	25	0.30	40	n.	serpentinized harzburgite.
022	50	30	12	0.20	30	n.	serpentinized harzburgite.
023	60	30	25	0.20	40	n.	serpentinized harzburgite.
024	40	25	25	0.20	30	1.5 mm	serpentinized harzburgite.
025	35	27	25	0.20	25	n.	serpentinized harzburgite.
026	40	25	15	0.20	20	n.	serpentinized harzburgite.
027	27	17	13	0.20	5	n.	serpentinized harzburgite.
028	20	15	12	0.20	5	n.	serpentinized harzburgite.
051					6300		serpentine sand.
052					7200		serpentine sand.
053					6050		serpentine sand.
054					5100		serpentine sand.
055					2150		serpentine sand.
D03-001	260	200	160	0.20	11500	n.	serpentinized dunite (to harzburgite?).
002	320	210	110	0.30	12500	f.	serpentinized tectonized harzburgite.
003	260	200	190	0.30	9900	f.	serpentinized layered harzburgite ((two?) Pyroxene layer of 1 cm).
004	190	150	130	0.30	4500	f.	serpentinized tectonized harzburgite.
005	220	120	100	0.20	2400	f.	serpentinized harzburgite.
006	150	110	100	0.30	2150	n.	serpentinized tectonized harzburgite.
007	180	160	80	0.20	1150	f.	serpentinized harzburgite.
008	190	160	80	0.20	1850	f.	serpentinized dunite.
009	140	140	45	0.30	1230	f.	serpentinized harzburgite (weakly tectonized).
010	140	100	80	0.30	1350	f.	serpentinized harzburgite (containing layter stage of talc ? veins).
011	120	90	70	0.20	940	f.to 0.1	serpentinized dunite.
012	160	90	80	0.30	1300	n. to f.	serpentinized dunite containing pyroxene layers.
013	130	80	80	0.20	920	n.	serpentinized harzburgite (shear fracture of serpentine).
014	100	90	65	0.30	860	n.	serpentinized tectonized harzburgite.
015	140	100	40	0.30	630	f.	serpentinized harzburgite.
016	120	90	50	0.30	820	f.	serpentinized harzburgite (weakly tectonized).
017	140	95	40	0.30	590	f.	serpentinized dunite.
018	130	80	60	0.20	890	f.	serpentinized tectonized harzburgite.
019	120	85	65	0.30	680	f.	serpentinized tectonized harzburgite.
020	140	70	50	0.20	700	f.	serpentinized harzburgite.
021	100	90	50	0.20	685	f.	serpentinized tectonized harzburgite.
022	100	90	80	0.20	770	f.	serpentinized dunite.
023	110	85	50	0.20	430	f.	serpentinized harzburgite.
024	100	60	55	0.30	490	f.	serpentinized tectonized harzburgite.
025	100	75	65	0.35	390	n.	serpentinized dunite.
026	90	75	55	0.40	440	f.	serpentinized dunite.
027	95	70	60	0.40	360	f.	serpentinized dunite.
028	130	70	55	0.30	500	n. to f.	serpentinized dunite.
029	110	70	60	0.30	430	f.	serpentinized dunite, later stage of veins.
030	80	75	60	0.40	340	n. to f.	serpentinized dunite, later stage of veins.
031	110	100	30	0.20	300	f.	serpentinized harzburgite.
032	80	70	60	0.30	360	f.	serpentinized harzburgite.
033	190	120	70	0.30	1800	f.	serpentinized harzburgite, tectonite layering of pyroxene.
034	170	120	80	0.30	1900	f.	dunite with small vein of serpentine, olivine shows mesh texture.

Sample No.	Diameter L	M	S	Round-ness	Wt. (g)	Mn-coating	Lithology & Remarks
D03-035	140	120	80	0.40	1220	f.	tectonized dunite with altered olivine. olivine turn to iddingsite.
036	140	120	80	0.40	1480	3 mm	serpentinized harzburgite with magnetite.
037	140	110	80	0.30	1320	n.	dunite, olivine with mesh texture.
038	130	90	70	0.40	1020	3 mm	weakly tectonized serpentinized harzburgite.
039	110	100	60	0.30	1180	f.	serpentinized harzburgite weakly tectonized.
040	120	80	70	0.40	1030	1 mm	serpentinized harzburgite tectonite
041	120	110	65	0.40	950	f.	serpentinized harzburgite tectonite
042	200	100	50	0.20	1200	f.	serpentinized dunite
043	110	70	60	0.30	730	f.	serpentinized dunite tectonite. olivine (2.5x1.5 cm) kinked
044	100	90	70	0.30	810	f.	serpentinized dunite tectonite.
045	130	90	70	0.30	850	f.	serpentinized dunite
046	90	90	70	0.40	880	2 mm	serpentinized dunite
047	130	70	65	0.40	750	n.	serpentinized dunite
048	100	70	70	0.30	520	f.	dunite tectonite (serpentinized)
049	120	85	60	0.30	530	1 mm	serpentinized harzburgite
050	100	70	60	0.30	450	1 mm	serpentinized dunite tectonite
051	90	70	60	0.40	400	f.	serpentinized dunite
052	75	75	50	0.30	300	f.	serpentinized dunite
053	100	80	50	0.30	370	f.	serpentinized dunite
054	115	60	40	0.30	410	n.	serpentinized dunite
055	140	70	30	0.20	380	n.	serpentinized dunite
056	90	60	40	0.40	340	1 mm	serpentinized dunite
057	80	70	65	0.40	360	f.	serpentinized dunite with xenolith of harzburgite
058	110	90	50	0.40	350	f.	altered serpentinized dunite
059	100	75	40	0.40	300	1 mm	serpentinized dunite
060	65	55	55	0.60	280	f.	serpentinized dunite
061	70	65	50	0.60	250	n.	serpentinized dunite
062	80	60	50	0.40	290	2 mm	serpentinized dunite
063	95	65	30	0.20	300	f.	serpentinized dunite
064	100	75	50	0.20	330	n.	serpentinized dunite (brecciated)
065	80	50	45	0.40	110	n.	serpentinized harzburgite with serpentine vein
201	120	90	70	0.40	1000	f.	weakly foliated two pyroxene basalt. plagioclase lass than 10 %. pyroxene average 1~2 mm
202	120	90	70	0.40	800	n.	amphibolite. amphibole 6x4 mm in diameter.
203	120	90	60	0.30	750	3 mm	olivine pyroxene basalt. olivine pseudomorph, py 0.2~0.3 mm
204	110	100	65	0.30	650	n.	aphyric basalt with serpentine vein.
205	90	60	50	0.40	300	f.	olivine pyroxene gabbro, highly altered
206	110	70	25	0.20	300	n.	amphibole pyroxene (Opx) gabbro
207	60	60	60	0.30	250	n.	plagioclase pyroxene basalt. intersertal? neddle 4 mm in diameter.
208	60	35	35	0.20	200	n.	hornblende pyroxene gabbro. hlb; 6x7 mm, px; 4x4 mm
209	40	30	20	0.40	150	n.	amphibolite
210	95	55	35	0.20	250	n.	gneissose amphibole gabbro
301	130	110	95	0.30	980	f.	conglomerate of serpentinized dunite
401	80	65	40	0.40	130	n.	layered pumice
411					140		pebbles of pumice
D04-001	300	220	220	0.30	18100	n. to f.	Andesite, Px poor, Pl common, weakly altered, Zeolite in cavity.
2	330	230	140	0.20	9800	f.	Andesite, Px poor, Pl common, glassy, weakly altered, Pl 2.5mm, Zeolite in cavity.
3	280	250	140	0.40	4700	f.	Px andesite, Pl common, max. 1.5mm, Px rich, max. 3mm.
4	200	190	120	0.30	4850	f.	Ol bearing basaltic andesite, weakly to medium altered, glassy.
5	270	190	140	0.20	6750	f.	Ol bearing basaltic andesite, Pl rich 1mm, glassy.
6	200	170	140	0.30	4500	f.	Boninite? Pl rare, pores, nearly aphiric.
7	170	170	90	0.40	3500	f.	Andesite, Px 1.5mm common, Pl rich, max. 1mm, patchy altered.
8	160	110	100	0.40	2350	f.	Ol, two Px andesite, altered Ol iddingsite, phyric.
9	190	130	120	0.40	2700	n. to f.	Nearly ophitic andesite, Pl poor, glassy and porous.
10	170	140	110	0.40	2650	f.	(Boninite?) andesite, Ol rare, Px rich 2mm, Pl rare.

Sample No.	Diameter L	M	S	Round-ness	Wt. (g)	Mn-coating	Lithology & Remarks
D04-11	120	120	110	0.30	1500	f.	Ol bearing basaltic andesite, weakly to medium altered.
12	160	120	100	0.40	1470	f.	Px andesite, Cpx rich, max. 4mm, Pl 3mm, Groundmass bluish gray.
13	130	90	70	0.40	1000	f.	Ol bearing andesite, Pl rich, max. 4mm.
14	140	110	100	0.40	1350	f.	Andesite, Pl rich, max. 4mm, patchy cavity, Groundmass heterogeneous.
15	150	90	80	0.20	1000	f.	Andesite, Px rare, Pl common, max. 1.5mm, partly cavity, Groundmass patchy heterogeneous.
16	170	100	90	0.20	1200	f.	Andesite, Px rare to none, Pl rich max.3mm. Groundmass heterogeneous, white vein.
17	140	100	90	0.20	1430	f.	Boninite? aphyric andesite, glassy and porous, zeolite in cavity.
18	140	130	100	0.40	1100	f.	Aphyric andesite, Pl poor, max. 1.5mm, Gm heterogeneous (boninite?).
19	140	100	80	0.30	940	f.	Boninite or aphyric andesite, glassy and porous.
20	180	140	90	0.40	2320	f.	Greenish altered andesite, Pl common, max. 3mm, Xenolith including.
21	130	100	70	0.40	1280	a little f.	Andesite, Ol, Px poor to rare, Pl common, max. 2mm, glassy porous.
22	140	110	80	0.40	1310	a little f.	Px andesite, Px poor to common, Pl rich, max.5mm, greenish vein.
23	150	120	80	0.30	1600	a little f.	Px andesite, Px common, max. 2mm, Pl common, max.2.5mm, Gm heterogeneous.
24	170	130	90	0.30	2650	a little f.	Nearly aphyiric andesite, Px rare, Pl poor, max. 1.5mm,Gm patchy heterogeneous.
25	180	130	100	0.30	2050	f.	Ol bearing nearly aphyric andesite, glassy and porous.
26	120	110	80	0.40	1650	f.	Px andesite, Px common to poor, max. 1mm, Pl very rich, max. 2.5mm, glassy and a little porous.
27	130	90	90	0.30	1190	a little f.	Px andesite, Px poor, max. 0.7mm, Pl common, max. 1mm, glassy and porous.
28	150	150	70	0.30	1260	f.	Andesite, Px poor to rare, Pl rich, max. 2mm, porous, glassy, weakly altered.
29	100	90	70	0.30	615	f.	Andesite, Px poor to rare, zeolite in cavity, Pl common, max. 2mm, glassy,well altered.
30	120	100	90	0.40	990	f.	(Ol bearing?) Px andesite, Px max. 1mm, Pl poor, max. 1.5mm, glassy, weakly altered.
31	100	100	60	0.40	710	f.	Px andesite, Px poor, max. 1mm, Pl very rich, max. 3mm, Gm greenish, medium altered.
32	220	70	70	0.20	610	f.	Andesite, Px rare to none, Pl rich, max. 3mm, altered, white vein.
33	90	80	60	0.40	410	f.	Px andesite, Px common to rich, max. 3mm, Pl common 3mm, weakly altered.
34	100	80	50	0.40	495	a little f.	Andesite, Px rare to none, Pl common, max. 3mm, glassy, patchy porous.
35	120	70	70	0.30	750	f.	Px andesite, Px common, max. 1.5mm, Pl common, max. 3mm, Gm heterogeneous, weakly altered.
36	90	70	50	0.40	375	f.	Andesite, Px rare to none, Pl very rich, max. 4mm, dusty, Gm heterogeneous.
37	100	80	40	0.40	420	f.	Px andesite, Px common, max. 0.7mm, Pl common max. 2.5mm, Gm light gray.
38	110	80	70	0.30	480	f.	(Ol bearing?) Px andesite, Px very rich, max.6mm, Pl rich, max. 5mm, weakly altered.
39	100	70	60	0.60	345	n.	Px andesite, Px common, max. 0.5mm, Pl rich, max.4mm, medium altered.
40	120	100	40	0.20	295	f.	(Ol bearing?) Px andesite, Px poor, Pl common, max. 2mm, well altered, red vein.
41	110	80	40	0.20	290	f.	Px andesite, Px common, max. 2.5mm, Pl rich, max. 3mm, well altered, secondary mineral rich.
42	80	80	50	0.30	340	n.	Px andesite, Px common to poor, max. 2mm, Pl rich, max. 1mm, a little porous, alittle altered.

Sample No.	Diameter L	M	S	Round-ness	Wt. (g)	Mn-coating	Lithology & Remarks
D04-43	90	60	60	0.40	440	f.	Px andesite (or tuff?) Px common,max. 1.5mm, Pl rich, max. 2mm, glassy, Gm patchy heterogeneous.
44	130	90	60	0.20	430	f.	(Nearly aphyric) andesite, Px very poor, max. 1mm, Pl poor, max. 2mm, altered, Gm greenish gray.
45	90	60	45	0.30	420	2mm	Px andesite, Px common, max. 1mm, Pl rich, max. 3mm. a little glassy, reddish brown vein.
46	105	65	60	0.30	570	n.	Px andesite, Px common, max. 3mm, Pl rich, max. 3mm, Gm heterogeneous, partly weakly altered.
47	110	80	45	0.30	380	f.	Px andesite, Px rich(15 to 20%), max. 2.5mm, Pl very rich(30%), max. 3mm, Gm heterogeneous, weakly altered.
48	110	70	45	0.30	405	f.	Px andesite, Px poor to common, max. 1.5mm, Pl rich, max. 2.5mm, a little porous, white vein 3mm.
49	100	70	60	0.20	380	f.	Px andesite, Px poor, max. 0.7mm, Pl poor to common, max. 2mm, glassy, Gm a little heterogeneous.
50	100	60	50	0.20	410	f.	Px andesite, Px common, max. 1.5mm, Pl common to rich, max. 2.5mm, glomeroporphyritic texture including.
51	105	105	90	0.40	1250	n. to f.	Px andesite, Px poor, max. 1mm, Pl rich(30%), max. 6mm, Gm glassy, partly altered.
52	100	75	65	0.30	680	n. to f.	Andesite, Px rare to poor, max. 1mm, Pl common, max. 2mm, Gm hetereogeneous.
53	110	90	50	0.30	720	n. to f.	(Ol bearing?) Px andesite, Px common, max. 1.5mm, Pl rich(25 to 30%), dusty, max. 3mm, weakly altered.
54	90	90	40	0.40	550	n. to f.	Andesite, Px rare to poor, max. 1mm, Pl rich(25 to 30%), dusty, max. 2mm, glassy, weakly altered.
55	85	70	50	0.30	500	n.	Px andesite, Px poor to common, max. 1mm, Pl rich(30%), max. 8mm, dusty, Gm glassy, light gray.
56	90	80	35	0.30	570	n. to f.	Px andesite, Px common, max. 1.5mm, similar to No.55.
57	100	70	40	0.40	505	n. to f.	Px andesite, Px common, max. 1mm, Pl common, max. 1mm, glassy, medium altered.
58	80	80	45	0.40	500	n.	Ol bearing Px andesite, Ol iddingsite, Px common, max. 1mm, Pl rich(30%), max. 8mm. Gm altered.
59	90	65	50	0.40	360	n.	Andesite, Px rare to poor, max. 0.5mm, Pl rich(20 to25%), max. 3mm, Gm glassy, altered.
60	80	65	55	0.40	450	n.	Andesite, similar to No. 59. more porous, zeolite in cavity.
61	75	70	45	0.40	385	n.	Px andesite, Px poor, max. 0.7mm, Pl common, max. 4mm,dusty, Gm heterogeneous.
62	70	60	60	0.40	340	n.	Px andesite, Px common, max. 1mm, Pl rich(25%), max. 4mm, dusty, Gm glassy.
63	65	50	50	0.40	395	n.	Andesite, similar to No.59, Gm heterogeneous,partly porous.
64	80	75	40	0.40	295	f.	Andesite, similar to No.59, Gm a little porous, glassy.
65	95	65	50	0.40	360	n.	Andesite, similar to No.59, Px poor to common, Pl dusty, max. 5mm, secondary minaral in cavity.
66	70	60	40	0.40	190	n. to f.	Px andesite, Px common, max. 1mm, Pl rich(20%), max. 3mm, Gm weakly altered, granular, glassy.
67	70	60	35	0.40	220	n. to f.	Andesite, Px poor, max. 1.5mm, Pl common, dusty, max. 3mm, Gm altered, glassy.
68	80	50	40	0.40	255	f.	Andesite, Px poor, max. 1mm, Pl common to rich(15 to 20%), max. 8mm, dusty, Gm glassy heterogeneous.
69	70	60	50	0.40	215	n. to f.	Px andesite, Px common, max. 1mm, altered, Pl rich(25 to 30%), max. 4mm, dusty, Gm glassy, porous.
70	85	50	50	0.30	185	n. to f.	Px andesite, Px poor to common, max. 1mm, Pl rich(30%), max. 8mm, dusty, Gm glassy, weakly altered.
71	60	50	40	0.40	200	n. to f.	Andesite, Px rare to poor, Pl rich(30%), max. 5mm, dusty, Gm glassy, porous, heterogeneous.
72	60	55	25	0.30	125	f.	Andesite, Px rare to poor, altered, Pl rich(20% to 25%), max. 6mm, dusty, Gm glassy.
73	85	55	50	0.40	340	n. to f.	Andesite, Px poor, max. 1mm, alittle porous, Pl rich(30%), max. 10mm, dusty, Gm glassy.
74	70	45	35	0.30	225	n. to f.	Porous and glassy Px andesite and glassy andesite contact with white to gray quench glass zone(5mm).

Sample No.	Diameter L	M	S	Round-ness	Wt. (g)	Mn-coating	Lithology & Remarks
D04-75	60	40	40	0.30	160	n. to f.	(Px?) andesite, Px? common altered(green), Pl common, max. 2mm, tabular, altered.
76	70	40	30	0.25	145	n. to f.	(Ol bearing?) Px andesite, Px poor, max. 0.7mm, Pl common, max. 1.5mm, Gm altered.
77	50	40	40	0.30	140	f.	Andesite, Px poor to rare, Pl rich(30%), max. 6mm, dusty, Gm heterogeneous, weakly altered.
78	60	50	40	0.30	175	n. to f.	Nearly aphyric andesite, Px poor, max. 7mm, Pl poor, max. 3mm, dusty, glassy, partly porous.
79	70	60	30	0.40	220	n. to f.	Nearly aphyric andesite, similar to No.78, Pl poor (to common), partly altered.
80	70	60	30	0.30	225	half f.	Nearly aphyric andesite, similar to No.78, Pl poor (to common).
81	95	60	40	0.30	355	n. to f.	Nearly aphyric andesite, similar to No.78, Pl poor (to common), zeolite in cavity.
82	65	35	30	0.30	120	n. to f.	Nearly aphyric andesite, similar to No.78, Pl poor (to common), partly zeolite in cavity.
83	70	50	30	0.35	220	n. to f.	Px andesite, similar to No. 76, Ol none, Gm altered.
84	80	60	30	0.30	225	n. to f.	Nearly aphyric andesite, Pl poor (to common), max. 3mm, Gm similar to No. 83.
85	130	80	80	0.30	1300	n. to f.	Nearly aphyric to aphyric andesite (boninite?), Pl poor, max. 2mm, small and well vesiculated.
86	140	90	80	0.20	1180	f.	Nearly aphyric to aphyric andesite (boninite?), Gm heterogeneous.
87	110	80	70	0.30	1050	f.	Nearly aphyric to aphyric andesite (boninite?), Gm heterogeneous.
88	120	80	70	0.20	700	n. to f.	Nearly aphyric to aphyric andesite, Gm heterogeneous, Pl poor to common, max. 2mm, cavity rich.
89	120	80	70	0.30	900	n. to f.	Nearly aphyric to aphyric andesite (boninite?), Gm heterogeneous, clay mineral in cavity.
90	145	80	50	0.30	850	half f.	Px andesite, Px common, max. 2mm, altered, Pl common, max. 1.5mm, altered.
91	120	70	50	0.30	630	f.	Nearly aphyric to aphyric andesite (boninite?), Gm heterogeneous, partly clay mineral in cavity.
92	100	60	60	0.30	410	f.	Nearly aphyric to aphyric andesite (boninite?), Gm heterogeneous cavity rich.
93	110	100	50	0.40	530	n. to f.	Nearly aphyric to aphyric andesite, altered, Gm heterogeneous, Pl poor to common, clay mineral in cavity.
94	90	70	60	0.40	480	f.	Nearly aphyric to aphyric andesite (boninite?), Gm heterogeneous cavity rich.
95	80	60	55	0.20	320	f.	Nearly aphyric to aphyric andesite (boninite?), Gm heterogeneous, clay mineral in cavity.
96	95	55	50	0.30	390	f.	Nearly aphyric to aphyric andesite (boninite?), Gm heterogeneous, cavity common.
97	90	55	50	0.30	360	n. to f.	Nearly aphyric to aphyric andesite (boninite?), Gm heterogeneous.
98	90	55	40	0.30	300	n. to f.	Nearly aphyric to aphyric andesite (boninite?), Gm spherulitic heterogeneous.
99	70	60	40	0.30	300	n. to f.	Nearly aphyric to aphyric andesite (boninite?), Gm partly spherulitic heterogeneous.
100	75	70	50	0.40	340	n. to f.	Nearly aphyric to aphyric andesite (boninite?), Gm heterogeneous, partly clay mineral in cavity.
101	90	70	50	0.30	405	n. to f.	Nearly aphyric to aphyric andesite (boninite?), Gm partly spherulitic heterogeneous in cavity.
102	80	55	45	0.30	340	n. to f.	Nearly aphyric to aphyric andesite (boninite?), Gm heterogeneous.
103	65	40	40	0.30	320	poorly f. to n.	Px andesite, Px common, max. 2mm, altered, Pl poor, Mn? in cavity, altered.
104	90	55	40	0.40	310	poorly f.	Px andesite, Px poor, max. 1mm, altered, Pl rich, max. 3mm, small and well vesiculated.
105	80	50	40	0.30	295	n. to f.	Nearly aphyric to aphyric andesite (boninite?), Gm heterogeneous.
106	70	50	45	0.30	210	n. to f.	Andesite, Px rare, Pl rich(20 to 25%), max. 2mm, glassy, small and well vesiculated.
107	75	45	40	0.40	215	poorly f.	Nearly aphyric to aphyric andesite (boninite?), Gm partly spherulitic heterogeneous in cavity.

Sample No.	Diameter L	M	S	Round-ness	Wt. (g)	Mn-coating	Lithology & Remarks
D04-108	95	55	30	0.35	230	n. to f.	Nearly aphyric to aphyric andesite (boninite?), Gm heterogeneous around in cavity.
109	75	50	45	0.30	210	n. to f.	Nearly aphyric to aphyric andesite (boninite?), Gm partly spherulitic heterogeneous.
110	80	50	40	0.40	230	poorly f.	Nearly aphyric to aphyric andesite (boninite?), Gm partly spherulitic heterogeneous.
111	70	60	40	0.30	215	n. to f.	Nearly aphyric to aphyric andesite (boninite?), Gm heterogeneous, altered clay mineral in cavity.
112	60	45	45	0.40	165	f.	Nearly aphyric to aphyric andesite (boninite?), partly altered, Gm partly clay mineral in cavity.
113	80	65	40	0.40	215	f.	Px andesite, Px poor to common, max. 0.5mm, Pl rich(20%), max.1.5mm, very small and well vesiculated, glassy.
114	90	45	45	0.30	210	n. to f.	Nearly aphyric to aphyric andesite (boninite?), Gm heterogeneous, cavity poor, zeolite, chlorite, clay mineral in cavity.
115	145	90	80	0.35	1260	n.	Strongly altered dacitic andesite and alteredandesite, glassy, chlorite in cavity.
116	110	90	75	0.35	800	n.	Px andesite, Px common, max. 1.5mm Pl rich(25 to 30%), max. 2mm, glassy, altered, zeolite in cavity.
117	90	90	80	0.40	1100	n.	Px andesite, Px common, max. 2mm, Pl common, max. 4mm, dusty, weakly to medium altered.
118	100	75	70	0.40	670	f.	Ol bearing Px basaltic andesite, Px rich, max. 1mm, Pl common, max. 1.5mm, very small vesiculated, altered..
119	95	80	60	0.30	440	n. to f.	Px andesite, Px poor, max. 0.5mm, altered, Pl common, max. 3mm, dusty, chlorite, zeolite in cavity.
120	90	55	55	0.20	260	f.	Px andesite, Px rich, max. 2mm, Pl common, max. 2.5mm, dusty, glomeroporphiritic texture.
121	100	90	45	0.30	590	f. to 1mm	Nearly aphyric andesite, Px poor, Pl poor, max.2mm, Gm flow structure, weakly altered.
122	100	60	65	0.25	250	n. to f.	Aphyric to nearly aphyric andesite, Pl poor, max. 2mm. flow texture.
123	95	60	50	0.30	310	f. to 1mm	Andesite, Px poor to common, max. 1mm, altered, Pl poor, max.3mm, chlorite and clay mineral in cavity.
124	140	80	60	0.40	800	partly	Nearly aphyric andesite, Px poor, Pl poor, max. 3mm, dusty, zeolite in cavity.
125	125	85	70	0.35	810	f.	(Nearly aphyric) dacitic andesite, Px poor, Pl poor (to common), max. 2.5mm, Gm heterogeneous, weakly flow structure.
126	110	90	70	0.40	610	f.	Nearly aphyric dacitic andesite to dacite, Pl poor, max. 3mm, weakly altered.
127	100	80	70	0.20	415	n. to f.	Andesite, Px rare, Pl common, max. 2mm, reddish brown vein, max. 1.5mm, partly altered.
128	100	60	50	0.25	305	n. to f.	Andesite, Px common, max. 1mm, Pl common, max. 1.5mm, very small vesiculated.
129	95	75	60	0.25	370	f.	Nearly aphyric dacitic andesite to dacite, Pl poor, max. 4mm, dusty, Gm a little heterogeneous.
130	80	70	70	0.25	275	n. to f.	Nearly aphyric dacitic andesite to dacite, Px poor, max. 2mm, Pl poor, max. 3mm, fresh.
131	115	75	60	0.30	465	f. to 1mm	Nearly aphyric dacitic andesite to dacite, Pl common, max. 4mm, dusty, weakly altered.
132	85	70	55	0.30	420	f.	Px andesite, Px common, max. 2mm, Pl common to rich, max. 2.5mm; zeolite in vein, altered.
133	75	45	40	0.30	115	f.	Aphyiric dacitic andesite.
134	85	60	35	0.30	165	f.	Nearly aphyric dacitic andesite to dacite, Pl poor, max. 2mm, thin red and white vein.
135	65	55	40	0.30	110	f.	Nearly aphyric dacitic andesite to dacite, Pl common to poor, max. 3mm, Gm dark gray.
136	70	50	35	0.25	105	f.	Px andesite, Px common, max. 1mm, weakly altered, Pl common to rich, max. 1.5mm, very small vesiculated.
137	100	60	60	0.30	370	n.	Px andesite, Px common, max. 1mm, weakly altered, Pl common to rich, max. 1.5mm, very small vesiculated, altered.

Sample No.	Diameter L	M	S	Round-ness	Wt. (g)	Mn-coating	Lithology & Remarks
D04-138	90	70	40	0.25	270	n. to f.	Ol bearing Px andesite, Ol max. 1mm, Px common, max. 1mm, Pl common, max. 3.5mm. altered.
139	80	60	55	0.40	330	f. to 1mm	Ol bearing Px basaltic andesite, Ol max. 1mm, Px common, max. 1mm, Pl common, max. 2.5mm. altered.
140	80	80	60	0.35	445	n. to f.	Px andesite, Px poor to common, max.1mm, Pl common, max. 3mm, altered.
141	115	75	40	0.25	385	f. to 1mm	Px andesite, Px poor to common, 1.5mm, Pl common, max. 3mm, glassy, Gm heterogeneous.
142	95	60	40	0.40	260	n. to f.	Px andesite, Px poor, max. 1mm, Pl common 1.5mm, altered.
143	65	55	50	0.45	245	n. to f.	Px andesite, Px poor to common, max.1mm, Pl common, max. 3mm, small vesiculated, altered.
144	90	55	50	0.30	250	n. to f.	Px basaltic andesite, Px rich(20%), max. 6mm, Pl rich(30%), max. 4mm, small vesiculated, altered.
145	80	80	40	0.35	280	half f.	Px andesite, Px poor to common, 1.5mm, Pl common, max. 3mm, glassy, Gm reddish gray, altered.
146	95	65	60	0.20	280	n.	Px andesite, Px poor to common, 1.5mm, Pl common to rich, max. 4mm, dusty, glassy, Gm heterogeneous.
147	80	70	50	0.25	240	n. to f.	Px andesite, Px poor to common, 1.5mm, Pl rich(30%), max. 4mm, dusty, Gm heterogeneous.
148	80	70	50	0.30	275	n. to f.	Px andesite, Px poor, max. 0.7mm, altered, Pl very rich(35 to 40%), secondary mineral rich.
149	90	65	60	0.30	340	n. to f.	Px andesite, Px common, max. 2mm, Pl common to rich(15 to 20%), max. 3mm, glassy.
150	90	65	40	0.30	270	f.	Px andesite, Px poor to common, max.1mm, Pl poor, max. 3.5mm, weakly altered.
151	90	85	70	0.40	510	poorly f.	Andesite, Px poor, max. 1mm, Pl rich(25 to 30%), tabular, dusty, white and brown vein, max. 8mm.
152	85	70	60	0.40	480	n. to f.	Px andesite, Px common to rich, max. 4mm, Pl rich(25 to 30%), small vesiculated, glassy.
153	70	60	40	0.40	170	n. to f.	Andesite, Px poor, max. 0.5mm, Pl common, max. 1.5mm, weakly altered.
154	70	50	45	0.40	185	n. to f.	Nearly aphyric andesite, Pl poor, max. 2mm, weakly altered.
155	80	60	60	0.30	340	n. to f.	Px andesite, Px poor to common, max. 1mm, Pl common, max.2mm, altered.
156	70	60	40	0.60	210	n. to f.	Px andesite, Px poor to common, max. 1mm, Pl common, max.2mm, Gm heterogeneous, weakly altered.
157	80	50	40	0.30	195	n. to f.	Px andesite, Px poor to common, max. 1mm, Pl common, max.2mm, altered.
158	60	50	40	0.30	180	n.	Px andesite, Px common to rich, max. 3mm, Pl common 3mm, dusty.
159	90	60	30	0.30	210	n. to f.	Px andesite, Px poor to common, max. 1mm. Pl poor to common, max. 1mm, weakly altered.
160	60	50	40	0.30	185	n. to f.	Px andesite, Px common, max. 0.5mm, Pl common to rich, max. 3.5mm, dusty, Gm heterogeneous, weakly altered.
161	70	50	30	0.30	200	f.	Px andesite, Px common to rich, max. 1mm, Pl common, max. 1.5mm, small vesiculated, chlorite in cavity, weakly altered.
162	80	60	55	0.30	195	f.	(Ol bearing ?) basaltic andesite to andesite, Px poor to rare, Pl common, max. 4mm, glassy, Gm heterogeneous.
163	80	60	50	0.30	190	f.	Px andesite, Px common, max. 2mm, Pl rich, max. 1mm, glassy, very small vesiculated.
164	60	50	40	0.30	170	n. to f.	Px andesite, Px rich, max. 2.5mm, Pl common, max. 2mm, glassy, very small vesiculated.
165	60	40	40	0.30	90	n.	Px basaltic andesite to andesite, Px common, max. 2mm, Pl, max. 3mm, dusty, glassy, clay mineral in cavity, altered.
166	70	65	45	0.23	160	thinly f.	Px andesite, Px poor, max. 0.3mm, Pl common, 3.5mm, Gm heterogeneous, weakly altered.
167	90	65	40	0.20	180	n. to f.	Px andesite, Px rich, max. 3mm, dusty, Gm heterogeneous.
168	65	50	30	0.20	90	n. to f.	Px andesite, Px poor to common, max. 0.6mm, Pl common to rich, max. 2mm, glassy, very small vesiculated.

Sample No.	Diameter L	M	S	Round-ness	Wt. (g)	Mn-coating	Lithology & Remarks
169	80	65	25	0.25	140	n. to f.	(Ol bearing?) Px basaltic andesite, Px common to rich, max. 0.4mm, Pl common, max. 2mm, altered.
170	75	45	35	0.25	110	f.	Px basaltic andesite to andesite, Px common to rich, max. 2mm, Pl common, max. 4mm, glassy, vesiculated, clay mineral in cavity.
171	65	35	35	0.20	90	n. to f.	Px basaltic andesite to andesite, Px common, max. 1mm, Pl common, max. 6mm, glassy, vesiculated.
172	90	65	30	0.20	210	n. to f.	Px basaltic andesite to andesite, Px common, max. 1mm, Pl rich (20 to 30%), max. 4mm, glomeroporphyritic texture, glassy, clay mineral in cavity.
173	75	55	35	0.30	130	n. to f.	*Nearly aphyric basalt to basaltic andesite, Pl poor ,max. 1.5mm, Gm heterogeneous, glassy, very small well vesiculated.
174	95	55	30	0.23	200	f.	Reddih altered andesite, Pl common, max. 12mm, dusty, flow texture of occurrence of vesicule, clay mineral in cavity.
175	65	45	35	0.20	95	thinly f.	Px andesite. Px common, max. 1mm, Pl rich (20 to 25%), max. 3mm, glassy, weakly altered.
176	70	55	50	0.4	150	film	Px andesite, Px poor, max. 0.5mm, Pl common, max. 3.5mm, dusty, weakly altered, clay mineral in cavity.
177	60	50	40	0.4	130	n to f	Px andesite, Px poor, max. 0.7mm, Pl common, max. 1.5mm, Gm heterogeneous, waekly vesiculated.
178	60	40	40	0.3	110	film	*Px basaltic andesite, Px poor, max. 2mm, Pl poor to common, max. 5mm,glassy (quenched).
179	75	65	45	0.2	230	n to f	*Px andesite. Px poor to common, max. 2mm, Pl common, max. 5mm, dusty, rich in boundary.
180	95	75	40	0.4	315	n to f	*Px andesite, Px poor, max. 4mm, Pl common, max. 4mm, dusty, glassy(quenched), brown vein 2mm.
181	80	60	40	0.4	190	n to f	Gray tuff to tuffaceous sand.
182	60	45	25	0.4	75	film	Px andesite, Px poor, max. 1mm, Pl max. 4mm, dusty, altered.
183	75	40	35	0.3	85	thinly film	Px andesite, Px common, max. 3mm, Pl common, max. 9mm, altered.
184	205	145	130	0.3	2050	film	*Nearly aphyric andesite, Pl poor, max. 3mm, Gm glassy, partly well vesiculated.
185	180	130	110	0.4	1600	film	*Px andesite, Px poor to common, max. 2mm, Pl poor to common, 3mm, flow structure of occurrence of vesicular.
186	160	125	90	0.4	1500	8	*Nearly aphyric andesite, Pl poor, max. 3mm, Gm glassy, partly well vesiculated, flow structure of occurrence of vesicular.
187	100	95	50	0.3	580	none	Px andesite, Px poor, max. 1mm, Pl common, max. 3mm, Gm heterogeneous, glassy, weakly altered.
188	110	110	50	0.2	610	thinly film	*Px andesite, Px poor, max.1.5mm, Pl poor to common, max. 1.5mm, glassy, clay mineral in cavity.
189	80	75	60	0.2	260	poorly film	*Ol bearing basalt to basaltic andesite, altered Ol, Px common, max.0.5mm, Pl common, max. 1mm, vein 5mm.
190	105	95	50	0.3	400	poorly film	Pl, Px basalt, Ol, Px common, max. 0.5mm, Pl rare to poor, max. 0.7mm, glassy, altered.
191	80	65	50	0.3	240	poorly film	Reddish altered basaltic andesite and greenish altered andesite (magma mixing?).
192	100	70	45	0.3	280	n to f	Px andesite, Px poor to common, max. 0.5mm, Pl common, max.2mm, Gm heterogeneous, weakly altered..
193	80	60	50	0.4	310	none	Ol bearing Px basaltic andesite, Px rich, max. 1mm, Pl rich, max. 3mm, strongly altered..
194	85	70	55	0.3	280	n to f	Greenish altered Px andesite and yellow altered Px dacitic andesite (magma mixing?).
195	70	70	55	0.3	220	thinly film	*Aphyric to nearly aphyric basaltic andesite, vesiculated, Gm heterogeneous.
196	70	60	45	0.3	170	poorly film	Lapilli tuff? mainly composed of basaltic andesite (15mm), weakly altered.
197	75	55	40	0.3	180	poorly film	Greenish altered Px andesite, Px poor, max. 1mm, Pl common, max. 4mm.
198	90	60	30	0.4	190	poorly film	Ol bearing basalt to basaltic andesite, altered Ol, Px common, max.0.5mm, Pl common, max. 1mm, vein 5mm.

Sample No.	Diameter L	M	S	Round-ness	Wt. (g)	Mn-coating	Lithology & Remarks
199	60	60	40	0.25	110	thinly film	Strongly altered greenish lapilli tuff, mainly composed of altered andesite.
D04-201	200	170	150	0.2	6600	f.	White lapilli tuff with very fine matrix, lapilli: green andesite, altered
202	120	95	85	0.3	980	f.	White very fine pumiceous tuff, px: rare, pl: poor 1mm
203	80	70	30	0.4	200	n.	Lapilli tuff composed of white pumice(5mm), andesite(4.5mm) and crystals in volcanic ash
204	80	65	50	0.4	210	n. to f.	Pale green fine~very fine tuff
205	75	65	45	0.3	180	n. to f.	Light grey fine tuff including andesitic lapilli
206	80	60	40	0.3	185	n. to f.	Lapilli tuff composed of white pumice (4mm); green altered andesite (4mm) and grey andesite (3mm) in volcanic ash
207	65	50	50	0.3	170	f.	Lapilli tuff composed of pale green tuff (15mm) in glassy volcanic ash
208	100	75	40	0.4	355	f.	Similar to 204
209	115	75	50	0.3	420	n. to f.	Grey coarse grained tuff composed of basaltic andesite, green altered andesite and pumice, weak flow banding
210	75	60	50	0.4	300	n. to f.	Reddish brown coarse grained tuff composed of red altered andesite and grey andesite in altered ash
211	70	65	30	0.4	135	f.	Pale grey pumiceous tuff, rich in crystals (px and pl)
212	95	85	45	0.5	350	f.	Yellow and black lapilli tuff composed of basalt, altered materials and crystals (px, pl) in volcanic ash
213	70	55	40	0.6	140	f.	Similar to 212, more coarse grained
214	70	55	40	0.3	155	f.	Yellowish brown coarse grained tuff composed of basaltic andesite, pumice and crystals in ash
215	70	55	35	0.4	120	f.	Pale yellowish grey fine tuff rich in crystals (ol, px, pl)
216	80	70	35	0.3	190	f.	Pale yellow pumiceous tuff composed of pumice (4mm) rich in crystals (ol, px, pl)
217	115	90	50	0.5	500	n.	Lapilli tuff composed of ash(5mm), pumice(2.5mm), basalt(4mm), andesite(5mm) and crystals in volcanic ash
218	75	55	40	0.5	115	f.	Lapilli tuff composed of greenish yellow pumice(4mm), basalt (3mm), andesite(2.5mm) in volcanic ash
219	70	60	25	0.3	115	n.	Similar to 217
220	80	70	20	0.3	130	n. to f.	Pale greenish grey fine ~ very fine tuff dark green (chlorite ?) vein ~1mm
221	75	65	45	0.4	210	n. to f.	Similar to 206, grey andesite 5mm
222	75	50	50	0.3	150	f.	Lapilli tuff composed of green altered andesite (8mm), basalt (5mm) and pumice (4mm) in ash
223	90	70	60	0.4	310	n. to f.	Similar to 222
224	55	45	35	0.6	100	f.	Lapilli tuff composed of basalt (6mm), altered andesite (5mm) and crystals cemented in white altered materials
225	60	45	35	0.6	90	f.	Lapilli tuff composed of scoria (12mm), basalt (4mm) and crystals (px, pl) in altered yellowish brown glass
226	85	70	40	0.4	270	n. to f.	Lapilli tuff composed of green altered andesite (2mm), andesite (3mm), pumice (4mm) and basalt (1.5mm) in volcanic glass
227	70	65	30	0.3	170	f.	Strongly altered green lapilli tuff composed of basalt or basaltic andesite (8mm) and pumice (2mm) in altered glass
228	75	60	45	0.3	115	f.	Lapilli tuff composed of pumice (4mm), basaltic andesite (4mm) in pumiceous ash
229	85	40	40	0.3	130	n. to f.	Similar to 228
230	125	85	55	0.3	900	n. to f.	Greenish altered lapilli tuff composed of pumice (4mm) andesite (1.5mm) and crystals (px, pl) in volcanic glass
231	130	80	50	0.3	780	n. to f.	Similar to 230, basaltic andesite (7mm), altered
232	105	70	65	0.4	610	n. to f.	Strongly altered green lapilli tuff composed of pumice (84mm) and andesite (8mm) in altered glass
233	100	75	75	0.4	620	n. to f.	Pale greenish altered lapilli tuff composed of pumice, including andesite block (67mm Å~50mm)

Sample No.	Diameter L	M	S	Round-ness	Wt. (g)	Mn-coating	Lithology & Remarks
234	120	75	60	0.4	445	f.	Pale greenish altered lapilli tuff composed of pumice (3mm) and crystals, green (chlorite) vein (~1mm)
235	105	75	60	0.4	550	n. to f.	Lapilli tuff composed of pumice (10mm), andesite (13mm), red altered andesite (4mm) in altered glass
236	115	80	65	0.3	550	n. to f.	Pale greenish altered lapilli tuff composed of pumice (8mm), mainly pale green tuff
237	140	80	50	0.2	690	n. to f.	Strongly altered green lapilli tuff composed of greenish altered andesite (25mm) and pumice (7mm)
238	130	110	60	0.3	850	n. to f.	Strongly altered green lapilli tuff composed of altered andesite (15mm) and pumice (5mm)
239	90	80	55	0.4	400	f.	Lapilli tuff composed of altered andesite (13mm), green tuff (15mm) in greenish altered glass
240	105	65	45	0.3	305	n. to f.	Similar to 238 including andesite (30mm)
241	95	65	60	0.6	450	n. to f.	Strongly altered dark green lapilli tuff composed of andesite in
242	85	85	45	0.2	310	n. to f.	Lapilli tuff composed of andesite (35mm), green tuff in glass
243	80	75	50	0.4	300	f.	Pale green altered lapilli tuff composed of pumice (4mm), including andesite (45mmÅ~35mm)
244	85	65	45	0.3	270	f.	Green tuff or lapilli tuff composed of pumice (3mm)
245	85	70	45	0.3	260	n. to f.	Similar to 239, greenish altered
246	95	60	50	0.3	350	n. to f.	Similar to 242 including andesite (40mmÅ~25mm)
247	100	60	45	0.2	320	n. to f.	Lapilli tuff composed of pumice (5mm), andesite (5mm) and crystals (px, pl) in volcanic glass
248	100	70	45	0.3	270	n. to f.	Lapilli tuff composed of andesite (3mm), pumice (2mm) in greenish altered glass
249	110	70	40	0.2	260	n. to f.	Similar to 248 greenish altered
250	100	75	20	0.3	225	n. to f.	Similar to 227
251	75	55	40	0.3	170	n. to f.	Lapilli tuff composed of nearly aphyric andesite (20mm), greenish or reddish altered andesite (8mm) and green tuff (10mm) in altered glass
252	115	80	50	0.1	360	n.	Strongly altered dark greenish lapilli tuff composed of altered andesite (6mm) cemented in white materials
253	90	50	45	0.3	230	f.	Lapilli tuff composed of andesite (20mm), and nearly aphyric dacite (25mm) in altered glass. green vein (2mm)
254	90	65	55	0.2	360	f.	Lapilli tuff composed of green tuff (15mm) altered andesite (15mm) and pumice (5mm) in glass
255	75	60	45	0.4	250	f.	Similar to 232, pale green altered andesite (35mm)
256	65	55	40	0.5	160	n. to f.	Strongly altered pale green lapilli tuff including pale green tuff (45mm)
257	75	55	40	0.4	180	n. to f.	Lapilli tuff composed of nearly aphyric andesite (12mm), greenish altered andesite (15mm) in altered glass
258	80	50	40	0.4	190	n.	Lapilli tuff composed of green tuff (23mm), basaltic andesite (3mm), altered andesite (7mm) and pumice (2.5mm)
259	75	55	50	0.5	260	n.	Lapilli tuff composed of basalt (50mm), basaltic andesite (8mm) and pumice (1.5mm) in pumiceous glass
260	60	60	40	0.4	170	f.	Lapilli tuff composed of grey tuff (12mm), greenish altered andesite (6mm), pumice (3mm) and crystals in altered glass
261	95	45	35	0.2	180	f.	Pale greenish altered lapilli tuff composed of green tuff (10mm) in altered glass. dark green (chlorite) vein (~1mm)
262	75	45	45	0.4	160	n. to f.	Similar to 237
263	70	60	40	0.3	150	n. to f.	Similar to 239 altered andesite (10mm)
264	70	55	25	0.3	160	n. to f.	Greenish altered lapilli tuff composed of altered andesite (15mm) and green tuff (5mm) in altered glass
265	85	45	35	0.3	150	n. to f.	Strongly altered lapilli tuff composed of altered andesite (20mm) and green tuff (10mm), partly flow structure
266	100	65	25	0.3	140	n. to f.	Greenish altered lapilli tuff composed of green tuff (9mm) and altered andesite (6mm)
267	75	45	40	0.4	150	f.	Similar to 234
268	60	50	40	0.3	130	n.	Similar to 232, andesite (30mm)

Sample No.	Diameter L	M	S	Round-ness	Wt. (g)	Mn-coating	Lithology & Remarks
269	80	50	30	0.3	120	n. to f.	Lapilli tuff composed of green tuff (13mm), altered andesite (5mm) and crystals in volcanic glass
270	70	65	25	0.3	140	n. to f.	Pale green lapilli tuff mainly composed of grey or green tuff in altered glass. dark green vein (1.5mm)
271	70	55	30	0.3	110	f.	Lapilli tuff composed of altered andesite (11mm), green tuff (6mm) and pumice (4mm) in altered glass
272	60	55	30	0.3	110	n. to f.	Similar to 250 (227)
273	60	45	25	0.2	90	n. to f.	Similar to 251
274	75	55	25	0.3	110	f.	Greenish altered lapilli tuff composed of pumice (3mm), altered andesite (8mm) and green tuff (3mm) in altered glass
275	90	75	40	0.1	230	f.	Strongly altered greenish lapilli tuff composed of altered andesite (35mm), green tuff(10mm) in altered glass. dark green vein (1mm)
276	105	55	50	0.3	310	n. to f.	Lapilli tuff composed of andesite (22mm), pumice (3mm), pale green tuff (2mm) in volcanic glass
277	145	90	30	0.1	460	f.	Lapilli tuff composed of andesite (15mm) and green tuff (2mm), calcite or silica mineral in cavity
278	105	70	45	0.3	340	f.	Tuff breccia composed of andesite (70mm), altered andesite (5mm) in altered volcanic glass
279	90	45	45	0.3	200	n. to f.	Lapilli tuff comlposed of altered andesite (20mm) and green tuff (3mm) in altered glass
280	75	55	45	0.3	190	n. to f.	Lapilli tuff mainly composed of andesite (23mm) and altered andesite (23mm) in greenish tuf
281	65	50	40	0.4	150	n. to f.	Lapilli tuff composed of basaltic andesite (23mm) and altered andesite (3mm) in altered glass
282	65	55	40	0.3	170	n. to f.	Lapilli tuff composed of aphyric andesite (15mm), grenn tuff (3mm) and crystals (px, pl) in altered glass
283	65	55	40	0.3	120	n.	Similar to 280
284	50	50	40	0.6	80	f.	Lapilli tuff composed of a little vesiculated basaltic andesite (40mm) and tuff in altered volcanic glass
285	50	45	40	0.4	60	f.	Similar to 284
286	18	13	12	0.4	295	f.	Strongly altered brown lapilli tuff mainly composed of altered basalt or basaltic andesite in altered glass
D04-301	145	70	65	0.2	640	n.	Dark reddish brown tuffaceous sandy mudstone, weakly laminated, partly mixed by bioturbation
302	95	80	35	0.15	340	n.	Dark reddish brown tuffaceous sandy mudstone, weakly laminated, white vein 1mm
303	100	70	40	0.15	310	poor	Dark reddish brown tuffaceous sandy mudstone and dacite block(2,5cm), white bein 2mm
304	110	85	40	0.2	360	n.	Similar to 302, white vein 4mm
305	100	70	20	0.15	240	poor	Similar to 301, white vein 1.5mm
306	95	60	45	0.15	270	n.	Similar to 302, white vein 1mm
307	115	55	45	0.15	260	n.	Similar to 302, white vein 2mm
308	70	55	40	0.15	130	n.	Similar to 302, white vein 2mm
309	110	70	30	0.3	210	poor	Grey tuffaceous sandstone
310	90	70	30	0.35	220	poor	Greenish grey tufaceous sandstone
D04-501	80	60	50	0.3	480	n.	Ol-px basalt, ol: rich 0.7mm, px: rich 1mm, pl: 1mm, glassy, altered
502	80	50	50	0.3	310	n.	Px basaltic andesite or andesite, glassy, px: common 1.5mm, pl: common 2mm, weakly altered
503	120	80	30	0.1	370	n.	Px basaltic andesite or andesite, glassy, px: common 1.5mm, pl: common 1.8mm, weakly altered
504	110	60	40	0.2	330	n.	Ol-px basalt, ol: common or rich 0.6mm, glassy, px: common or rich 1mm, pl common 1mm, altered
505	110	80	20	0.1	170	f.	Similar to 504, strongly altered
506	90	50	50	0.2	230	f.	Nearly aphyric basalt, ol and px: rare, pl: poor 1.5mm, glassy, weakly altered
507	80	50	50	0.3	190	n. to f.	Px andesite, px: common 2.5mm, pl: common 3mm, gm: heterogeneous

Sample No.	Diameter L	M	S	Round-ness	Wt. (g)	Mn-coating	Lithology & Remarks
508	80	40	50	0.3	185	n. to f.	Aphyric basaltic andesite, altered, quartz or calcite in cavity, chlorite vein
509	70	50	30	0.3	130	n. to f.	Ol-px basalt or basaltic andesite, glassy, ol: common 0.5mm, px: common 0.7mm, pl: rich 3mm, altered
601					5880		The bag package of pebbles.
602					2360		The bag package of pebbles.
603					1760		The bag package of pebbles.
604					880		The bag package of pebbles.
605					870		The bag package of mud.
606					4350		The bag package of sand.
D05-001	330	260	260	0.40	15900	n.	vesicular pillow basalt
002	290	270	220	0.40	9900	n.	vesicular pillow basalt
003	300	290	220	0.40	11800	n.	vesicular pillow basalt
D05-004	300	240	170	0.40	11550	n.	vesicular pillow basalt
005	270	190	180	0.40	9200	n.	vesicular pillow basalt
006	300	220	190	0.40	9450	n.	vesicular pillow basalt
007	240	220	170	0.50	7150	n.	vesicular pillow basalt
008	190	200	185	0.50	3700	n.	vesicular pillow basalt
009	210	200	150	0.40	3700	n.	vesicular pillow basalt
010	220	130	150	0.50	4300	n.	vesicular pillow basalt
011	240	180	120	0.30	5400	n.	vesicular pillow basalt
012	210	200	160	0.20	4000	n.	vesicular pillow basalt
013	240	170	150	0.40	3150	n.	vesicular pillow basalt
014	210	160	160	0.40	2650	n.	vesicular pillow basalt
015	210	160	110	0.40	2450	n.	vesicular pillow basalt
016	210	150	130	0.40	2950	n.	vesicular pillow basalt
017	230	130	130	0.40	4000	n.	vesicular pillow basalt
018	200	150	130	0.30	2550	n.	vesicular pillow basalt
019	230	180	190	0.20	5900	n.	vesicular pillow basalt
020	180	120	120	0.40	1700	n.	vesicular pillow basalt
021	190	140	160	0.30	2700	n.	vesicular pillow basalt
022	260	120	90	0.20	1750	n.	vesicular pillow basalt
023	210	170	120	0.30	3050	n.	vesicular pillow basalt
024	200	170	120	0.30	2500	n.	vesicular pillow basalt
025	230	130	110	0.20	2000	n.	vesicular pillow basalt
026	180	130	140	0.40	1900	n.	vesicular pillow basalt
027	210	135	100	0.40	2000	n.	vesicular pillow basalt
028	200	100	95	0.20	1050	n.	vesicular pillow basalt
029	170	145	85	0.20	1400	n.	vesicular pillow basalt
030	150	130	105	0.40	1050	n.	vesicular pillow basalt
031	205	105	85	0.30	1150	n.	vesicular pillow basalt
032	150	135	130	0.30	1650	n.	vesicular pillow basalt
033	90	110	95	0.20	1250	n.	vesicular pillow basalt
034	150	120	85	0.40	700	n.	vesicular pillow basalt
035	170	115	105	0.30	1420	n.	vesicular pillow basalt
036	145	145	110	0.30	1470	n.	vesicular pillow basalt
037	170	85	105	0.10	1080	n.	vesicular pillow basalt
038	135	110	85	0.40	1150	n.	vesicular pillow basalt
039	145	110	90	0.60	780	n.	vesicular pillow basalt
040	125	90	70	0.60	650	n.	vesicular pillow basalt
201	190	180	135	0.50	5200	f.	vesicular basalt to basaltic andesite
202	260	180	130	0.40	4650	f.	vesicular basalt rich in large vesicular
203	160	145	90	0.40	3500	f.	vesucular basalt rich in small vesicular
204	170	140	110	0.30	3100	f.	vesucular basalt rich in small vesicular
205	160	130	100	0.50	2350	f.	vesucular basalt rich in small vesicular
206	150	135	70	0.40	1100	f.	vesicular basalt rich in large vesicular

Sample No.	Diameter L	M	S	Round-ness	Wt. (g)	Mn-coating	Lithology & Remarks
301	80	65	45	0.30	160	half f.	strongly hydrothermally altered tuff breccia deseminated by pyrite and galena
302	50	40	30	0.40	85	n.	fragment of blacksmorker chimney comprising mostly pyrite
303	60	50	30	0.30	45	half f.	strongly hydrothermally altered tuff breccia deseminated by pyrite
304	40	30	25	0.30	15	half f.	strongly hydrothermally altered tuff breccia deseminated by pyrite
305	40	30	30	0.30	20	half f.	strongly hydrothermally altered tuff breccia deseminated by pyrite
311					50		other rocks
401	40	80	70	0.40	430	f.	low temperature and oxidizing altered basalt
402	90	65	50	0.30	250	f.	low temperature and oxidizing altered basalt
403	65	55	50	0.40	180	f.	low temperature and oxidizing altered basalt
404	65	55	50	0.40	130	f.	low temperature and oxidizing altered basalt
405	70	60	40	0.40	135	f.	low temperature and oxidizing altered basalt
406	65	55	40	0.40	120	n. to f.	low temperature and oxidizing altered basalt
411					180		other rocks
501					11200		volcanic rock gravels
502					12500		volcanic rock gravels
D05-503					10200		volcanic rock gravels
504					12500		volcanic rock gravels
505					6500		volcanic rock gravels
506					11800		volcanic rock gravels
507					10500		volcanic rock gravels
508					11500		volcanic rock gravels
511					1860		pebble
512					1190		sand
513					2680		sand
514					20		sand
D06-001	350	250	200	0.20	26500		
002	360	200	150	0.30	12800	thin stain	aphyric vesicular basalt (rounded vesicular)
003	350	200	140	0.20	12670	thin stain	aphyric vesicular basalt (elongated vesicule)
004	250	150	90	0.40	6550	stain	aphyric vesicular basalt, small phenocryst plagicoclase, max. 2mm
005	240	200	120	0.10	4250	stain	aphyric basalts with elongated vesicules max. 8cm
006	220	160	120	0.10	3800	thin stain	aphyric loapy basalts, vesiculous , elongated vesicules
007	170	170	130	0.30	3400	stain	aphyric basalt with rare pl. phenocrysts and elongated vesicules
008	170	110	50	0.10	1200	stain	aphyric basalt with rare pl. phenocrysts less than 1 mm, elongated vesicules
009	160	150	170	0.20	1700	stain	aphyric basalt with about 1 cm vesicules and xenolith of gabbroic rock?
010	180	140	80	0.20	1600	stain	loapy and aphyric basalt with rare pl. and elongated vesicules.
011	160	100	60	0.20	1300	thin stain	loapy and aphyric basalt with elongated vesicules of about 1 cm.
012	130	100	50	0.10	1030	stain	loapy and aphyric basalt with pl. and elongated vesicules.
013	120	120	50	0.20	1060	stain	aphyric basalt with 1 cm vesicular, pl. poor, max. 2 mm
014	140	100	60	0.10	1200	stain	highly vesiculous basalt with 1 mm pl.
015	140	90	60	0.20	850	stain	aphyric basalt with elongated vesicules
016	120	100	90	0.40	1290	partly f.	altered basalt with vesicules filled with zeolite?
017	120	90	50	0.50	970	none	basalt with much amounts of vesicules and a few mm pl.
018	140	50	60	0.40	820	f.	altered basalt with vesicules and pl. less than a few mm.
019	120	70	50	0.30	600	none	basalt , pl. less than 1 mm with small vesicules, quench glass.
020	120	110	40	0.30	630	stain	loapy aphyric basalt with pl. and elongated vesicules.
D06-101	200	130	120			stain	Plutonic rock, containing large amount of magnetite, foliated, Xenolith, max. 3cm.

Sample No.	Diameter L	M	S	Round-ness	Wt. (g)	Mn-coating	Lithology & Remarks
102	230	160	100	0.20	3250	n.	Vesicular basalt, Pl common, max.3mm, basaltic gabbroic xenocryst including.
103	140	120	80	0.30	1020	stain	Vesicular basalt, Pl common, Ol max.5mm, max. 3cm basaltic gabbroic xenocryst including.
104	130	100	60	0.30	1050	n.	Vesicular basalt, Pl common, gabbroic xenocryst(1cm) including.
105	120	100	60		800	n.	Vesicular basalt, Pl common, max. 3mm, basalt xenolith(3cm) including.
106	120	100	80	0.30	835	weakly stain	Vesicular basalt, Pl common, max 2mm, gabbroic xenolith(2 to 10mm) including.
107	130	90	70		690	n.	Vesicular basalt, Pl common, max. 1mm, basalt xenolith(5cm) including.
201	180	130	70		2750	f.to stain	Basalt breccia, sulfered with low Temp. alteration.
301	65	40	25		50	n.	Semi-altered scoria.
302	55	40	30	0.30	70	n.	altered pumice.
303	60	50	35	0.30	30		altered tuffacous pumice.
311					175		other rocks.
401					12000		Volcanic rock gravel.
402					16000		Volcanic rock gravel.
403					3200		Volcanic rock gravel.
411					3020		Pebbles and sand.
412					4700		Pebbles and sand.
413					3350		Pebbles and sand.
414					2300		Pebbles and sand.
D07-001	340	300	270	0.40	20000	n.	Vesicular pillow basalt with a few mm Pl phenocrysts, lateral stratified structure oc occurrence of vesiculation.
002	270	210	180	0.30	10600	n.	Vesicular pillow basalt with a few mm Pl phenocrysts, lateral stratified structure oc occurrence of vesiculation.
003	350	220	190	0.30	10800	n.	Vesicular pillow basalt with a few mm Pl phenocrysts, lateral stratified structure oc occurrence of vesiculation.
004	310	210	200	0.30	12000	n.	Vesicular pillow basalt with a few mm Pl phenocrysts, lateral stratified structure oc occurrence of vesiculation.
005	330	190	170	0.40	10200	n.	Vesicular pillow basalt with a few mm Pl phenocrysts, lateral stratified structure oc occurrence of vesiculation.
006	260	240	190	0.40	12800	n.	Vesicular pillow basalt with a few mm Pl phenocrysts, lateral stratified structure oc occurrence of vesiculation.
007	280	200	150	0.40	12200	n.	Vesicular pillow basalt with a few mm Pl phenocrysts, lateral stratified structure oc occurrence of vesiculation.
008	280	200	180	0.40	16050	n.	Vesicular pillow basalt with a few mm Pl phenocrysts, lateral stratified structure oc occurrence of vesiculation.
009	220	190	180	0.50	9350	n.	Vesicular pillow basalt with a few mm Pl phenocrysts, lateral stratified structure oc occurrence of vesiculation.
010	320	220	190	0.40	12250	n.	Vesicular pillow basalt with a few mm Pl phenocrysts, lateral stratified structure oc occurrence of vesiculation.
011	280	190	180	0.40	9350	n.	Vesicular pillow basalt with a few mm Pl phenocrysts, lateral stratified structure oc occurrence of vesiculation.
012	190	190	130	0.40	5800	n.	Vesicular pillow basalt with a few mm Pl phenocrysts, lateral stratified structure oc occurrence of vesiculation.
013	230	180	100	0.30	5350	n.	Vesicular pillow basalt with a few mm Pl phenocrysts, lateral stratified structure oc occurrence of vesiculation.
014							VOID
015	200	160	150	0.50	6350	n.	Vesicular pillow basalt with a few mm Pl phenocrysts, lateral stratified structure oc occurrence of vesiculation.
016	190	150	130	0.50	4000	n.	Vesicular pillow basalt with a few mm Pl phenocrysts, lateral stratified structure oc occurrence of vesiculation.

Sample No.	Diameter L	M	S	Round-ness	Wt. (g)	Mn-coating	Lithology & Remarks
017	190	130	100	0.50	4300	n.	Vesicular pillow basalt with a few mm Pl phenocrysts, lateral stratified structure oc occurrence of vesiculation.
018	230	140	140	0.40	4800	n.	Vesicular pillow basalt with a few mm Pl phenocrysts, lateral stratified structure oc occurrence of vesiculation.
019	180	170	130	0.40	4650	n.	Vesicular pillow basalt with a few mm Pl phenocrysts, lateral stratified structure oc occurrence of vesiculation.
020	180	130	110	0.50	2480	n.	Vesicular pillow basalt with a few mm Pl phenocrysts, lateral stratified structure oc occurrence of vesiculation.
021	150	120	100	0.50	2450	n.	Vesicular pillow basalt with a few mm Pl phenocrysts, lateral stratified structure oc occurrence of vesiculation.
022	160	110	90	0.50	1850	n.	Vesicular pillow basalt with a few mm Pl phenocrysts, lateral stratified structure oc occurrence of vesiculation.
023	140	130	90	0.50	1330	n.	Vesicular pillow basalt with a few mm Pl phenocrysts, lateral stratified structure oc occurrence of vesiculation.
024	130	120	100	0.40	1900	n.	Vesicular pillow basalt with a few mm Pl phenocrysts, lateral stratified structure oc occurrence of vesiculation.
025	160	120	90	0.40	1800	n.	Vesicular pillow basalt with a few mm Pl phenocrysts, lateral stratified structure oc occurrence of vesiculation.
026	140	110	80	0.50	1030	n.	Vesicular pillow basalt with a few mm Pl phenocrysts, lateral stratified structure oc occurrence of vesiculation.
027	140	130	100	0.40	1380	n.	Vesicular pillow basalt with a few mm Pl phenocrysts, lateral stratified structure oc occurrence of vesiculation.
028	150	100	80	0.40	1165	n.	Vesicular pillow basalt with a few mm Pl phenocrysts, lateral stratified structure oc occurrence of vesiculation.
029	130	110	90	0.40	945	n.	Vesicular pillow basalt with a few mm Pl phenocrysts, lateral stratified structure oc occurrence of vesiculation.
030	110	90	70	0.50	910	n.	Vesicular pillow basalt with a few mm Pl phenocrysts, lateral stratified structure oc occurrence of vesiculation.
031	110	100	70	0.40	810	n.	Vesicular pillow basalt with a few mm Pl phenocrysts, lateral stratified structure oc occurrence of vesiculation.
032	120	100	80	0.50	790	n.	Vesicular pillow basalt with a few mm Pl phenocrysts, lateral stratified structure oc occurrence of vesiculation.
033	110	90	70	0.40	840	n.	Vesicular pillow basalt with a few mm Pl phenocrysts, lateral stratified structure oc occurrence of vesiculation.
034	110	100	60	0.50	790	n.	Vesicular pillow basalt with a few mm Pl phenocrysts, lateral stratified structure oc occurrence of vesiculation.
035	120	80	70	0.40	585	n.	Vesicular pillow basalt with a few mm Pl phenocrysts, lateral stratified structure oc occurrence of vesiculation.
036	120	60	55	0.50	570	n.	Vesicular pillow basalt with a few mm Pl phenocrysts, lateral stratified structure oc occurrence of vesiculation.
037	80	80	75	0.50	575	n.	Vesicular pillow basalt with a few mm Pl phenocrysts, lateral stratified structure oc occurrence of vesiculation.
038	100	75	75	0.50	480	n.	Vesicular pillow basalt with a few mm Pl phenocrysts, lateral stratified structure oc occurrence of vesiculation.
039	85	75	60	0.50	450	n.	Vesicular pillow basalt with a few mm Pl phenocrysts, lateral stratified structure oc occurrence of vesiculation.
040	110	90	60	0.40	580	n.	Vesicular pillow basalt with a few mm Pl phenocrysts, lateral stratified structure oc occurrence of vesiculation.
041	100	90	50	0.40	495	n.	Vesicular pillow basalt with a few mm Pl phenocrysts, lateral stratified structure oc occurrence of vesiculation.
042	110	70	60	0.40	390	n.	Vesicular pillow basalt with a few mm Pl phenocrysts, lateral stratified structure oc occurrence of vesiculation.
043	90	60	50	0.40	350	n.	Vesicular pillow basalt with a few mm Pl phenocrysts, lateral stratified structure oc occurrence of vesiculation.
D08-001						n.	flesh pillow lava including glass
002	260	180	60	0.10		n.	flesh pillow lava including glass
003	150	120	70	0.10		n.	flesh pillow lava including glass
004	200	100	50	0.10		n.	flesh pillow lava including glass
005	120	50	45	0.10		n.	flesh pillow lava including glass

Sample No.	Diameter L	M	S	Round-ness	Wt. (g)	Mn-coating	Lithology & Remarks
006	190	130	80	0.10		n.	flesh pillow lava including glass
007	180	90	45	0.10		n.	flesh pillow lava including glass
008	100	100	50	0.10		n.	flesh pillow lava including glass
009	140	75	60	0.10		n.	flesh pillow lava including glass
010	100	80	60	0.10		n.	flesh pillow lava including glass
011	180	100	60	0.10		n.	flesh pillow lava including glass
012	150	60	55	0.10		n.	flesh pillow lava including glass
013	110	90	50	0.10		n.	flesh pillow lava including glass
014	80	80	70	0.10		n.	flesh pillow lava including glass
015	100	70	40	0.10		n.	flesh pillow lava including glass
016	70	70	50	0.10		n.	flesh pillow lava including glass
017	80	60	30	0.10		n.	flesh pillow lava including glass
018							fragment of flesh pillow lava including glass
019							fragment of flesh pillow lava including glass
020							fragment of flesh pillow lava including glass
021							fragment of flesh pillow lava including glass
022							fragment of flesh pillow lava including glass
023							fragment of flesh pillow lava including glass
024							fragment of flesh pillow lava including glass
025							fragment of flesh pillow lava including glass
026							fragment of flesh pillow lava including glass
027							fragment of flesh pillow lava including glass
028							fragment of flesh pillow lava including glass
029							fragment of flesh pillow lava including glass
030							fragment of flesh pillow lava including glass
031							fragment of flesh pillow lava including glass
032							fragment of flesh pillow lava including glass
033							fragment of flesh pillow lava including glass
034							fragment of flesh pillow lava including glass
035							fragment of flesh pillow lava including glass
036							fragment of flesh pillow lava including glass
037							fragment of flesh pillow lava including glass
038							fragment of flesh pillow lava including glass
039							fragment of flesh pillow lava including glass
040							fragment of flesh pillow lava including glass
D09-001	170	140	70	0.1	1800	none	Pillow andesitic basalt lava with the part of several tube structure, Pl (max. 5mm) concentrated in quench glass rim(max. 12mm), and scattered in the inner part with small vesiculation.
002	150	120	50	0.1	1100	none	Pillow andesitic basalt lava with the part of one tube's structure, Pl (max. 5mm) concentrated in quench glass rim(max. 12mm), and scattered in the inner part with small vesiculation.
003	180	100	60	0.1	620	none	Pillow andesitic basalt lava with the part of one tube's structure, Pl (max. 5mm) concentrated in quench glass rim(max. 12mm), and scattered in the inner part with small vesiculation.
004	110	100	40	0.1	430	none	Pillow andesitic basalt lava with the part of one tube's structure, Pl (max. 5mm) concentrated in quench glass rim(max. 12mm), and scattered in the inner part with small vesiculation.
005	150	120	60	0.1	610	none	Pillow andesitic basalt lava with the part of one tube's structure, Pl (max. 5mm) concentrated in quench glass rim(max. 12mm), and scattered in the inner part with small vesiculation.
006	130	80	70	0.1	415	none	Pillow andesitic basalt lava with the part of one tube's structure, Pl (max. 5mm) concentrated in quench glass rim(max. 12mm), and scattered in the inner part with small vesiculation.
007	100	60	40	0.1	360	none	Similar to 001 and 002, the part of two tube's structure.
008	80	70	40	0.1	290	none	Similar to 001 and 003, the part of two tube's structure.
009	160	70	50	0.1	495	none	Similar to 001 and 003, the part of two tube's structure.

Sample No.	Diameter L	M	S	Round-ness	Wt. (g)	Mn-coating	Lithology & Remarks
010	150	100	90	0.1	910	none	Pillow andesitic basalt lava with the part of one tube's structure, round shape of tube and filled by lava, partly vesiculated, Pl (max. 5mm) concentrated in quench glass rim(max. 12mm), and scattered in the inner part with small vesiculation.
011	100	80	60	0.1	405	none	Same as 010.
012	80	50	30	0.1	150	none	Pillow andesitic basalt lava with the part of one tube's structure, Pl (max. 5mm) concentrated in quench glass rim(max. 12mm), and scattered in the inner part with small vesiculation.
013	70	60	40	0.1	240	none	Pillow andesitic basalt lava with the part of one tube's structure and thick inner part, Pl (max. 5mm) concentrated in quench glass rim(max. 12mm), and scattered in the inner part with small vesiculation.
014	80	75	50	0.1	335	none	Same sa 010, and perfectly preservated tube morphology.
015	80	70	45	0.1	240	none	Same as 010, and partly well preservated tube morphology.
016	75	70	40	0.1	210	none	Same as 015.
017	75	70	50	0.1	230	none	Same as 014.
018	80	60	45	0.1	205	none	Same as 015.
019	70	50	35	0.1	155	none	Same as 015.
020	65	45	30	0.1	100	none	Quench glass of pillow andesitic basalt lava with perfectly preservated tube morphology.
021	65	45	20	0.1	80	none	Same as 002.
022	70	30	30	0.1	90	none	Same as 007.
023	45	30	25	0.1	65	none	Same as 013, (23mm).
024	65	40	10	0.1	55	none	Same as 002.
025	45	25	20	0.1	60	none	Same as 002.
026	110	90	50	0.1	525	none	Same as 014, rounded and lobe like shape, perfectly.
027	100	50	40	0.1	125	none	Same as 013, (29mm) reddish black zone and yellowish block zone in inner part.
028	55	45	30	0.1	85	none	Same as 013 (25mm).
029	70	40	7	0.1	40	none	Quench glass rim of pillow andesitic basalt lava.
051					1185		Fragment of pillow andesitic basalt.
052					315		Fragment of pillow andesitic basalt.
053					195		Fragment of pillow andesitic basalt.
D10-001	2.5	2	2	0.5 than 10g		none	Black scoria, small and medium to ill vesiculated, Pl rare, max. 2mm.
002	2.5	1.5	1	0.4 than 10g		none	Black and gray banded scoria, small and well vesiculated, Pl rare, max. 1mm.
003	1.5	1	0.7	0.4 than 10g		none	Black scoria, small and well vesiculated, nearly aphyric, Pl rare, max. 2mm.
004	1.5	1	0.8	0.4 than 10g		none	Brownis black scoria, small and very well vesiculated, Pl rare.
005	2	1.2	1	0.3 than 10g		none	Black scoria, small and medium to well vesiculated, aphyric.
006	1.7	1.1	1	0.4 than 10g		none	Yellowish brown pumice (scoria?), small and ill vesiculated, Px poor max.0.8mm, Pl poor max. 0.7mm.
007	1.5	0.8	0.7	0.3 than 10g		none	Brown gray scoria (pumice ?), small and very ill vesiculated, Px rare max.0.7mm, Pl poor max. 3mm, elongate vesicule.
008	1.2	0.9	0.7	0.4 than 10g		none	Dark brown scoria, small and medium to ill vesiculated, Px common max. 0.5mm, Pl poor max. 0.5mm.
009	1	0.8	0.7	0.1 than 10g		none	Dark brown scoria, small and medium to ill vesiculated, Px common max. 0.5mm, Pl poor max. 0.5mm.
010	1	0.7	0.6	0.5 than 10g		none	Black scoria, small and medium to ill vesiculated, Pl rare, max. 2mm.
011	1	1	0.5	0.4 than 10g		none	Dark gray scoria, small and ill vesiculated, Pl poor to rare, max. 0.5mm, partly banded.
012	1	0.7	0.5	0.4 than 10g		none	Brown gray scoria (pumice ?), small and ill vesiculated, Px poor max.0.5mm, Pl poor max. 0.5mm.
013	1	0.8	0.5	0.3 than 10g		none	Brown gray scoria, small and medium to well vesiculated, Px rare, Pl poor max. 0.5mm.

Sample No.	Diameter L	M	S	Round-ness	Wt. (g)	Mn-coating	Lithology & Remarks
014	0.9	0.8	0.7	0.4	than 10g	none	Yellowish brown pumice, small and very ill vesiculated, Pl poor, max. 0.5mm.
015	1.3	1.2	0.8	0.3	than 10g	none	Dark brown lapilli tuff, mainly composed of ill vesiculated scoria in volcanic ash.
021	60	50	25				Pale brown mud.
D11-001	410	270	190	0.3	26820	4	Highly altered serpentinized harzburgite.
002	300	205	195	0.5	18000	7	Highly altered serpentinized harzburgite.
003	310	270	185	0.4	14700	1	Highly altered serpentinized harzburgite.
004	200	175	110	0.5	4800	7	Semi-highly altered serpentinized harzburgite.
005	190	180	95	0.5	2900	2	Medium altered serpentinized dunite.
006	165	150	135	0.3	3400	f.	Highly altered serpentinized harzburgite.
007	210	150	135	0.4	3900	n. to f.	Fresh to low altered harzburgite.
008	180	145	100	0.5	3000	3	Fresh to low altered harzburgite to dunite.
009	190	135	105	0.4	3200	f.	Fresh to low altered harzburgite.
010	195	150	135	0.4	3500	n. to 6	Medium altered serpentinized harzburgite.
011	185	130	120	0.5	3120	3	Highly altered serpentinized harzburgite to dunite.
012	180	130	100	0.3	2100	2	Highly altered serpentinized harzburgite to dunite.
013	140	130	100	0.3	1850	n. to 6	Highly altered serpentinized dunite.
014	175	140	65	0.3	1990	3	Medium to high altered serpentinized harzburgite.
015	140	110	80	0.4	1400	2	Fresh to low altered dunite.
016	140	100	90	0.5	1600	1 to 2	Semi-highly altered serpentinized harzburgite.
017	130	90	70	0.5	920	1	Fresh to low altered harzburgite.
018	255	180	130	0.2	2450	n. to 6	Low to medium altered harzburgite.
019	180	180	50	0.2	2020	f. to 6	seim-altered serpentinized hartbergite.
020	140	140	60	0.2	1400	f. to 1	seim-altered serpentinized hartbergite.
021	150	110	100	0.4	1990	f. to 1	fresh low altered harzergite to dunite.
022	140	120	75	0.4	1280	1 to 5	low-semi altered dunite.
023	190	100	90	0.5	1650	5	high-altered serpentinized hartzbergite.
024	120	120	65	0.4	930	1	fresh- low altered hartzbergite.
025	150	100	90	0.4	1120	1 to 2	fresh- low altered hartzbergite.
026	130	120	95	0.5	1330	5	fresh- low altered hartzbergite to dunite.
027	155	115	75	0.4	1300	4	fresh- low altered hartzbergite.
028	125	105	65	0.4	730	4	fresh- low altered dunite.
029	115	105	65	0.4	810	4	high-altered serpentinized dunite.
030	125	115	70	0.4	830	3	high-altered serpentinized hartbergite.
031	135	120	40	0.4	670	n. to 2	high-altered serpentinized dunite.
032	95	85	55	0.4	370	1	low-semi altered serpentinized hartzbergite.
033	125	100	65	0.4	660	n. to 1	low altered hartzbergite.
034	125	95	60	0.4	630	1 to 2	semi altered serpentinized hartzbergite.
035	130	85	55	0.3	520	2	low altered hartzbergite.
036	100	75	55	0.4	440	2	high altered serpentinized dunite.
037	95	75	55	0.5	410	3 to 5	high altered serpentinized dunite.
038	110	95	53	0.5	390	n. to f.	semi to high altered serpentinized hartzbergite.
039	115	75	52	0.3	350	1	low altered hartzbergite
040	90	90	60	0.3	380	1	semi altered serpentinized hartzbergite.
041	95	65	55	0.4	355	5	high altered serpnetinized hartzbergite.
042	80	75	50	0.4	240	1	semi altered serpentinized dunite.
043	75	65	60	0.5	210	1 to 2	semi altered serpentinized hartzbergite.
044	100	75	60	0.3	300	1	high altered serpentinized hartzbergite.
045	95	70	55	0.5	295	1 to 5	semi altered serpentinized hartzbergite.
046	95	60	45	0.4	210	1	semi altered serpentinized hartzbergite.
047	95	50	35	0.4	160	2 to 5	semi altered serpentinized hartzbergite.
048	90	65	30	0.5	200	1	fresh to low altered hartzbergite.
D11-101	145	100	85	0.40	1500	f. to 1	low to semi altered massive gabbro.
102	135	115	85	0.40	1200	f.	low altered px-pl gabbro.
201	115	85	65	0.50	870	f.	low altered aphyric basalt.

Sample No.	Diameter L	M	S	Round-ness	Wt. (g)	Mn-coating	Lithology & Remarks
301	120	80	65	0.50	430	none	px-bearing low vesicularity basaltic scoria.
401	210	145	70	0.40	1800	f. to 2	coarse serpentinized sandstone.
402	175	100	55	0.50	1070	1	middle to fine serpentinized sandstone.
403	90	75	20	0.50	150	1	middle to fine serpentinized sandstone.

Crustal evolution and back arc tectonics of the southern end of the Mariana Trough

H. MASUDA,
Department of Geosciences, Osaka City University
ISHII T., GAMO T., HARAGUCHI S., HIRATA U.
Ocean Research Institute, University of Tokyo
Y. NISHIO,
Graduate School of Science, University of Tokyo
T. YAMANAKA,
Department of Earth and Planetary Science, Kyushu University
HAYASAKA Y., Maejima T.,
Department of Earth and Planetary Science, Hiroshima University
SATO H.,
Graduate School of Natural Sciences, Tsukuba University
TANIGUCHI H.,
Komazawa-Daigaku High School

Introduction

The Mariana Trough is the crescent shaped back arc basin formed in relation to the subduction of the Pacific Plate under the old oceanic island arc, which is the active Mariana Ridge and inactive West Mariana Ridge at the present. The Mariana Trough has been thought to be opened during the Miocene earlier than 5.5 Ma from the southern part (Scott et al., 1981). The presently active arc volcanic chain is aligned in the back arc side of the Mariana Ridge (Fig. 1). In the southern part of the volcanic chain from 15°N, the top of the volcanoes are beneath the ocean surface. The southernmost submarine volcano belonging to the Mariana Arc volcanism known before the Yokosuka cruise was Tracy Seamount located at 144°00'E and 13°40'N. Until the research cruise by Yokosuka and submersible Shinkai 6500 in 1992 and 1993, no research was persuaded in the southern Mariana Trough except only one topographic survey concerned with submarine telephone cable (Hagen et al., 1992). However, seamount chains parallely aligned between 143°45'E, 13°08'N and 144°05'E, 13°40'N were found in 1992, and an active hydrothermal field was found at the summit of the one of those (B seamount). In 1993, diffusive emanation of low temperature hydrothermal fluids were observed at the C and X seamounts. Based on the shore based analyses of the rocks from the four seamounts, chemical characteristics of those rocks are those of island arc volcanisms (Masuda et al., in prep.). Thus, it is evident that the newly found seamount chains are

on the extension of active volcanic zone of the Mariana Arc.

In this cruise, we are targeting the seamounts comprising the southernmost segment between 12°35'N and 12°50N. To clarify the type of volcanism and possibility of present activity, we tried to dredge and hydrocast. In this section, the dredge sites and the results of dredged samples are briefly described.

Dredge site and obtained samples

The location and depths of dredged sites are in the Table 1. The topography and obtained samples are as follows.

D-5

The targeted area is a conical seamount aligned on the western seamount chain of the presumed arc volcanic chains. The dredged trace is from the west to east. Most of the obtained samples are highly vesicular pillow basalts, which have fresh quenched glass surface without manganese coating. Some basalt blocks coated by thin manganese film seem to be more silica rich, and probably have basaltic andesite composition. If manganese coating indicates the exposure time at the ocean bottom, the basaltic andesite is derived from the older volcanic activity than the basalt having fresh glass rim.

It is notable that the hydrothermal sediments concerned with high temperature fluid were recovered from this site. Those are fragments of hydrothermally altered brecciated rocks and a small piece of sulfide deposit. The hydrothermally altered rocks, which would originally be tuff breccia, color white, indicating acidic alteration to form silica and aluminous clay minerals.

D-6

The targeted site was the seamount having a crater on the top, and the dredger traced from the bottom to the wall of the crater.

Most of the obtained rocks are vesicular pillow basalts. The basalts include small amounts of plagioclase phenocrysts of less than 3 mm. From the optical observation, the basalts would be grouped into two different types, although those can not be defined without detailed shore based analyses. One of the basalts have vesicles having elongated shape, and those length are more than 8 cm at the maximum. Joints parallel to the elongation direction of the vesicles are developed in an each few cm. The other type of the basalts have the spherical shaped vesicles of ~3 cm diameters. Also this type of basalts seems to be more vesiculous than the former one. The former type of the basalt would have more basic composition, e.g., lower viscosity, than the other.

More detailed analyses must be needed to clarify the identification of these basalts, two types of basalt would indicate two different stages of volcanic eruption.

Some of the basalt which have spherical shaped vesicles contained xenolith of basic rocks; plutonic rocks and basalt. The largest xenolith was a foliated plutonic rock containing large amounts of feldspar and magnetite and minor olivine, suggesting gabbroic composition. Altered basalt fragments less than 5 mm are also observed as xenolith. These xenoliths should be crustal component under the seamount.

Thin red stain occasionally coat the surface of basalts, although manganese coating was not observed. A few small fragments of weakly hydrothermally altered basalts are present in the obtained rocks. Brown colored sediment and a few small pieces of ferrous sediments were also dredged from this site. All of these samples indicate that low temperature hydrothermal fluid is issuing from somewhere in the crater.

D-7

The targeted area is a conical shaped seamount comprising the western seamount chain. Apparent character of the recovered rocks are optically monotonous; vesicular pillow basalt having plagioclase of a few cm. The shape of vesicles are spherical, and looked resemble to those obtained from the site of D-5. Manganese coating was not recognized, and thin red stein was also rarely observed. Thus, the sampled rocks would be very young, however, the present hydrothermal activity is in doubt.

D-8

The dredged line is estimated to cut the westernmost part of the transform fault, running in east-west direction at 13。08'N, and finished at slope of the one of the segments of the narrow ridge located parallel in the west of the arc volcanic chains. The ridge has en échelon alignment and running through in the direction of NNE to SSW, and the summit depths is about 3000m. The targeted ridge is a segment located from 13°07'N to 13°32'N. The dredge was planned to collect the rocks from the both sides of the fault, although the recovered rocks are thought to be collected only from the northern part from the fault.

All sampled rocks were fresh loapy pillow basalts, on which surface a few cm thick quenched glass having scraped texture on the surface remains. No manganese or red stain coating was observed. Thus, volcanic activity of the area would be very young.

The basalt is aphyric, however, it contains small amount of plagioclase phenocryst of less than 2 mm. Low occurrence of vesicles, which are elongated,

indicates low viscosity of the basalt.

D-9

Although the targeted area was a high temperature active hydrothermal field named the Alice Spring field in the middle Mariana Trough, the obtained samples were only fresh pillow basalts. The basalts are optically monotonous, which have fresh quenched glass rim of about a few cm thick, and which contain moderate amount of plagioclase phenocrysts of 2~5 mm lengths.

□ualthough

Present volcanisms and tectonic field in the studied area

The research ot this cruise is successful to find the following important discoveries.

1 Active hydrothermal fields which have not been known are strongly presumed in the studied area. Especially, a piece of sulfide ore deposit is an important indicator for high temperature blacksmoker type fluid emanation at somewhere on the summit area of a conical seamount located on 12°35'N, 143°25'E. and aome fragments of hydrothermally altered tuff breccia aresAlso, red Also, reddish sediments recovered from the seamount having a crater at 12°50'N, 143°43.6'N indicate a low temperature hydrothermal field on the bottom of the crater. Anomalous changes of conductivity, dissolved oxygen and Mn contents in the seawater column taken from the inside of the caldera are notable to suggest a presence of hydrothermal plume from the seamount located at 12°45'N, 143°30'E (written by Gamo, this volume).for the southern Mariana Trough

2 The pillow basalt collected from the site of D-8 is estimated to be very young. Although no indicator for hydrothermal activity was found in this area, the ridges running on the westernmost part of the map is active at the present. If so, the ridges would be an active spreading center of the back arc basin.

Forthgoing study

The studied area is active volcanic zone, where the arc volcanism and back arc spreading occou in the adjacent area. Probably, the convergent area is located at 12°35'N, 143°15'E and its surroundings. In order to define the tectonics of back arc spreading in this area, shore based analyses of petrology and chemisty of collected rocks and seawaters. Moreover, if we will have chances to return the area, we should survey the western ridge which is presumed to be a back arc spreading center and the convergent

area of it and arc volcanic chains. Such a research will define the principle driving force for back arc opening of the Mariana Trough in an oceanic island arc.

Selected papers of the studied field

Alt J. C., Shanks III W. C. and Jackson M. C. (1993) Cyclying of sulfur in subduction zones: The geochemisty of sulfur in the Mariana Island Arc and back-arc trough. Earth Planet. Sci. Lett., 119, 477-494.

Barone A. M., Lonsdale P. F. and Puteanus D. (1990) Formation of axial volcanic ridges of the Mariana slow spreading center from spaced magma sources. EOS Trans. Am. Geophys. Union, 71, 1637

Bibee L. D. Shor G. G. and Lu R. S (1980) Inter-arc spreading in the Mariana Trough. mar. Geol. 35, 183-197.

Bracey D. R. and Ogden T. A. (1972) Southern Mariana Arc: Geophysical observations and hypothesis of evolution. Geol. Soc. Amer. Bull., 83, 1509-1522.

Crock J. G. and Lichte F. E. (1982) Determination of rare earth element in geological materials by inducting coupled argon plasma/atomic emission spectrometry. Anal. Chem., 54, 1329-1332.

Davidson J. P. (1987) Crustal contamination versus subduction zone enrichment: Examples from the Lesser Antilles and implications for mantle source composition of island arc volcanic rocks. Geochim. Cosmochim. Acta. 51, 2185-2198.

Delaney J. R., D. W. Muenow and Grayham D. G. (1978) Abundance and distribution of water, carbon and sulfur in the glassy rims of submarine pillow basalts. Geochim. Cosmochim. Acta. 42, 581-594.Dixon J. E., Stolper E. and Delaney J. R. (1988) Infrared spectroscopic measurements of CO2 and H2O in Juan de Fuca Ridge basaltic glasses. Earth Planet. Sci. Lett., 90, 87-104.

Dixon T. H. and Stern R. J. (1983) Petrology, chemistry, and isotopic composition of submarine volcanoes in the southern Mariana arc. Geol. Soc. Amer. Bull., 94, 1159-1172.

Dixon T. H. and Batiza R. (1979) Petrology and chemistry of recent lavas in the northern Marianas: Implications for the origin of island arc basalts. Contrib. Mineral. Petrol., 70, 167-181.

Fryer P. (1993) The relationship between tectonic deformation, volcanism, and fluid venting in the southeastern Mariana convergent margin. Proc. JAMSTEC Symp. Deep Sea Res., 9, 161-179.

Fryer P. (1995) Geology of the Mariana Trough. In Backarc Basins: Tectonics and

magmatism, B. Taylor (ed.). Plenum press: New York. 237-279.
Gamo T., Chiba H., Fryer P., Ishibashi J., Ishii T., Jhonson L. E., Kelly K., Masuda H., Ohta H., Reysenbach A.-L., Rona P. A., Shibata T., Tamaoka J., Tanaka H., Tsunogai U. and Yamaguchi T. (1993) Revits to the mid-Mariana Trough hydrothermal site and discovery of new venting in the soutehrn Mariana region by the Japanese submerible SHINKAI 6500.
Gamo T., Tsumogai U., Ishibashi J., Masuda H. and Chiba H. (1997) Chemical characteristics of hydrothermal fluids from the Mariana Trough.
Garcia M. O., Liu N. W. K. and Muenow D. W. (1979) Volatiles in submarine volcanic rocks from hte Mariana Island arc and trough. Geochim. Cosmochim. Acta., 43, 305-312.
Hagen R. A., Shor A. N. and Fryer P. (1992) Sea MARC II evidence for the locus of seafloor spreading in the southern Mariana Trough. Mar. Geol., 103, 311-322.
Hawkins J. W. and Melchior J. T. (1985) Petrology of Mariana Trough and Lau Basin basalts. Jour. Geophys. Res., 90, 11431-11468.
Hart S. R., Glassley W. E. and Karig D. E. (1972) Basalts and sea floor spreading behind Mariana island arc. Earth Planet. Sci. Lett. 15, 12-18.Hawkins J. W. and Melchior J. T. (1985) Petrology of Mariana Trough and Lau Basin basalts. Jour. Geophys. Res., 90, 11431-11468.
Hawkins J. W., Lonsdale P. F., Macdaugall J. D. and Volpe A. M. (1990) Petrology of the axial ridge of the Mariana Trough backarc spreading center. Earth Planet. Sci. Lett., 100, 226-250.
Hawkesworth C. J. and Ellam R. (1989) Chemical fluxes and wedge replenishment rates along recent destructive plate margins. Geology. 17, 46-49.
Hawkesworth C. J., Hergt J. M., Ellam R. and McDermott F. (1991) Element fluxes associated with subduction related magmatism. Phils. Trans. R. Soc. London, Ser. A 335. 393-405.
Hickey-Vergas R. (1991) Isotope characteristics of submarine lavas from the Phillipine Sea: implications for the origin of arc and basin magmas of the Philippine tectonic plate. Earth Planet. Sci. Lett., 107, 290-304.
Hole M. J., Saunders A. D., Marriner G. F. and Tarney J. (1984) Subduction of pelagi sediments: implications for the origin of Ce-anomalous basalts from the Mariana Islands. Geol. Soc. London., 141, 453-472.
Horibe Y., Kim K.-R. and Craig H. (1986) Hydrothermal methane plumes in the Mariana back-arc spreading centre. Nature, 324, 131-133.
Johnson L. E., Fryer P., Taylor B., Silk M., Jones D. L., Sliter W. V., Itaya T. and

Ishii T. (1991) New evidence for crustal accretion in ther outer Mariana fore ar: Cretaceous radiolarian cherts and mid-ocean ridge basalt-like lavas. Geology, 19, 811-814.

Johnson L. E., Fryer P., Masuda H., Ishii T. and Gamo T. (1993) Hydrothermal vent deposits and two magma source for volcanoes near 13。20'N in the Mariana backarc basin: a view from Shinkai 6500 (abstract). EOS Trans. AGU Fall Meeting Suppl., 74(43): 681.

Karig D. E. (1971) Structural history of the Mariana Island Arc system. Geol. Soc. Amer. Bull., 82, 323-344.

Karig D. E., Anderson R. N. and Bibee L. D. (1978) Characteristics of back arc spreading in the Mariana Trough. Jour. Geophys. Res., 83, 1213-1226.

Karig D. E. (1971) Origin and development of marginal basins in the western Pacific, J. Geopys. Res. 76, 2452-2561.

Kasahara J., Sato T. and Fujioka K. (1994) Intensive thermal upwelling at a Seamount in the southern Mariana Trough observed by Ocean Bottom Seismic instruments Using "Shinkai 6500" submsersible. JAMSTEC J. Deep Sea Res., 10, 163-174.

Kimura G., Koga K. and Fujioka K. (1989) Deformed soft sediments at the junction betwen teh Mariana and Yap Trenches. Jour. Structural Geol. 11, 463-472.

Larson E. E., Reynolds R. L., Merrill R., Levi S., Ozima M., Aoki Y., Kinoshita H., Zasshu S., Kawai N., Nakajima T. and Hirooka K. (1974) Major-element peroochemistry of some extensie rocks from the volcanically active Mariana Islands. Bull. Volcanologique, 38, 1-17.

Lin P.-N., Stern R. J. and Bloomer S. H. (1989) Shoshonitic volcanism in the Northern Mariana Arc 2. Large-ion lithosphile and rare element abundances: Evidence for the source of incompatible element enrichments in intraoceanic arcs. J. Geophys. Res. 94, 4497-4514.

Masuda H., Gamo T., Fryer P., Ishii T., Johnson L. E., Tanaka H., Tshunogai U., MatsumotoT., Masumoto S. and Fujioka K. (1993) The major element chemistry of sumbarine volcanic rocks from the southern Mariana Trough and its relation to the topography. Proc. JAMSTEC Symp. Deep Sea Res., 9, 181-189. (in Japanese with English abstract)

Masuda H., Lutz R. A., Matsumoto T., Masumoto S. and Fujioka K. (1994) Topography and geochemical aspects on the most recent volcanism around the spreading axis of the southern mariana Trough at 13。N. JAMSTEC J. Deep Sea. Res., 10, 175-185. (in Japanese with English abstract)

Meijer A. (1976) Pb and Sr isotopic data bearing on the origin of volcanic rocks from

the Mariana island-arc system. Geol. Soc. Amer. Bull., 87, 1358-1369.
Morris J. D. and Hart S. R. (1983) Isotopic and imcompatible element constraints on the genesis of island arc volcanics from Cold Bay and Amark Island, Aleutians, and implications for mantle structure. Geochim. Cosmochim. Acta., 47, 2015-2030.
Pearce J. A. and Cann J. R. (1973) Tectonic setting of basic volcanic rocks determined using trace element analysis. Earth Planet. Sci. Lett., 19, 290-300.
Poreda R. and Craig H. (1989) Helium isotope ratios in circum-Pacific volcanic arcs. Nature, 338, 473-478.
Poreda R. (1985) Helium-3 and deuterium in back-arc basalts: Lau Basin and the Mariana Trough. Earth Planet. Sci. Lett., 73, 244-254.
Scott R. B., Kroenke L., Zakariadze G. and Sharaskin A. (1981) Evolution of the south Phillipne Sea: Deep Sea Drilling Project Leg 59 results. Init. Repts. DSDP 59: Washington (U. S. Govt. Printing Office), 803-815.
Shibata T. and Segawa K. (1985) Basaltic glasses from the northern Marana trough, in Preliminary Report of the Hakuho maru cruise KH 84-1. pp. 215-224. Ocean Res. Inst. Univ. Tokyo, Tokyo.
Stern R. J., Morris J., Bloomer S. H. and hawkins Jr. J. W. (1991) The source of the subduction in convergent margin magmas: Trace element and radiogeni isotope evidence from Eocene boninites, Mariana Arc. Geochim. Cosmochim. Acta., 55, 1467-1481.
Stern R. J. and Bibee L. D. (1984) Esmeralda Bank: Geochemistry of an active submarine volcano in the Mariana Island Arc. Contrib. Mineral. Petrol., 86, 159-169.
Stern R. J., Lin P.-N., Morris J. D., Jackson M. C., Fryer P., Bloomer S. H. and Ito M. (1990) Enriched back-arc basin basalts from the northern Mariana Trough: implications for the magmatic evolution of back-arc basins. Earth Planet. Sci. Lett., 100, 210-225.
Stern R. J., Jackson M. C., Fryer P. and Ito E. (1993) O, Sr, Nd and Pb isotopic composition of the Kasuga cross-chain in the Mariana Arc: A new pwerspective on the K-h relationship. Earth Planet. Sci. Lett., 119, 459-475.
Stolper E. and Newman S. The role of water in the pertogenesis of Mariana trough magmas. Earth Planet. Sci. Lett., 121, 293-325.
Stern D., Taibi N. E,, McMurtry G. M., Scholten J., Stoffers P. and Zhang D. (1994) Growth histogy of hydrotermal silica chimney from the Mariana back arc spreading center (southwest Pacific, 18。13'N). Chem. Geol., 113, 273-296.
U. S. Japan paleomagnetic Cooperation Project in Micronesia (larson E. E., Reynolds R. L., Merrill R., Levi S., Ozima M., Aoki Y., Kinoshita H., Zasshu S., Kawai N., Nakajima T., Hirooka K. (1974) Major-element petrochemistry of some extensive rocks from the volcanically active Mariana Islands. Bull. Volcanol. 38, 1-17.

Volpe A. M., Macdougall J. D., Lugmair G. W., Hawkins J. W. and Lonsdale P. (1990) Fine-scale isotopic variation in Mariana Trough basalts: evidence for heterogenuity and a recycled component in backarc basin mantle. Earth Planet. Sci. Lett., 100, 251-264.

Volpe A. M., Macdougall J. D. and Hawkins J. A. (1987) Mariana Trough basalts (MTB): trace element and Sr-Nd isotopic evidence for mixing between MORB-like and Arc-like melts. Earth Planet. Sci. Lett., 82, 241-254.

Wright I. C. (1993) Pre-spread rifting and herogenous volcanism in the southern Havre Trough back-arc basin. Marine Geol., 113, 179-200.

Wessel J. K., Fryer P., Wessel P. and Taylo B. (1994) Extention in the northern Mariana Inner forearc. Jour. Geophys. Res., 99, 15181-15203.

Woodhead J. D (1989) Geochemistry of the Mariana arc (western Pacific): Source composition and processes. Chem. Geol., 76, 1-24.

Yamatani Y., Masuda H., Amakawa H., Nozaki Y. and Gamo T. (1994) Rare earth element chemistry of submarine volcanic rocks from a spreading axis, the southern Mariana Trough. JAMSTEC J. Deep Sea Res., 10, 187-193.

Table 1 The lacations of dredge site during KH-98-1 Leg III in the Mariana Trough

Site	Start position			Final position		
	Altitude	Longitude	Depths (m)	Altitude	Longitude	Depths (m)
D-5	12°33.91'N	143°24.83'E	2711	12°33.86'N	143°25.71'E	2059
D-6	12°52.00'N	143°50.02'E	2486	12°51.37'N	143°50.02'E	2128
D-7	12°58.45'N	143°43.65'E	3216	12°58.04'N	143°44.90'E	2776
D-8	13°08.72'N	143°41.41'E	2929	13°09.19'N	143°40.60'E	2962
D-9	18°12.94'N	144°42.06'E	3718	18°12.69'N	144°42.97'E	3788

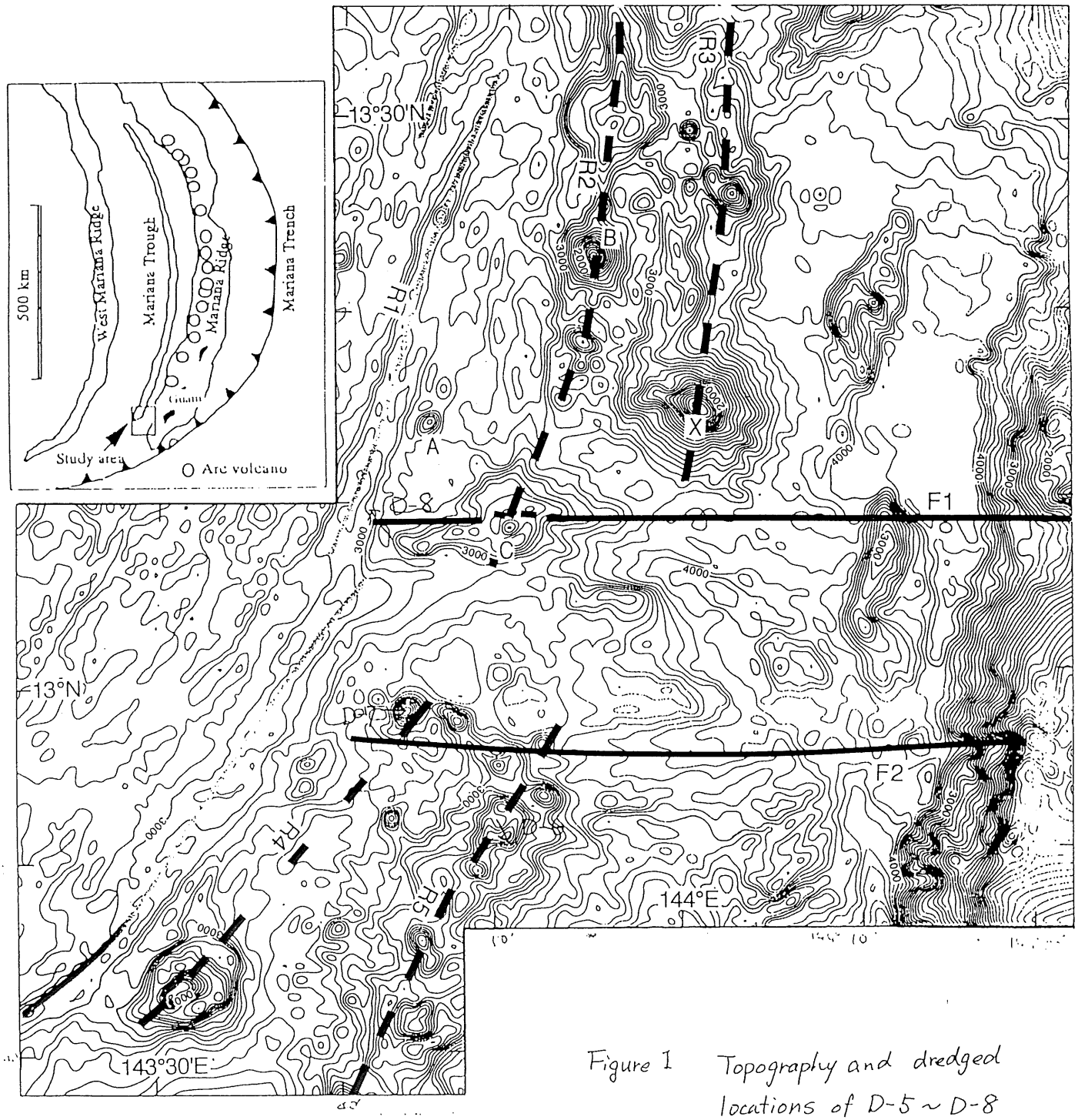

Figure 1 Topography and dredged locations of D-5 ~ D-8 in the southern Mariana Trough during KH 98-1 Leg 3.

D-5
→⊕

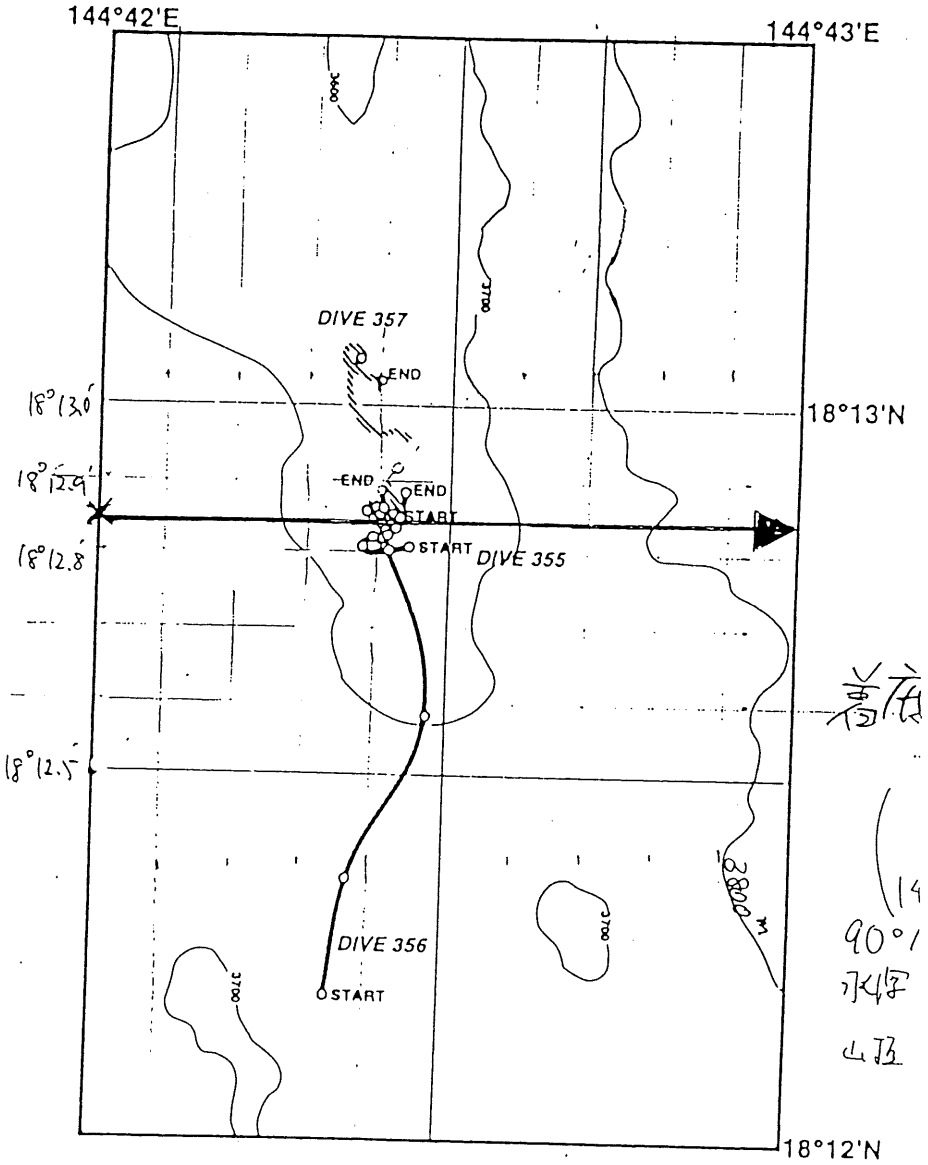

Figure 2 Dredged site of D-9 in the middle Mariana Trough during KH 98-1 Leg 3.

Search for and chemical characterization of hydrothermal plumes in the Mariana Trough during the KH-98-1 Cruise

T. Gamo, H. Hasumoto, S. Kitagawa, K. Okamura
Ocean Research Institute, University of Tokyo
E. Nakayama, H. Obata
University of Shiga Prefecture
J. Ishibashi, Y. Nishio
Graduate School of Science, University of Tokyo
H. Masuda
Osaka City University
T. Yamashiro
Kagoshima University
T. Yamanaka
Kyushu University

1. Introduction: previous studies and purposes of this study

Mariana Trough is a present-day spreading back arc basin behind the Mariana Trench, where the Pacific plate subducts under the Philippine Sea plate. The spreading rate is thought to be ~3 cm y^{-1} as a full rate for these 3 m.y. (Hussong and Uyeda, 1981). Mariana Trough is also characterized by active hydrothermal circulation with heat and material flux from seafloor (e.g. Ishibashi and Urabe, 1995), as evidenced by the existence of hydrothermal active sites in the mid- and southern Mariana Trough as described below.

In efforts to locate and characterize ocean bottom hydrothermal systems, water column distributions of various chemical components give us much information. Although submarine hydrothermal activity is a very localized phenomenon at sea bottom, it usually accompanies hydrothermal plumes, cloud-like widely dispersing water masses, which are the mixture of hydrothermal end members and ambient bottom seawater. Areal extent of hydrothermal plumes can be traced from water column anomalies of chemical components such as methane, manganese, helium-3, which are particularly enriched in hydrothermal solutions (e.g. Klinkhammer et al., 1985; Horibe et al., 1986; Gamo et al., 1987; Nojiri et al., 1989; Charlou et al., 1991a,b; Gamo et al., 1993; 1996). In addition, light transmission is also known to be useful for the detection of hydrothermal plumes (e.g. Baker et al., 1995)

In the mid-Mariana Trough, water column CH_4 anomalies were found for the first time between 18°12'N and 18°15'N during the CEPHEUS (KH-82-1) Expedition of R/V *Hakuho Maru* (Ocean Research Institute, University of Tokyo) in 1982 (Horibe et al., 1986). Five years later, detailed bottom surveys using DSRV *Alvin* (Woods Hole Oceanographic Institution, U.S.A.) discovered hydrothermal activity (18°13'N, 144°42'E; depth: 3,600 m; Alice springs field) with high temperature vent fluids (up to 287°C) and biological communities along the axial region centered on 18°13'N in the mid-Mariana Trough (Craig

et al., 1987; Campbell et al., 1987; Hessler et al., 1988). DSRV *Shinkai 6500* (Japan Marine Science and Technology Center, JAMSTEC) revisited this site in 1992 and 1996, confirming almost steady duration of hydrothermal activity (Gamo et al., 1993; 1994; 1997; Fujikura et al., 1997).

In the southern Mariana Trough, a high temperature hydrothermal active site (13°24'N, 143°55'E; depth: 1470 m; Forecast vent field) was found in 1992 by DSRV *Shinkai 6500* in spite of no information of hydrothermal plumes (Gamo et al., 1993; 1994; 1997; Masuda et al., 1993; Fryer et al., 1993; Johnson et al., 1993). This site was also revisited by *Shinkai 6500* in 1993 and 1996 for detailed observation (Masuda et al., 1994; Tsunogai et al., 1994; Tsunogai, 1995; Gamo et al., 1997; Fujikura et al., 1997)

Chemical characteristics (major element compositions, dissolved gas concentrations, isotope ratios etc.) of the hydrothermal fluids from the Alice springs field in the mid-Mariana Trough (maximum fluid temperature: 264-287°C) and from the Forecast vent field in the southern Mariana Trough (195-210°C) have shown that the former activity is a sediment-starved backarc type, while the latter a sediment-starved arc type, although the data on fluid chemistry have not necessarily been accumulated enough so far (Gamo et al., 1997).

The purposes of this study, i.e. water column surveys in the Mariana Trough during the KH-98-1 cruise are: (1) observation of areal distribution of hydrothermal plumes and their detailed chemical characterization, and (2) search for hydrothermal active sites by detecting new hydrothermal plumes if any. This is the first hydrothermal plume survey in the southern Mariana Trough. As a newly developed observational instrument, an *in situ* Mn analyzer (GAMOS-II) was introduced for the first time, in order to elucidate super-fine chemical structure of hydrothermal plumes. The data from the mid-Mariana Trough will be compared with those previously observed (Horibe et al., 1986) to detect any temporal variability of the hydrothermal plumes.

2. Methods

2-1. CTD Carousel Multi Sampling (CTD-CMS) system

The CTD-CMS (CTD-Carousel Multi Sampling system) used during the KH-98-1 cruise consists of the following instruments.

CTD fish (Seabird, Model 9 plus, pressure rating: 6800m) with a DO sensor
Carousel Multi-Sampling system (Seabird, Carousel-24)
Lever-action Niskin samplers (General Oceanics, 12-liter type)
Niskin Samplers (General Oceanics, 12-liter type)
Pinger (Benthos, Model 2216)
Light transmissometer (SeaTech, 25cm light path, 5000m-type)
GAMOS-II (Geochemical Anomaly Monitoring System)

The above CTD-CMS system, attached at the end of the titanium armored cable (8mm o.d.) from the No.2 winch of R.V. Hakuho Maru, was controlled

on board the ship by a CTD deck unit (Seabird, Model 11 plus) connected with an IBM compatible desktop computer (Endeavor Pro-300). The array frame (Carousel) has a capability to hold 24 water samplers with a volume of 12 liters. During this cruise, however, 19 samplers (11 Lever-action Niskin samplers and 8 Niskin samplers) were attached because the space for the rest five samplers was shared by the in situ Mn analyzer GAMOS-II and a pinger for monitoring the distance between the system and the sea bottom. The ship stays at a fixed location, where the system is lowered to a depth of several meters above the bottom. Water samples are taken by triggering the samplers at appropriate depths while the system is coming up to the surface.

2-2. Water samplers

Two kinds of water samplers were used: lever-action Niskin samplers and ordinary Niskin samplers. In order to reduce the contamination level as low as possible, all the samplers had been completely coated with teflon paint on their inside walls before the cruise. Silastic tubing (a kind of silicone rubber) is utilized as rubber spring for the Niskin samplers because of its contamination-free characteristics. On board the ship, the samplers were cleaned thoroughly using 2% Extran MA01 (Merck) solution, 0.1M HCl solution and Milli-Q pure water.

2-3. Shipboard chemical analyses

Collected samples were split for analyses of salinity, dissolved oxygen, and manganese. Subsamples for Si measurement were divided from the samples for Mn analysis. Brief descriptions for the shipboard measurements are as follows.

2-3-1. Salinity (by H. Obata)

Salinity was measured with a salinometer, (Autosal, Model 8400A) in the usual way. The cell temperature was 24°C. IAPSO standard seawater (Ocean Scientific International Ltd., Batch : P127, Date14-Feb-95, K15=0.99990, S=34.996) was used for calibration.

2-3-2. Dissolved Oxygen (by T. Gamo, H. Masuda, T. Yamashiro, S. Kitagawa)

Each seawater is collected to an oxygen bottle with a volume of 100 cm^3, avoiding the introduction of bubbles. After the collection, 0.5 cm^3 of $MnCl_2$ solution and 0.5 cm^3 of KI-NaOH solution are successively added to the bottle. This procedure quantitatively fixes dissolved oxygen in seawater sample as $MnO(OH)_2$. After standstill for a day or so for the precipitate to settling down to the bottom of the bottle, the supernatant (10-20 cm^3) is removed to reduce the sample volume. Then, 5 ml of 6M HCl is added to dissolved the precipitation to release I_2. Then, I_2 (yellow color) is titrated by sodium thiosulfate ($Na_2S_2O_3$) standard solution using an automatic titrating machine (Hirama, Model ART-3). The sodium thiosulfate standard solution is calibrated by using CSK standard of 0.0100M potassium iodate (KIO_3) solution (WAKO Pure Chemical Industries, LTD., Lot No. KCP8418).

2-3-3. Silica (by J. Ishibashi)

B-molybdosilicic acid is formed by the reaction of silicate with molybdate at a pH of 1 to 1.8. The B-molybdosilicic acid is reduced by tin(II) to form molybdenum blue with an absorbance maximum at 820 nm. Shimadzu xx-1200 spectrophotometer was used for the analysis.

2-3-4. Manganese (by E. Nakayama, H. Obata)

Manganese was determined on board by the automated-Mn analysis system which is based on the column electrolysis preconcentration and the chemiluminescence(CL) detection (Nakayama et al., 1989). In brief, 50 cm^3 of unfiltered seawater adjusted at pH 5.0 by adding ammonium acetate buffer solution is introduced to the system. Mn in the sample is adsorbed onto glassy carbon column electrode. The column is rinsed with the cleaning solution (pure water), and then hydrogen peroxide solution adjusted to pH 4 with ammonium acetate buffer solution is passed through the column. The eluent is mixed with alkaline luminol solution and the mixture is introduced into the CL cell through the mixing coil. Finally, Mn is determined by measurement of the CL intensity. Mn determined with this system is called "total adsorbable Mn", which contains Mn(II) ion and part of colloidal Mn. The relative standard deviation for five replicate measurements at 3.6 nM is 3.2 % and the determination limit(3σ) is 0.14 nM for the typical analysis condition. The total throughput of analysis is 8 samples per hour. In addition to the measurement of total adsorbable Mn, total Mn was determined in the following manner: the samples were heated to boil with a microwave oven after adding hydrogen peroxide to decompose inert colloidal and particulate Mn. After this pretreatment, Mn was determined in the same manner as total adsorbable Mn. The obtained data will be compared with the *in situ* data by GAMOS-II.

2-4. Shorebased analyses

Subsamples were stored for the following measurements in shorebased laboratories: concentrations of CH_4, CO_2, Fe, stable isotope ratios of CH_4, CO_2 and He. These measurements will be done with the collaboration of Drs. U. Tsunogai (Nagoya Univ.) and M. Maruo (Univ. Shiga Prefecture). In addition, several samples (mostly surface samples) were taken for Dr. N. Nakamura (Kobe Univ.), who will measure stable isotope ratios of Cl and Sr.

2-5. *In-situ* chemical analyzer GAMOS-II (by K. Okamura)

GAMOS (Geochemical Anomalies MOnitoring System) is an in-situ chemical analyzer used to detect manganese anomalies in neutrally buoyant plumes and to map manganese distribution in bottom seawater over vent fields. GAMOS analyzes dissolved manganese continuously by a flow-through analysis method (Okamura et al., submitted). Dissolved manganese concentration is determined using a H2O2-luminol chemiluminescence method. Development of the GAMOS system was started in 1994. The first version of GAMOS was used successfully at Manus Basin, Papua New Guinea (Shinkai 6500/YOKOSUKA ManusFlux cruise, 1995).

2-5-1. Analytical Method

Sample fluid or standard solution is passed through a filter (10 μm) to remove large particles. The solution is mixed with a pH 5 buffer solution and passed through a Kelex-100 (commercial name for 7-dodecenyl-8-quinolinol, Ashland Chemical Co.) column, which removes interfering metals (mainly Fe, Cu and Zn) from solution. The solution is mixed with hydrogen peroxide, aqueous ammonia, and luminol solution and then transported to a detector. Manganese concentration is determined by measuring the resulting chemiluminescence intensity. Detection range can be adjusted by altering reagent concentrations.

2-5-2. GAMOS-II

GAMOS-II was designed for either tow-yo surveys from a surface ship or for submersible operations.

As shown in Fig. 1, GAMOS-II is composed of four parts: (i) an acrylic oil and water-filled vessel containing a flow-through analyzer system, (ii) an aluminum pressure housing for electronic modules, (iii) an acrylic cylinder to arrange flexible plastic bags of analytical reagents, and (iv) a battery for power supply (DC24V). The battery can be omitted if power is supplied directly from a ship or submersible.

The acrylic vessel holds a peristaltic pump, four stop valves and a reaction manifold. The peristaltic pump supplies a constant flow of the sample solution (seawater, standard or blank solution) and the chemiluminescence reagents. The electromagnetic stop valves (Takasago, clean valve, MTV-2) are programmed to select the appropriate flow path for these solutions. The reaction manifold for the chemiluminescence reaction is made from 1 mm I.D. Teflon tubing. The acrylic vessel has a rubber diaphragm (Bellofram) at its top for pressure balance between the inside and outside of the vessel.

The Al pressure housing, with a pressure rating of 450 atm, holds a CPU, 2 photomultiplier detectors with amplifiers, an A/D converter, and a 2M-byte flash memory for data logging. These electronic modules serve the following functions: (1) time-keeping with a quartz crystal oscillator clock in the CPU, (2) generating commands to control a motor of the peristaltic pump motor and stop valves according to a time schedule program, (3) amplifying and recording detected chemiluminescence intensity, and (4) communication with a computer using a RS-232C interface to control the functions of the GAMOS system and to transfer obtained data. The pressure housing is connected to the acrylic vessel using underwater connectors (Brantner & Associates, Inc., XSK-8). The data is logged every one second during operation.

3. Location of stations

Water column observations using the CTD-CMS were performed at the following stations:

V371 (Control station, 11°26'N, 138°44'E)

V372-2 (Control station, 12°06'N, 138°53'E)
KH981-H01 (Southern Mariana Trough; 12°43.4'N, 143°31.25'E)
KH981-H02 (Southern Mariana Trough; 12°59'N, 143°45'E)
KH981-H03 (Southern Mariana Trough; 13°23.7'N, 143°55.2'E)
KH981-H04 (Mid-Mariana Trough; 18°12.8'N, 144°42.4'E)
KH981-H05 (Mid-Mariana Trough; 18°24'N, 144°39'E)

KH981-H01 locates inside a seamount caldera, where P. Fryer (Univ. of Hawaii) has ever dredged to find strong signature of hydrothermal activity (Fryer, pers. comm.). KH981-H02 is the station also for dredging during this cruise, where hydrothermal activity is expected. KH981-H03 and KH981-H04 correspond to "Forecast vent field" discovered by *Shinkai 6500* in 1992 and "Alice springs field" discovered by *Alvin* in 1987, respectively. KH981-H05 is a large seamount north of "Alice springs field", where no hydrographic data is yet available.

4. Preliminary results

The transmissometer detected significant hydrothermal plumes (probably three layers) at station KH981-H01 as shown in Fig.2. These plumes are accompanied by remarkably high Mn concentrations (Fig.3). It is of interest that the most significant plume at pressure ranging from 2650 to 2850 decibar seem to be also accompanied by slight decrease of dissolved oxygen (Figs.2, 3), possibly reflecting a signature of reducing characteristics of hydrothermal fluids.

Little transmission anomaly was observed at stations KH981-H02 and KH981-H05 as well as the control stations.

Contrary to our expectation, stations KH981-H03 and KH981-H04, where high temperature fluid venting has been observed by the previous submersible observations as mentioned above, showed little transmission anomaly. This may be related with the fact that hydrothermal fluids observed at both sites were transparent (clear smokers).

Particle-rich (low transmission) characteristics of hydrothermal plumes observed at station KH981-H01 may suggest the existence of black or white smoker chimneys inside this caldera.

References

Baker, E.T., C.R.German, and H. Elderfield (1995): Hydrothermal Plumes Over Spreading-Center Axes: Global Distributions and Geological Inferences. In: Seafloor Hydrothermal Systems. Physical, Chemical, biological, and Geological Interactions (AGU Geophysical Monograph 91), 47-71.

Campbell, A.C., J.M. Edmond, D. Colodner, M.R. Palmer and K.K. Falkner (1987): Chemistry of hydrothermal fluids from the Mariana Trough back arc basin in comparison to mid-ocean ridge fluids. EOS Trans. AGU, 68(44), 1531 (abstract).

Charlou, J.L., H. Bougault, P. Apprio, T. Nelsen and P. Rona (1991a): Different TDM/CH4 hydrothermal plume signatures: TAG site at 26°N and serpentinized ultrabasic diapir at 15°05'N on the Mid-Atlantic Ridge. Geochim. Cosmochim. Acta, 55, 3209-3222.

Charlou, J.L., H. Bougault, P. Appriou, P. Jean-Baptiste, J.-Etoubleau and A. Birolleau (1991b): Water column anomalies associated with hydrothermal activity between 11°40'

and 13°N on the East Pacific Rise: discrepancies between tracers. Deep-Sea Res., 38, 569-596.

Craig, H., Y. Horibe, K.A. Farley, J.A. Welhan, K-R. Kim and R.N. Hey (1987): Hydrothermal vents in the Mariana Trough: Results of the first Alvin dives. EOS Trans. AGU, 68(44), 1531 (abstract).

Fryer, P.(1993): The relationship between tectonic deformation, volcanism, and fluid venting in the southwestern Mariana convergent plate margin, Proc. JAMSTEC Symp. Deep Sea Res., 9, 161-179.

Fujikura, K., T. Yamazaki, K. Hasegawa, U. Tsunogai, R.J. Stern, H. Ueno, H. Yamamoto, Y. Maki, S. Tsuchida, T. Kodera, H. Yamamoto, C-H. Sun, & T. Okutani (1997): Biology and earth scientific investigation by the submersible "Shinkai 6500" system of deep-sea hydrothermalism and lithosphere in the Mariana Back-arc Basin. JAMSTEC J. Deep Sea Res., 13, 1-20 (in Japanese with English abstract).

Gamo, T., J. Ishibashi, H. Sakai and B. Tilbrook (1987): Methane anomalies in seawater above the Loihi submarine summit area, Hawaii. Geochim. Cosmochim. Acta, 51, 2857-2864.

Gamo, T. and the shipboard scientific party of the Y9204 cruise (1993): Revisits to the mid-Mariana Trough hydrothermal site and discovery of new venting in the southern Mariana region by the Japanese submersible Shinkai 6500, InterRidge News, 2, 11-14.

Gamo, T., H. Chiba, P. Fryer, J. Ishibashi, T. Ishii, L.E. Johnson, K. Kelly, H. Masuda, S. Ohta, A-L. Reysenbach, P.A. Rona, T. Shibata, J. Tamaoka, H. Tanaka, U. Tsunogai, T. Yamaguchi, and K. Fujioka (1994): Mariana 1992 diving survey by "Shinkai 6500" (Y9204 cruise): revisits to the mid-Mariana hydrothermal area and discovery of hydrothermal vents in the southern Mariana region, JAMSTEC J. Deep Sea Res., 10, 154-162 (in Japanese with English abstract).

Gamo, T., H. Sakai, J. Ishibashi, E. Nakayama, K. Isshiki, H. Matsuura, K. Shitashima, K. Takeuchi and S. Ohta (1993) Hydrothermal plumes in the eastern Manus Basin, Bismarck Sea: CH_4, Mn, Al and pH anomalies. Deep-Sea Res., 40 (11/12), 2335-2349.

Gamo, T., E. Nakayama, K. Shitashima, K. Isshiki, H. Obata, K. Okamura, S. Kanayama, T. Oomori, T. Koizumi, S. Matsumoto, and H. Hasumoto (1996): Hydrothermal plumes at the Rodriguez Triple Junction, Indian Ridge. Earth Planet. Sci. Lett., 142, 261-270.

Gamo, T., U. Tsunogai, J. Ishibashi, H. Masuda, and H. Chiba (1997): Chemical characteristics of hydrothermal fluids from the Mariana Trough. JAMSTEC J. Deep-Sea Res. Spec. Volume: Deep Sea Research in subduction zones, spreading centers and backarc basins, JAMSTEC, 69-74.

Hessler, R., P. Lonsdale and J. Hawkins (1988): Patterns on the ocean floor, New Scientist, 24(March), 47-51.

Horibe, Y., K.-R. Kim and H. Craig (1986): Hydrothermal methane plumes in the Mariana back-arc spreading centre, Nature, 324, 131-133.

Hussong, D.M. & S. Uyeda (1981): Tectonic processes and the history of the Mariana arc: A synthesis of the results of Deep Sea Drilling Project Leg 60, in Init. Repts. DSDP, 60 (D.M. Hussong, S. Uyeda et al. eds.), Deep Sea Drilling Project , Washington D.C., pp. 909-929.

Ishibashi, J. and T. Urabe (1995): Hydrothermal activity related to arc-backarc magmatism in the western Pacific, in Backarc Basins: Tectonics and Magmatism, ed by B. Taylor, Plenum Press, New York & London, pp. 451-495.

Johnson, L., P. Fryer, H. Masuda, T. Ishii & T. Gamo (1993): Hydrothermal vent deposits and two magma sources for volcanoes near 13°20'N in the Mariana backarc: a view from Shinkai 6500, EOS Trans. AGU, 74(43), Fall Meet. Suppl., 681 (abstract).

Klinkhammer, G.P., P. Rona, M. Greaves and H. Elderfield (1985): Hydrothermal manganese plumes in the Mid-Atlantic Ridge rift valley. Nature, 314, 727-731.

Masuda, H., T. Gamo, P. Fryer, T. Ishii, L.E. Johnson, H. Tanaka, U. Tsunogai, S. Matsumoto, S. Masumoto, and K. Fujioka (1993): The major element chemistry of submarine volcanic rocks from the southern Mariana Trough and its relation to the topography. JAMSTECTR Deepsea Res., 9, 181-189 (in Japanese with English abstract).

Masuda, H., R.A. Lutz, S. Matsumoto, S. Masumoto, & K. Fujioka (1994): Topography and geochemical aspects on the most recent volcanism around the spreading axis of the

southern Mariana Trough at 13°N. JAMSTEC J. Deep Sea Res., 10, 175-185 (in Japanese with English abstract).
Nakayama, E., K. Isshiki, Y. Sohrin, and H. Karatani (1989): Automated determination of manganese in seawater by electrolytic concentration and chemiluminescence detection. Anal. Chem., 61, 1392-1396.
Nojiri, Y., J. Ishibashi, T. Kawai, A. Otsuki and H. Sakai (1989): Hydrothermal plumes along the North Fiji Basin spreading axis. Nature, 342, 667-670.
Okamura, K., T. Gamo, H. Obata, E. Nakayama, H. Karatani, Y. Nozaki: Selective and sensitive determination of trace manganese in seawater by flow through technique using luminol-hydrogen peroxide chemiluminescence detection. Analytica Chimica Acta (submitted).
Tsunogai, U., J. Ishibashi, H. Wakita, H. Masuda, T. Gamo, & K. Fujioka (1994): Geochemical features of the southern Mariana Trough region as revealed by dissolved chemical composition of hydrothermal fluids, Japan Earth and Planetary Sciences Joint Meeting, H31-01 (abstract).
Tsunogai, U. (1995): Geochemical studies of migration process and source of fluids in the crust, Ph D. Thesis, University of Tokyo, 116pp.

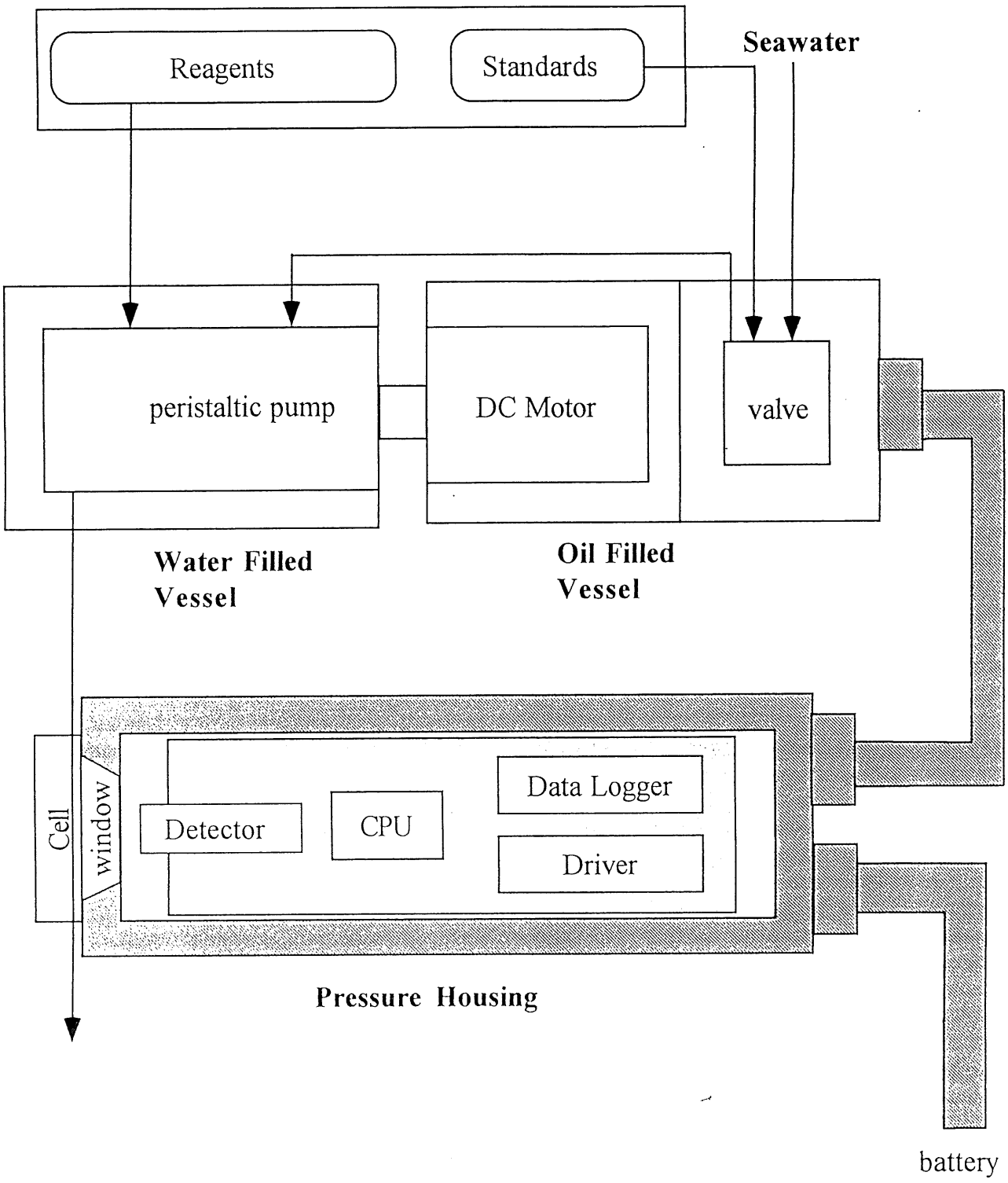

Fig . 1 Schematic diagram of GAMOS-II

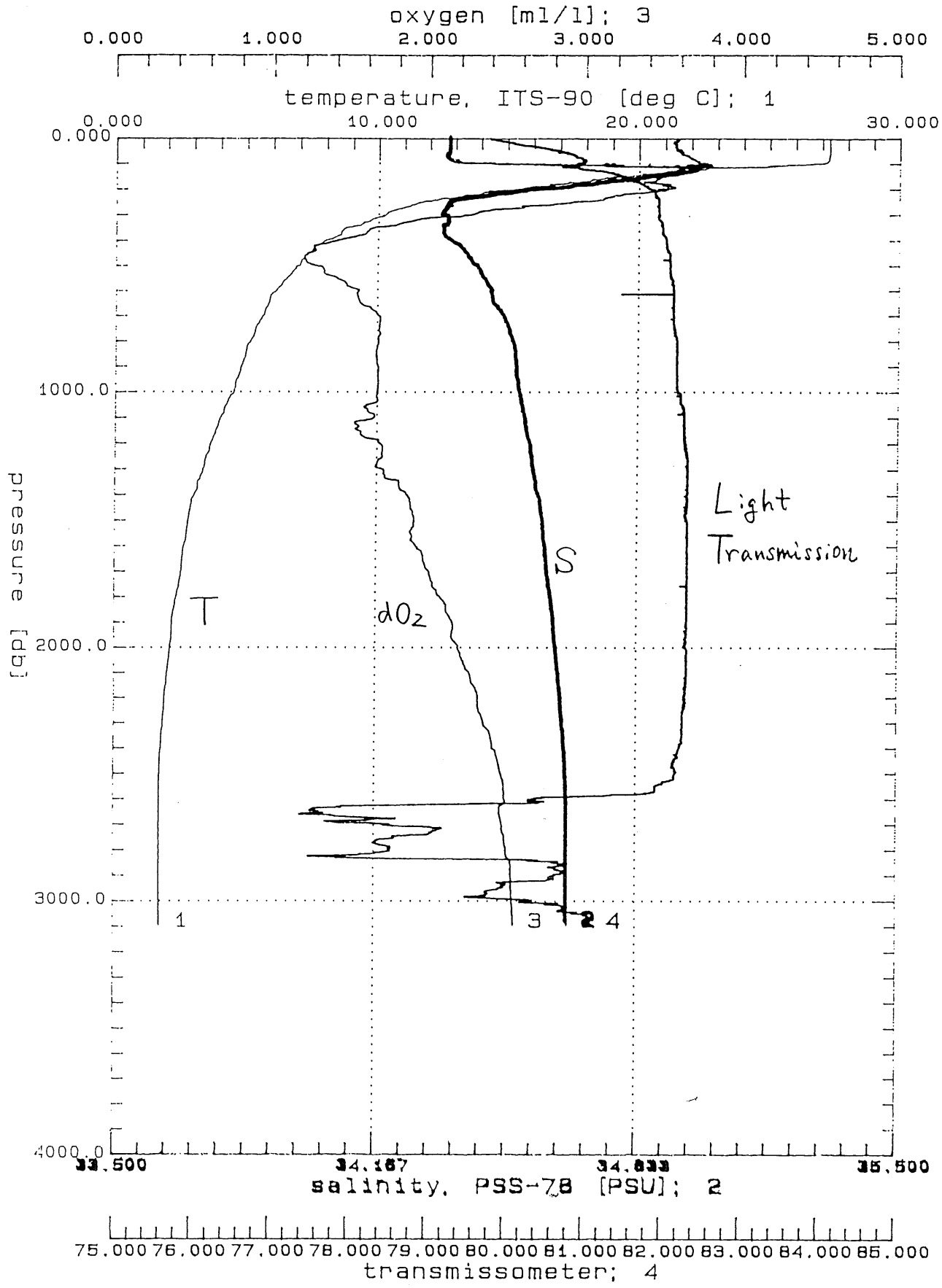

HYDRO-1U.CNV: KH-98-1

Fig. 2

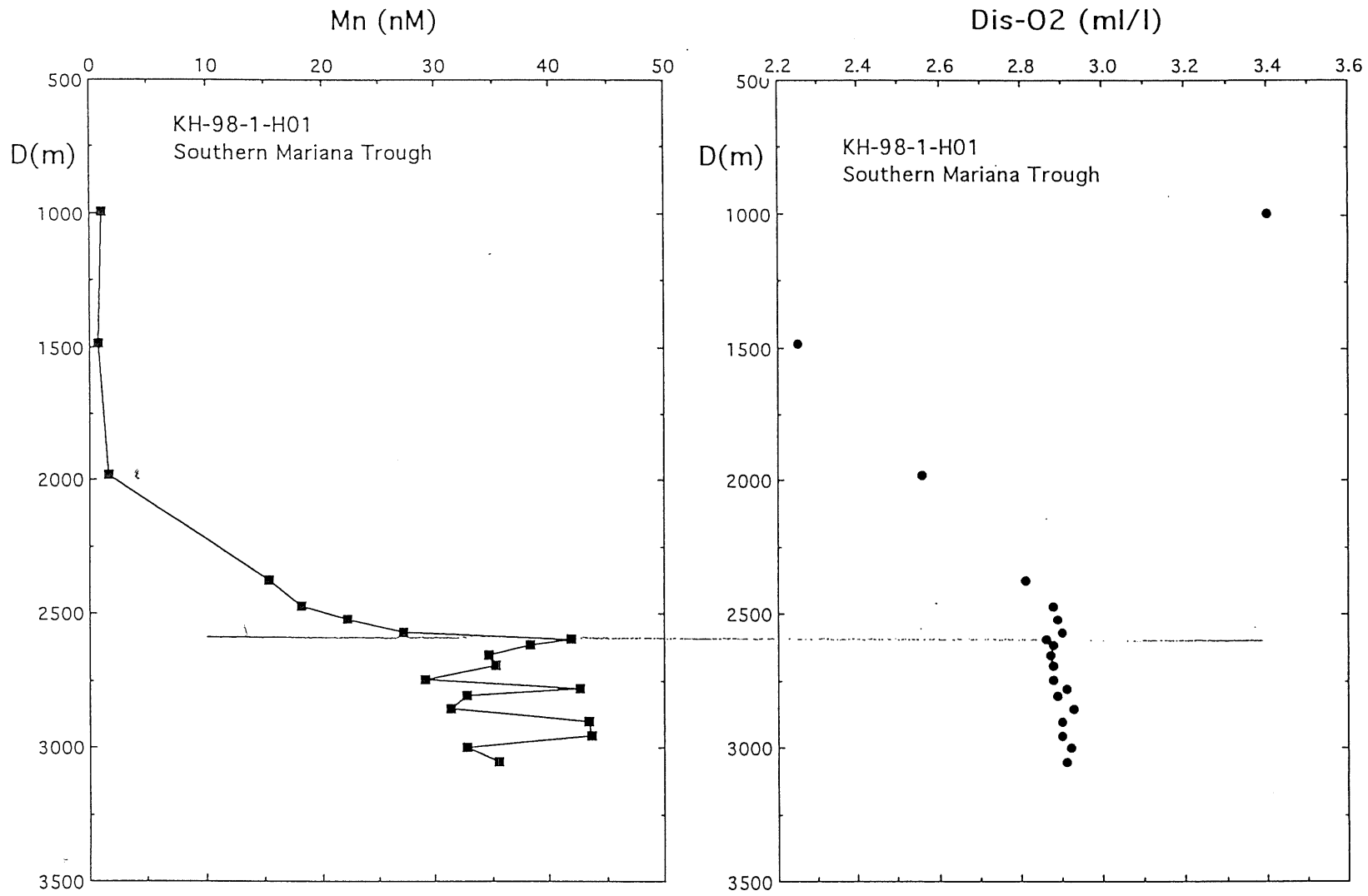
Mn (nM)
0
10
20
30
40
50
500
D(m)
1000
1500
2000
2500
3000
3500
KH-98-1-H01
Southern Mariana Trough
Dis-O2 (ml/l)
2.2
2.4
2.6
2.8
3.0
3.2
3.4
3.6
500
D(m)
1000
1500
2000
2500
3000
3500
KH-98-1-H01
Southern Mariana Trough

Fig. 3

Air sampling for measuring stable carbon isotopic composition of non-methane hydrocarbons (NMHC) and methyl chloride (CH_3Cl) in western Pacific atmosphere

U. Tsunogai and N. Yoshida
Institute for Hydrospheric-Atmospheric Sciences, Nagoya Univ. and JST

T. Gamo
Ocean Research Institute, University of Tokyo

Purpose:

Light molecular weight non-methane hydrocarbons (NMHC)(C2-C5) and methyl chloride (CH_3Cl) are commonly present in the lower regions of the atmosphere in cencentrations ranging from a few parts per billion by volume (ppbv) to a few parts per trillion (pptv). Many past investigations on the distributiohn of these compounds have revealed that they play an important role in the chemistry of atmosphere. However, many uncertainties still remain aboun nature, the strength and the distribution of their sources and removal processes.

Studies on the stable isotopic composition of atmospheric species with more than about ppmv mixing ratio, such as CO_2 and CH_4, have provided valuable information for understanding the distribution of production and removal processes involved in atmospheric cycling. In the case of trace components such as NMHC and methyl chloride, however, few data are available for their isotopoic composition, because it is difficult to collect sufficient quantity of samples for traditional $\delta^{13}C$ determination.

New isotope-ratio-monitoring gas chromatography / mass spectrometry (irm-GC/MS) systems require much smaller sample volume for isotopic analyses. We have developed an analytical sy6stem which is capable of on-line simultaneous analyses of concentration and $\delta^{13}C$ of low level NMHC and methyl chloride in atmosphere using irm-GC/MS. In this study, we will determine distributions of both mixing ratios and stable carbon isotopic compositions of NMHC and CH_3Cl in western Pacific atmosphere, by using the above method. The air mass composition reflect land sources followed by transport over the ocean, during which additional marine contribution and photochemical removal process occur. By using isotopic sugnatures, we will discuss the sources and removal processes of NMHC and methyl chloride in western Pacific.

Sampling and Analysis:

All the air samples are collected in 6.0-L pre-evaluated stainless steeel canisters (fused-silica coated) equipped with a diaphragm valve (fused-silica coated). At the air sampling port of a canister, an absorption trap, 30 cm long, 5 mm i.d., packed with 10-20 mesh Drierite (Hammond) and 20-30 mesh Ascarite II (Thomas), was attached to remove water water and carbon dioxide from the

sampled air. All the samples will be analyzed in the shorebased laboratory at IHAS, Nagoya University, within a few weeks after sampling, by using combination of (1) three step cryofocusing, (2) separation using HP 6890 gas chromatograph with a PoraPLOT Q capillarly column (0.32 mm i.d. x 25 m), (3) quantitative combustion of all separeted hydrocarbons to CO_2 by passing them through a 960 °C combustion interface (CuO/NiO/Pt catalyzer) and (4) sequantial determinations of $\delta^{13}C$ in the CO_2 by Finnigan MAT 252 mass spectrometer.

Sample list:

The following 9 air samples were taken at the front end of the sixth deck (over the bridge) of the Hakuho-Maru during sailing of the ship at a speed of about 16 knots (only the last sample, 0315-2, was taken at the ship speed of about 7 knots).

Sample No.	Canister No.	Sampling date	Sampling location
0303	SC-04	March 3, 1998	(6°05'N, 154°05'E)
0304	SC-02	March 4, 1998	(8°32'N, 151°06'E)
0306	SC-01	March 6, 1998	(12°05'N, 144°22'E)
0311	SC-03	March 11, 1998	(16°14'N, 144°23'E)
0312	SC-05	March 12, 1998	(21°41'N, 144°28'E)
0313	SC-06	March 13, 1998	(25°37'N, 143°20'E)
0314	SC-08	March 14, 1998	(30°06'N, 141°18'E)
0315-1	SC-07	March 15, 1998	(35°00'N, 139°43'E)
0315-2	SC-09	March 15, 1998	(35°32'N, 139°51'E)